International Journal of Hydrogen Energy 140 (2025) 745–776

Contents lists available at ScienceDirect

International Journal of Hydrogen Energy

journal homepage: www.elsevier.com/locate/he

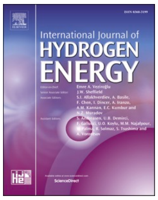

Advances in filler-crosslinked membranes for hydrogen fuel cells in sustainable energy generation

Aminul Islam [a,b,c,*], Mamun Shahriar [a,d], Md. Tarekul Islam [e], Siow Hwa Teo [f], M. Azizur R. Khan [d,**], Yun Hin Taufiq-Yap [g], Suman C. Mohanta [d], Ariyan Islam Rehan [h], Adiba Islam Rasee [i], Khadiza Tul Kubra [i], Md. Munjur Hasan [i], Md. Shad Salman [j], R.M. Waliullah [j], Md. Nazmul Hasan [h], Md. Chanmiya Sheikh [k], Tetsuya Uchida [k], Mrs Eti Awual [j], Mohammed Sohrab Hossain [i], Hussein Znad [l], Md. Rabiul Awual [l,***]

[a] *Department of Petroleum and Mining Engineering, Jashore University of Science and Technology, Jashore, 7408, Bangladesh*
[b] *Hydrogen energy and CO_2 conversion Lab, Department of Petroleum and Mining Engineering, Jashore University of Science and Technology, Jashore, 7408, Bangladesh*
[c] *College of Engineering, Korea University, 145 Anam-ro, Seongbuk-gu, Seoul, 02841, Republic of Korea*
[d] *Department of Chemistry, Jashore University of Science and Technology, Jashore, 7408, Bangladesh*
[e] *Department of Leather Engineering, Faculty of Mechanical Engineering, Khulna University of Engineering and Technology, Khulna, 9203, Bangladesh*
[f] *Industrial Chemistry Program, Faculty of Science and Natural Resources, Universiti Malaysia Sabah, 88400, Kota Kinabalu, Sabah, Malaysia*
[g] *Catalysis Science and Technology Research Centre, Faculty of Science, Universiti Putra Malaysia, Serdang, 43400, Malaysia*
[h] *Department of Chemistry, School of Science, The University of Tokyo, 7-3-1 Bunkyo-ku, Tokyo, 113-0033, Japan*
[i] *Department of Chemistry, Graduate School of Science, Osaka University, Osaka, 560-0043, Japan*
[j] *Institute for Chemical Research, Kyoto University, Gokasho, Uji, Kyoto, 611-0011, Japan*
[k] *Division of Applied Chemistry, Graduate School of Natural Science and Technology, Okayama University, 1-1 Tsushima-naka, 3-Chome, Okayama, 700-8530, Japan*
[l] *Western Australian School of Mines: Minerals, Energy and Chemical Engineering, Curtin University, GPO Box U 1987, Perth, WA, 6845, Australia*

ARTICLE INFO

Handling Editor: Dr Mehran Rezaei

Keywords:
Advanced materials
Fuel cell
Hydrogen gas generation
Proton exchange membrane
Polymer

ABSTRACT

Fuel cell membranes can be used in various ways to achieve zero-emission transport and energy systems, which offer a promising way to power production due to their higher efficiency compared to the internal combustion engine and the eco-environment. Perfluoro sulfonic acid membranes used for proton exchange membranes (PEMs) have certain drawbacks, like higher fuel permeability and expense, lower mechanical and chemical durability, and proton conductivity under low humidity and above 80 °C temperature. Researchers have drawn their attention to the production of polymer electrolyte membranes with higher proton conductivity, thermal and chemical resilience, maximum power density, lower fuel permeability, and lower expense. For sustainable clean energy generation, a review covering the most useful features of advanced material-associated membranes would be of great benefit to all interested communities. This paper endeavors to explore several types of novel inorganic fillers and crosslinking agents, which have been incorporated into membrane matrices to design the desired properties for an advanced fuel cell system. Membrane parameters such as proton conductivity, the ability of H_2 transport, and the stability of the membrane are described. Research directions for developing fuel cell membranes are addressed based on several challenges suggested. The technological advancement of nanostructured materials for fuel cell applications is believed to significantly promote the future clean energy generation technology in practice.

---

* Corresponding author. Department of Petroleum and Mining Engineering, Jashore University of Science and Technology, Jashore, 7408, Bangladesh.
** Corresponding author. Department of Chemistry, Jashore University of Science and Technology, Jashore-7408, Bangladesh.
*** Corresponding author. Western Australian School of Mines, Minerals, Energy and Chemical Engineering, Curtin University, GPO Box U 1987, Perth, WA, 6845, Australia.

E-mail addresses: aminul_pme@just.edu.bd (A. Islam), m.azizurrahman.khan@just.edu.bd (M.A.R. Khan), ariyan.islam@dims-bd.org (A.I. Rehan), munjur.hasan@dims-bd.org (Md.M. Hasan), shad.salman@dims-bd.org (Md.S. Salman), nazmul.hasan@dims-bd.org (Md.N. Hasan), chanmiya.sheikh@dims-bd.org (Md.C. Sheikh), rabiul.awual@dims-bd.org, rawual76@yahoo.com, rabiul.awual@curtin.edu.au (Md.R. Awual).

https://doi.org/10.1016/j.ijhydene.2025.05.197
Received 29 January 2025; Received in revised form 21 April 2025; Accepted 14 May 2025

Abbreviation

3D	Three Dimensional
AC	Alternating current
AFC	Alkaline fuel cell
AMPS	2-Acrylamido-2-methyl-1-propanesulfonic acid
BDC/bdc	1,4-Benzene-dicarboxylate
BEE	Benzoin ether Ether
BIm.HSO$_4$	1-Butylimidazolium hydrogensulfate
BMI.HSO$_4$	1-Butyl-3-methylimidazolium hydrogen sulfate
CHS	Cesium hydrogen sulfate
CNTs	Carbon nanotubes
CPE	Constant phase element
CS	Chitosan
DAB	Diaminobenzidine
DC	Direct current
DS	Degree of sulfonation
DVB	Divinyl benzene
DWCNTs	Double-walled carbon nanotubes
EIS	Electrochemical impedance spectroscopy
EPA	Ethyl phosphonic acid
ETFE	Poly(ethylene-*co*-tetrafluoroethylene)
FC	Fuel cell
FEP	Fluorinated ethylene propylene
FeSPP	Ferric sulfophenyl phosphate
GO	Graphene oxide
HPAs	Heteropolyacids
HP-IM	4-Hydroxypyridine and imidazole cross-links
HPW	Phosphotungstic acid
HTPEM	High temperature proton exchange membrane
HT-PEMFCs	High temperature polymer electrolyte membrane fuel cells
IL	Ionic liquid
IL-EMI-BF$_4$	1-Ethyl-3-methyl imidazolium tetrafluoro borate
ILS	Ionic liquid-functionalizedSiO$_2$
ImMCs	Imidazole microcapsules
MC	Methyl cellulose
MCFC	Molten Carbonate fuel cell
MEA	Membrane electrode assembly
MOF	Metal-organic framework
MWNTs	Multi-walled carbon nanotubes
NVP	N-vinyl-2-pyrrolidone
OPBI	Poly [2,20-(*p*-oxydiphenylene)- 5,50-benzimidazole]
PA	Phosphoric acid
PAFC	Phosphoric acid fuel cells
PAMPS	Poly (2-acrylamido-2-methyl-1-propanesulfonic acid)
PBI	Polybenzimidazole
PBINf	Polybenzimidazole nanofibers
PEEK	Poly(Ether Ether ketone)
PEG	Poly ethylene Glycole
PEM	Proton exchange membrane
PEMFC	Polymer electrolyte membrane fuel cell
PES	Poly ether sulfone
PVP	Polyvinyl pyrrolidone
PFA	Perfluoroalkoxy alkane
PFPE-GO	Perfluoropolyether grafted graphene oxide
PFSAs	Perfluorosulfonic acids
PFSMs	Perfluorosulfonicacid-based membranes
PGO	Phosphonated graphene oxide
PMA	Phosphomolybdic acid
PMCs	Methacrylic acid polyelectrolyte microcapsules
PSSA-MA	Polystyrene sulfonic acid-*co*-maleic acid
PTFE	Polytetrafluoro ethylene
PVA	Poly vinyl alcohol
PWA	Phosphotungstic acid
QA	Quaternary ammonium
rGO	Reduced graphene oxide
rGONR	Reduced graphene oxides nanoribbons
RH	Relative humidity
SATS	Sulfonated poly(arylene thioether sulfone)
SDG	Sustainable development Goals
sGO	Sulfonated graphene oxide
SiWA	Silicotungstic acid
SOFC	Solid oxide fuel cell
SPAEKs	Sulfonated poly(arylene ether ketones)
SPAES	Sulfonated poly (arylene ether sulfone)
SPEEK	Sulfonated Poly(Ether Ether ketone)
SPES	Sulfonated poly ether sulfone
SPI	Sulfonated polyimides
SPIs	Sulfonated polyimides
SPS	Sulfonated poly sulfone
SPTA	Sulphothalic acid
SPTA-GO	Sulfonated polytriazole grafted graphene oxide
SPVA	Sulfonated poly vinyl alcohol
SSA	Sulfosuccinic acid
SWA	Silicotungstic acids
SWCNTs	Single-walled carbon nanotubes
TAC	Triallyl cyanurate
TEA-PS.HSO$_4$	3-Triethylammonium propane sulfonic hydrogensulfate
TEOS	Tetraethyl orthosilicate
UiO-66	UiO: University of Oslo
UV	Ultra violet
VGO	Vinyl functionalized graphene oxide
VP	Vinylpyridine
VPA	Vinylphosphonic acid
WU	Water uptake
ZIF	Zeolitic-imidazolate frameworks

(*continued on next column*)

(*continued*)

1. Introduction

Sustainable energy generation through hydrogen fuel cells was recognized as a promising solution for reducing carbon emissions and reliance on fossil fuels [1–3]. These cells operated by converting chemical energy from hydrogen into electricity through electrochemical reactions, emitting only water as a byproduct, which minimized environmental pollution [4–6]. The efficiency of hydrogen fuel cells was enhanced under varied operational conditions, with proton exchange membrane fuel cells (PEMFCs) being favored for their low operating temperature and fast start-up time [7–10]. However, challenges such as the high cost of materials, including platinum catalysts and PFSA membranes, along with limited hydrogen infrastructure, restrict widespread adoption [11–13]. Advances in alternative catalysts, non-fluorinated membranes, and green hydrogen production were explored to address these limitations, promoting fuel cells as a viable component of sustainable energy systems [13–17].

Advanced membranes are defined as polymer electrolyte membranes that incorporate innovative materials or structural modifications aimed at addressing the limitations of traditional PFSA membranes. These advanced membranes typically exhibit improved proton conductivity, enhanced thermal and chemical stability, reduced fuel crossover, and a cost-effective production process [18–20]. The objective of developing advanced membranes is to achieve a combination of desirable properties that can meet the demands of various fuel cell applications. Inorganic fillers and crosslinking agents play crucial roles in enhancing the properties of these advanced membranes. Inorganic fillers, such as silica (SiO_2), titania (TiO_2), and carbon-based materials, are incorporated into the polymer matrix to improve mechanical stability, increase proton conductivity, enhance thermal stability, and aid in water retention [21–23]. These fillers reinforce the membrane, reducing dimensional changes during hydration cycles and preventing mechanical degradation. Furthermore, certain inorganic fillers can facilitate additional proton conduction pathways, thereby enhancing overall membrane conductivity. Crosslinking agents are employed to create stronger bonds between polymer chains, resulting in improved membrane characteristics. The cross-linking process helps to reduce swelling by limiting the mobility of polymer chains during hydration, thus enhancing mechanical stability [24–26]. This approach also increases the durability of the membrane, providing greater resistance to chemical and thermal degradation, and extending the operational lifespan of the membrane. By carefully selecting crosslinking agents, the membrane's flexibility and toughness can be optimized for specific fuel cell conditions, contributing to better performance.

Inorganic fillers have been utilized to advance the development of polymer electrolyte membranes (PEMs) by enhancing their performance in fuel cells [27–29]. Functionalized silica (e.g., sulfonated, phosphonated, and polydopamine-modified silica), titanium dioxide (e.g., amino acid-functionalized and PAMPS-grafted TiO_2), and carbon-based nanomaterials (e.g., sulfonated graphene oxide and multiwalled carbon nanotubes) were incorporated into polymer matrices to improve mechanical, thermal, and electrochemical properties [30]. Membrane stability was enhanced through the reduction of swelling, while proton conductivity was maintained, particularly under high-temperature and low-humidity conditions. For instance, the incorporation of sulfonated silica into Nafion® was found to decrease water uptake without compromising conductivity. Additionally, metal-organic frameworks (MOFs), such as UiO-66 and MIL101, contributed to improved structural stability and ion transport, attributed to their high surface area and tunable porosity [31]. Crosslinking agents, such as phosphotungstic acid (HPW), incorporated into reduced graphene oxide (rGO) structures, further enhanced proton conductivity by providing additional proton-conducting pathways [32].

Traditional perfluorosulfonic acid (PFSA) membranes, such as Nafion®, have been confronted with several significant challenges that limit their application in **p**roton exchange membrane fuel cells (PEMFCs). A Proton Exchange Membrane Fuel Cell (PEMFC) or a Direct Methanol Fuel Cell (DMFC) is an electrochemical energy conversion device that generates electricity through the reaction of a fuel with an oxidant, typically hydrogen or methanol with oxygen, respectively. Both systems operate at relatively low temperatures and rely on a solid polymer electrolyte, which selectively facilitates the transport of ions while acting as a barrier to gases. The core functional unit of these fuel cells is the membrane electrode assembly (MEA), which is composed of three primary components: the proton exchange membrane, catalyst layers, and gas diffusion layers. The membrane serves as the electrolyte, allowing for the conduction of protons (H^+) from the anode to the cathode in PEMFCs, or generated from methanol oxidation in DMFCs. Catalyst layers, typically composed of platinum or platinum-based alloys, are employed to accelerate the electrochemical reactions at both electrodes [33]. Gas diffusion layers support uniform distribution of reactants to the catalyst sites and facilitate the removal of by-products such as water and carbon dioxide. In DMFCs, methanol is directly oxidized at the anode, producing protons, electrons, and carbon dioxide, while in PEMFCs, hydrogen serves as the primary fuel. In both systems, the electrons generated at the anode travel through an external circuit, providing electrical power, before recombining with protons and oxygen at the cathode to form water [34]. The performance and durability of the fuel cell are strongly dependent on the design and integrity of the MEA, making it a critical area of research and optimization in fuel cell technology. One of the primary issues reported was high fuel permeability, which reduced fuel efficiency and diminished overall cell performance [35]. Proton conductivity was also observed to decrease under low-humidity conditions and at temperatures exceeding 80 °C, compromising operational stability in high-temperature fuel cells [36]. Moreover, the manufacturing cost of PFSA membranes was found to be a significant barrier, as the synthesis process was complex and required expensive fluorinated materials [37]. Mechanical and chemical durability concerns were raised due to the degradation that occurred under prolonged exposure to harsh operational conditions, ultimately impairing membrane lifespan and reducing fuel cell performance.

Non-fluorinated polymeric materials were found to present both advantages and disadvantages compared to PFSA membranes. A significant advantage identified was their lower cost, as non-fluorinated raw materials were more readily available, and their synthesis involved simpler processes [38]. Enhanced thermal stability was also demonstrated at elevated temperatures, rendering these materials suitable for fuel cells operating above 100 °C [38–40]. Additionally, non-fluorinated polymers were chemically tailored to achieve specific properties, including increased mechanical strength and improved resistance to chemical degradation. However, these membranes were reported to exhibit lower proton conductivity, especially under low-humidity conditions, which limited their performance in certain applications [41]. Greater dependence on water retention for proton transport was observed, reducing their effectiveness in low-humidity environments or at elevated temperatures [42]. Furthermore, these materials were found to be more susceptible to oxidative degradation, compromising their long-term stability in fuel cell applications.

Since the majority of sulfonated polymer electrolyte membranes are thermally and mechanically stable, they have higher water uptake over a broad extent of temperatures. Sulfonated polymer electrolyte membranes additionally have reduced gas crossover, compared with PFSA membranes. Sulfonated polymer electrolyte membranes (PEMs), such as Nafion®, have been employed as critical components in hydrogen fuel cells, facilitating proton conduction while acting as gas barriers between fuel and oxidant. Nafion®'s thermal stability was attributed to its perfluorinated backbone, which resisted oxidative degradation and retained functionality up to 190 °C, maintaining proton conductivity at elevated temperatures [41]. Mechanical degradation was reported during hydration-dehydration cycles, where repeated swelling and shrinking generated stress and fatigue, leading to microcracking in the membrane matrix [43,44]. To mitigate these effects, sulfonated silica was incorporated into Nafion®, resulting in enhanced mechanical strength by limiting dimensional changes and preventing mechanical failure while preserving proton conduction pathways [12]. However, proton conductivity was still reduced under dehydrated conditions, as water loss at high temperatures compromised membrane integrity. Further stabilization was achieved through hybrid membrane designs, where carbon nanotubes were integrated to improve both mechanical and thermal properties [45]. Although these developments advanced the durability of sulfonated PEMs, challenges remained in ensuring consistent performance over extended periods, necessitating ongoing research to optimize their structure for long-term applications in fuel cells.

In the past two decades, a large number of papers have been published on H_2 fuel cell technology, reflecting both its importance and rapid development. Although it is not possible to adequately cover all the aspects of the fuel cell research, a review covering the key features of advanced fuel cell membranes associated with clean energy generation would be of great benefit to all those involved. This review aims to study recent advancements in fuel cell membranes, focusing on novel inorganic fillers and crosslinking agents that enhance membrane properties. Emphasis is placed on improving proton conductivity, hydrogen transport efficiency, and membrane stability. The potential of these materials to drive future developments in fuel cell technology is discussed, providing insights into strategies that may be employed to overcome current challenges in the field.

2. Principles and proton conductivity mechanisms of fuel cell membranes

Polymer Electrolyte Membrane Fuel Cell utilizes hydrogen as a fuel where an electrochemical reaction occurs at the interface of electrodes and membrane for the production of electrical energy and a pair of redox reactions between H_2 and O_2 produces water. A proton exchange membrane (PEM) as an electrolytic membrane allows protonic movement when hydrogen is passed through it [46]. On the other hand, being an electronic insulator prevents electron transfer and short-circuiting of the cell. The membrane is sand-witched between the electrocatalyst layers. Electrocatalyst layers consist of anode and cathode electrodes. On the anode side, oxidation of hydrogen molecules occurs to produce protons and electrons. The electrons generated migrate toward the cathode through an outer electrical circuit [47]; the operating principle of PEM is shown in Fig. 1.

$$\text{anodic reaction}: H_2 \rightarrow\ 2H^+ + 2e^- \tag{1}$$

$$\text{cathodic reaction}: \frac{1}{2}O_2 + 2H^+ + 2e^- \rightarrow H_2O \tag{2}$$

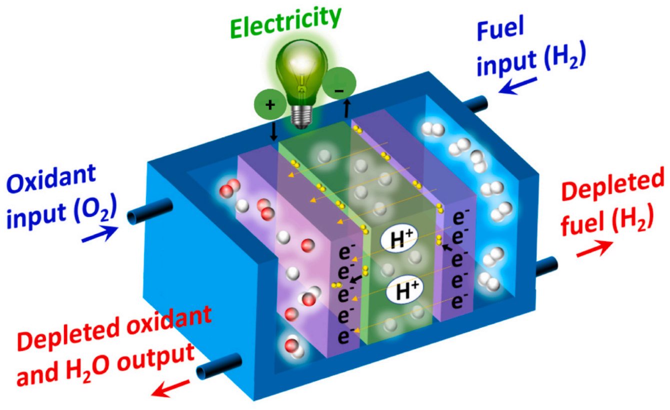

Fig. 1. Operating principle of PEMFCs **-** Proton Exchange Membrane cell uses hydrogen gas and oxygen gas as fuel. (Fuel cell diagram — Vector by serdiuk.igor.gmail.com).

$$\text{Overall reaction}: H_2 + \frac{1}{2}O_2 \rightarrow H_2O \tag{3}$$

At the cathode side, reduction of oxygen molecules occurs to produce O^{2-} ion, which finally reacts with H^+ ion and electrons to produce water as stated by Gagliardi et al. [48]. The power generated was due to the electronic conduction through the external electrical circuit attached with anode and cathode. There are two mechanisms, that can explain the proton conduction via the PEMs; the vehicular mechanism and the Grotthuss mechanism (hopping) [49]. The presence of better hydrophilic cluster interconnections as well as massive water uptake within PEM is necessary for proton diffusion in vehicular mechanism, whilst the proton leaps from protonic materials which include H^+ and H_3O^+ to some other protonic materials via the membrane. Therefore, von Grotthuss in 1806 proposed the authentic concept to explain a mechanism of proton transport among water molecules. In the Grotthuss mechanism, an "excess" proton is transferred via the H-bonded connections of water molecules or different H-bonded liquid species by the simultaneous construction and disruption of hydrogen bonds. It is supported by the short-route transfer of H_3O^+ ions to adjoining conducting reactive groups, as demonstrated in Fig. 2(b). As indicated by Karimi et al. [50], the free waters in the film facilitate the aqueous linkage arrangement inside the membranes and accordingly assisted the proton transport through the conducting reactive sites, for example, the sulfonic groups in Nafion. In this way, the Grotthuss mechanism is a cooperative system that boosts the slower proton transfer of the vehicular mechanism as well as facilitates the surprisingly higher transport rate of proton through the incessant construction and breaking of H-bond from one functional group to others. It was believed that at lower water content, each of the protons is combined with another free water molecule to produce a hydronium ion. Reversely in highly moisturized conditions, excess free water molecules easily combine with one proton to produce $H^+(H_2O)_n$, as stated by Yin et al. [51]**.** In vehicular mechanisms, the diffusion and migration of protons occur through the "vehicular service" of hydronium ion (H_3O^+) through the watered pathways.

Kreuer et al., 1982 introduced the vehicular transport system to explain the diffusion of the proton as a part of the complex structure due to the electro-osmotic drag with the formation of different ions H_3O^+, $H_5O_2^+$ (Zundel cation), and $H_9O_4^+$ (Eigen cation) with water molecules or different proton rich carrier existed within the electrolytes (e.g., NH_4^+, etc.) in aggregation with the chargeless molecular species (vehicle) that diffuses, as shown in pristine Nafion and composite membrane explained by Kuwertz et al. [52]**,** as shown in Fig. 2(c). High-pressure mass spectrometry has supported the explanation of proton hydration with many water molecules and the most possible structure of the solvated proton is the Zundel ion hydrated with the aid of using four water molecules. Recent research mentioned that the presence of one proton within a hundred water molecules is much more possible to be coordinated as the Zundel ion at 300K, while at elevated temperatures the persistence of Eigen ions is favorable. Eigen or Zundel ions permit proton transport through structural diffusion from one molecule to others via a very low energy resistance.

In Nafion membrane, Junoh et al. [53] showed, the cluster channel

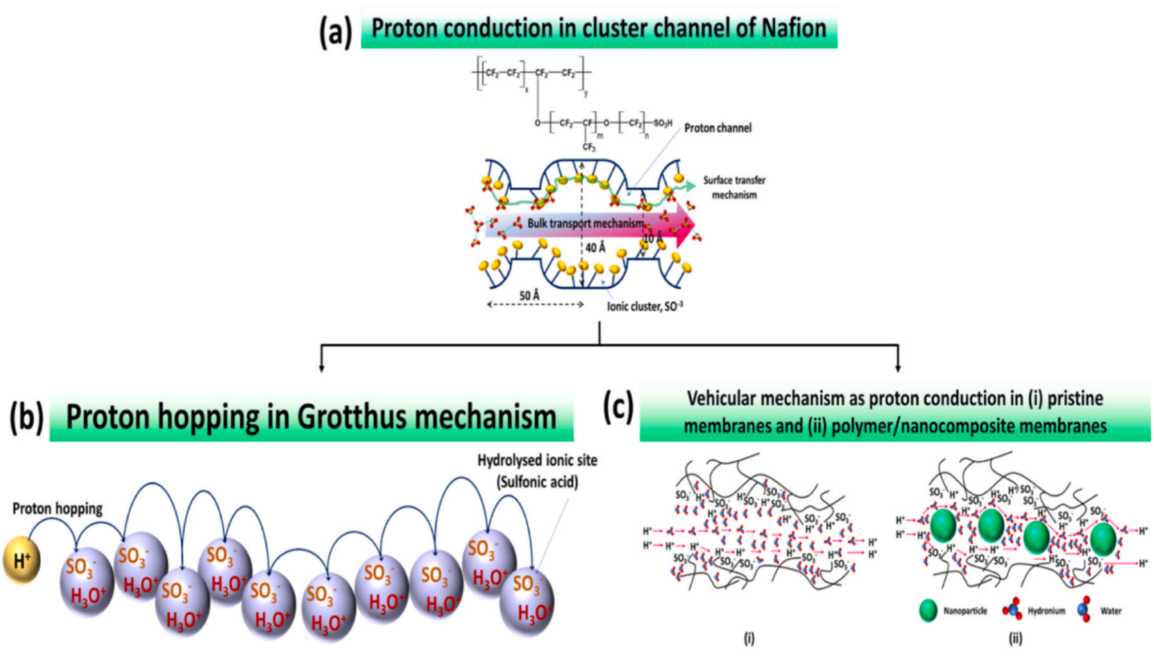

Fig. 2. (a)The cluster channel of Nafion [37]; (b) Proton transfer in Grotthus mechanism [38]; (c) Vehicular Mechanism as proton conduction in (i) pristine membranes and (ii) polymer/nanoparticle composite membranes [52].

of Nafion comprises four nano-meter sulfonated ion clusters connected with narrow water pathways of approximately 1 nm in diameter that are dispersed within the hydrophobic backbone, that's schematically delivered in Fig. 2(a). Esmaeili et al. [41] reported that highly hydrophilic –SO_3H groups can draw water molecules and accumulate to produce ionic clusters through which water and protons are transferred. In fact, proton transportation is caused due to the presence of these acidic sites in Nafion [54]. In the Grotthuss mechanism, the breakage and formation of bonds utilize more activation energy than that for the movement of solvated ions in vehicular species.

The Grotthuss mechanism, which is characterized by rapid proton hopping through a hydrogen-bonded network, generally involves lower activation energy than the vehicular mechanism. In the Grotthuss process, protons "hop" between adjacent water molecules or other hydrogen-bonded groups, leading to efficient charge transport with lower energy requirements [46,55]. This process is typically faster and more efficient, especially under hydrated conditions, because it relies on the rearrangement of hydrogen bonds rather than the bulk movement of molecules. Conversely, the vehicular mechanism entails proton transport via diffusion of protonated species through the electrolyte. This process requires the movement of the entire proton-carrying species, leading to comparatively higher activation energy due to greater mass transport requirements [47,56]. The difference in activation energies for these mechanisms becomes particularly significant in materials designed for proton exchange, as the Grotthuss mechanism offers a pathway for rapid conduction without the need for hydrated proton carriers, making it highly efficient in well-structured hydrogen-bonded environments.

3. Measurements of proton conductivity in membranes

Proton conductivity is the fundamental property of polymeric electrolyte membrane-based energy generation and transmission systems [57]. It is very difficult to measure the proton conductivity in insulating polymer films. Tang et al. [58] analyzed in detail the assessment result obtained from the measurement of the film resistance for a given polymer greatly depends on some factors, e.g., film casting conditions, relative humidity, cell configuration, and pressure applied between probe electrodes. The technique applied and the geometry of the cell under experiment strongly influence the resistance measurement. Considering the geometrical direction of measurement, in-plane assessment, and through-plane assessment techniques are used to determine the membrane resistance, also called impedance. In an in-plane assessment technique, the impedance of the membrane can be measured using facile support of a 2 or 4-electrodes arrangement. The greater cell constant, cell configuration, and more sensor electrodes in the 4-electrodes arrangement system ensured the high accuracy of measurement of this technique. Considering these facts**,** Escorihuela et al., [31] Suggested a 4-point-probe Electrochemical Impedance Spectroscopy (EIS) technique that determined PEM impedance over an extensive range of frequencies and thereby assessed the Proton conductivity (σ) of polymer electrolyte membrane successfully. A thin layer of membrane and Pt-plated electrodes are supported over a Teflon cell and the two parallel platinum electrodes are set on one facet of the membrane to assess in-plane proton conductivity. The measurement can be conducted by placing the cell in distilled deionized water or the cell can be positioned in a thermo-managed humid chamber at less than 100 % relative humidity (RH) [59,60]. The general expression to assess the in-plane proton conductivity is shown in Eq. (4).

$$\sigma = \mathrm{d/tlR} \tag{4}$$

Here, d represents the space separating the two electrodes, t is the thickness, l is the breadth, and R denotes the resistance of the membrane. A thin layer of membrane has been inserted between the platinum electrodes to assess the through-plane proton conductivity. The resistance is calculated from the semicircle intercept on the real axis of impedance at the higher frequency region of the Nyquist plot as shown by Al-Madani et al. [61]. The general expression to assess the Through-plane proton conductivity is provided in Eq. (5).

$$\sigma = t/AR \tag{5}$$

Where t is the membrane thickness, A is the effective area of the electrode and R is the resistance of the membrane.

Membrane thickness plays a crucial role in determining the overall performance of electrolyte membranes, particularly with respect to ionic conductivity and fuel cell efficiency. A decrease in membrane thickness generally leads to a reduction in ionic transport resistance, thereby enhancing the overall conductivity of the membrane [62]. Thinner membranes facilitate faster ion migration due to the shortened diffusion pathway, which is particularly beneficial for improving current density and power output in electrochemical devices. However, while reduced thickness may enhance conductivity, it can also lead to increased fuel crossover and decreased mechanical stability, potentially compromising the membrane's durability and selectivity [63]. Conversely, thicker membranes may offer improved mechanical integrity and reduced crossover, but at the cost of higher ohmic resistance and lower conductivity. Therefore, an optimal balance must be achieved between membrane thickness, ionic conductivity, and structural robustness. In fact, EIS has come up as an effective strategy to determine both the through-plane and in-plane proton conductivity of PEM over an extensive frequency range. Electrochemical Impedance Spectroscopy (EIS) has been widely regarded as a reliable method for evaluating the proton conductivity of polymer electrolyte membranes (PEMs), providing precise insights into ion transport properties. In the development of advanced fuel cell membranes, the blending of polymers and the incorporation of branched architectures have been regarded as effective strategies to enhance membrane performance. Through polymer blending, complementary properties of different polymers can be combined, allowing for the optimization of ionic conductivity, mechanical strength, thermal stability, and chemical resistance [64]. For instance, one polymer may provide high ionic conductivity, while the other contributes to structural integrity or improved film-forming capabilities. By carefully selecting and combining such polymers, membranes with synergistic properties can be fabricated. Similarly, the introduction of branching into polymer structures has been utilized to modify the morphology and ion transport behavior of the membranes. Branched polymers can provide a more interconnected ionic domain, facilitating more efficient ion conduction pathways [65]. Additionally, branching may lead to reduced crystallinity and enhanced segmental motion within the polymer matrix, thereby improving ion mobility. The phase separation behavior, water uptake, and dimensional stability can also be favorably influenced through controlled branching.

An alternating current (AC) perturbation was applied across the membrane, and the impedance spectrum was analyzed over multiple frequencies, enabling the differentiation between bulk conductivity, interfacial resistances, and electrode-related impedance [66]. The non-destructive nature of EIS allowed for long-term monitoring of membrane performance without compromising its integrity, making it ideal for studies conducted under dynamic conditions [67]. Consistent agreement with other techniques, such as four-probe measurements and proton NMR, was reported, further validating EIS as an accurate tool for assessing proton transport [68]. Additionally, the high-frequency region of the impedance spectrum enabled the isolation of proton conduction from other resistive or capacitive effects, enhancing measurement precision under varying hydration and temperature conditions [69]. Therefore, EIS has remained a preferred technique for investigating the complex conductive behavior of PEMs in fuel cells.

The membrane is dipped in 1.0-M H_2SO_4 solution for two days after washing it with water and then washed very well with deionized water overnight to eliminate the remaining acid. Subsequently investigated the proton conductivity within the hydrated membrane state [70,71]. The idea of impedance was taken from Ohm's law to circuits, that worked within the sinusoidal steady state. Basically, a small amplitude alternating current signal is imposed to take the impedance measurements at various frequencies. The result obtained is an alternating current signal, that may be resolved as a sum of sinusoidal features within the frequency region [59]. An EIS experimental setup includes a potentiostat/galvanostat, an electrochemical cell, and the frequency response analyzer. The sine wave was imposed to analyze the response using the frequency response analyzer and thereby determined the impedance of the membrane, as shown by Müller et al. [69] in their study. Impedance data is plotted to the Nyquist plots at different temperatures using equivalent circuits.

Like resistance, impedance (also called complex electrical resistance) is an assessment of the ability of a circuit to resist the flow of electrical current without limitations of ohm's law, which measure the barriers composed of various resisters and capacitors of a circuit. The AC current signal contains the excitation frequency and its harmonics. Since impedance, Z changes with applied frequency ϖ, Z must be measured as a function of frequency and resistance of sample evaluated. Therefore, Impedance Spectroscopy measures the impedance of a membrane to an applied voltage (Eq. (6)) [72].

$$Z(\varpi)=(E(\varpi))/(I\ (\varpi)) \tag{6}$$

Impedance takes into account the phase difference between the input voltage and output current and is thus defined as a complex resistance, which consists of real impedance Z' and imaginary impedance Z''. Real impedance is due to pure resistance R_o of homogeneous polyelectrolyte membrane and the resistance exerted from the migration of charges at the interface adjoining membrane and electrodes connected parallelly with a capacitor is R_p. The imaginary part comprises the constant phase element, mathematically given by the complex quantity, $Z_{CPE} = 1/[Y_o(j\varpi)^n]$ as shown by León et al. [72]; Bertok et al. [73]. When n equals 1, the constant phase element is an ideal capacitor and the Y_0 is its capacitance. In other cases, the constant phase element deviates from a capacitor and the Y_0 does not mean the capacitance.

The dc-conductivity is determined by plotting the $-Z''$ versus Z' into the Nyquist diagrams. The results obtained are expressed in terms of the equivalent circuits including the resistance R_o in series with the charge transfer resistance R_p, in parallel with a capacitor (C). Putting data, we have semicircles intersecting the abscissa axis at $Z' = R_o$, where the unreal part shows zero impedance with phase angle $\phi = o$ due to the intersection with the abscissa axis [74]. Then the dc-conductivity can be given by Eq.

$$\sigma_{dc} = \frac{LZ'}{S\left[(Z')^2 + (Z'')^2\right]} \tag{7}$$

where L is the thickness of the sample, and S is the effective area of the sample inserted in between the two electrodes during the measurement. On the other hand, the polarization relaxation processes in polymer electrolyte membranes are explained by the relaxation times extensively distributed over the semicircle. Therefore, the equivalent circuit should be composed of a resistance R_o in series with a congregation of N circuits. Each circuit comprises a polarization resistance R_i parallelly with the constant phase element (CPE) of admittance (in reverse of CPE of impedance) $Y^* = Y_o(i\varpi ɽ)^n\ (o \leq n \leq 1)$. The capacitance is well explained by the constant phase element (CPE) as indicated by the equation, $CPE = 1(j\omega C)^n$ where angular frequency $\omega = 2\pi f$ and the power n varies from zero to one [57]. However, the equation that represents the complex impedance of such circuit is –

$$Z^*(\varpi) = R_o + R_p/[1 + Y_o(\varpi ɽ_o)^n j^n] \tag{8}$$

Where $j = (-1)^{1/2}$ and $ɽ_o$ is a characteristic relaxation time [75,76]. Hence the real and imaginary components of the complex impedance of the equivalent circuit are used to determine the angular frequency of the electric field at $ɽ_o = 1/\varpi = R_oC$, the modulus of the complex conductivity, and phase angle. It is noticed from the Nyquist plot that at the ranges where angular frequencies ϖ tend to ∞ and o, the real part of impedance Z' tends to R_o and $R_o + R_1$, respectively, whereas, the imaginary part of impedance Z'' in both cases tends to zero. The semicircle of the Nyquist plot intersects the abscissa axis at $Z' = R_o$ at a higher frequency region, as shown by Cabello et al. [75].

The dc-conductivity can also be obtained from the Bode diagram to obtain R_0. Here the modulus of the complex conductivity versus the frequency ϖ is plotted. The complex conductivity increases reaching a plateau with frequency increases, whereas the phase angle $\phi = \tan^{-1}(Z''/Z')$ reaches a maximum (or tends to zero). When $\rightarrow\sigma_0$ and ϕ equals to zero, the proton conductivity of the membrane can be determined. The variation of the conductivity with the frequency for the PBI-Na [COSANE] composite membrane was shown by Fuentes et al. [77]. In the area where the conductivity presents a plateau, $\phi \rightarrow 0$ or a maximum, $Z'' = 0$, which represent the conductivity in the bulk phase of the samples, σ_{dc} and reflect the long-range proton transport. These are indirect methods to determine the value of the dc-conductivity, since the methods use the real and imaginary impedance elements of the sample membrane.

The proton conductivity in polymer electrolyte membranes (PEMs) is largely influenced by the intrinsic properties of the membrane material, as well as by the type and nature of fillers incorporated to enhance performance. Fillers, along with their crosslinking agents, play a significant role in modifying the proton conduction pathways, improving water retention, and stabilizing the membrane structure. Fillers modify the ionic conductivity by either facilitating proton transport through Grotthuss-type mechanisms or by enhancing vehicular proton conduction, depending on their structural and chemical properties [49,78]. The impact of these fillers on proton conductivity has been analyzed in subsequent sections, where different types of fillers and their crosslinking mechanisms are thoroughly discussed.

4. Filler and crosslinking agents of fuel cell membranes

4.1. Fillers of fuel cell membranes

Nanostructured materials with excessive surface area produce excessive opportunities for chemical and electrical reactions. The involvement of various constituents with their diverse physical, structural and chemical characteristics may bring about new materials, referred to as composites. Generally, composites encompass two phases, filler materials (dispersed segment) and a matrix (continuous segment). The filler segment is normally employed in the matrix segment to produce the composite membrane [79]. Different types of fillers such as inorganic oxides -MO_2, (where M is Si, Ti, Zr) carbonaceous nanofillers, metal-organic frameworks, phosphonic acid (H_3PO_3), heteropoly acids and ionic liquids fillers are added to the polymer matrix, which facilitates the proton transport ability through the membrane [80]. Different techniques were proposed to overcome some drawbacks such as agglomeration, absorption of more water with increasing the degree of functionating in the membrane and the hygroscopicity of the fillers, etc., which decrease the mechanical, dimensional, and physicochemical properties of the membrane. The addition of exact quantities of desired nano-particles, different cross-linking processes and/or blending with other polymer material, etc. are the most used procedures for the preparation of nanocomposite membranes to render expected physicochemical properties to the membrane [31,41].

The incorporation of different fillers can significantly influence the dominant proton conduction mechanism, thereby affecting membrane performance. Fillers modify the physicochemical properties of the membrane, such as water retention, ion exchange capacity, and microstructure, which in turn impact the proton conduction pathways.

Hydrophilic fillers, such as sulfonated silica or phosphonated TiO_2, promote water retention, favoring the vehicular mechanism under humid conditions [15,81]. In contrast, fillers like phosphotungstic acid or metal-organic frameworks (e.g., UiO-66-SO_3H) can facilitate the formation of hydrogen-bonded networks [82], supporting the Grotthuss mechanism, especially under low humidity or elevated temperature.

4.1.1. *Metal oxides as fillers*

Metal oxides as inorganic fillers render some excellent properties to polymer electrolyte membranes as explained by Sarirchi et al. [83]. The incorporation of hygroscopic oxides (e. g. SiO_2, TiO_2, ZrO_2) with high surface area introduces surface hydroxyl groups in the membranes that increase the water absorption and reserve of the membranes. Therefore, greater proton conductivity was achieved at higher temperatures and lower humidity conditions. The particle shape of metal oxides influences the properties of membranes, which are operated at temperatures above 100 °C [84]. The inclusion of higher loading of spherical particles with higher surface area resulted in a reduction in water uptake relative to the recast Nafion. However, in the case of nanotube metal oxides, the existing water molecules within the nanotube increase the water uptake with respect to the recast Nafion. The addition of metal oxide nanofillers increases the amorphous phase in the matrix, which assisted the proton transport in the polymer electrolyte membrane. Again, mesoporous materials carry great prospects as filler materials, since the minute pores (of size 8–10 nm) of these particles assist in reserving more water molecules and their higher surface area facilitates to attach functional groups, which improved proton transport [85].

However, all these composite membranes degraded significantly as the temperature is highly increased and displayed a decrease in polarization. The degradation of composite membranes in fuel cells was driven by chemical, mechanical, and thermal mechanisms, compromising long-term performance. Chemically, reactive oxygen species (ROS) such as hydroxyl (OH•) and hydroperoxyl (HO_2•) radicals, which originated from hydrogen peroxide (H_2O_2) byproducts, were found to degrade the membrane [86]. These radicals attacked sulfonic acid side chains, leading to ionic conductivity loss and membrane thinning. The presence of metal ions further accelerated radical formation, exacerbating chemical degradation [87]. Mechanical degradation was occurred through cyclic swelling and shrinking caused by hydration changes, which resulted in microcracks and stress accumulation at polymer-filler interfaces, especially when filler dispersion was poor [88]. Although the incorporation of silica and titania fillers improved mechanical stability by reducing swelling, insufficient polymer-filler interaction led to interfacial voids and microcracking [89]. Long-term stability has been evaluated through continuous performance testing over extended durations. For instance, PVDF/graphene oxide (GO) composite membranes have been reported to maintain more than 90 % of their original water flux after 60 days of continuous filtration, indicating strong antifouling and structural stability [90]. Additionally, KOH doped polybenzimidazole have shown retention of ion exchange capacity after 1000 h of immersion in alkaline environments, suggesting high chemical durability [91]. Furthermore, membranes embedded with nanomaterials such as zeolitic imidazolate framework-9 (ZIF-9) have demonstrated high mechanical integrity and operational stability [92].

Thermal degradation, including desulfonation, became significant at temperatures exceeding 140 °C, reducing proton conductivity and impairing membrane integrity [93]. While thermally stable fillers such as TiO_2 mitigated thermal degradation, organic fillers like MOFs were more prone to decomposition at higher temperatures. Crosslinking and functionalized fillers improved stability, but further optimization remained necessary for long-term durability. A major drawback of the hybridization of inorganic additives with the polymeric matrix is that the dispersion of inorganic solid additives produces heterogeneous composite membranes containing larger conglomerates of inorganic materials. To enhance the performance of PEMs in fuel cell applications, additives are crucial for boosting their mechanical strength and electrical conductivity. In proton exchange membranes (PEMs) used for fuel cell applications, the term "electrical properties" primarily refers to the membrane's ability to conduct protons (H^+ ions) effectively from the anode to the cathode. The efficiency of this proton transport directly influences the overall performance and power output of the fuel cell [79]. However, the intrinsic proton conductivity of base polymer materials such as Nafion or polybenzimidazole (PBI) can be limited, especially under low-humidity or high-temperature conditions. To address this, various additives are incorporated into the membrane matrix to improve its electrical performance. The improvement in electrical properties by additives involves several mechanisms. One common strategy is the introduction of inorganic additives such as silica (SiO_2), titanium dioxide (TiO_2), or zirconium phosphate (ZrP), which enhance water retention within the membrane. Since proton conductivity in many PEMs relies on the presence of water molecules to form hydrogen-bonded networks necessary for the Grotthuss mechanism of proton hopping, maintaining hydration is critical, particularly at elevated temperatures. By retaining water more effectively, these additives help sustain high proton conductivity even in dry environments. Other additives, such as heteropoly acids (e.g., phosphotungstic acid) or ionic liquids, can directly contribute to proton conduction by introducing additional proton carriers or forming alternative proton-conducting networks [49]. For instance, in phosphoric-acid-doped PBI membranes, the acid itself forms a hydrogen-bonded structure that supports anhydrous proton conduction, making these membranes suitable for high-temperature operation. Moreover, functionalized nanomaterials such as sulfonated graphene oxide or carbon nanotubes can provide both proton-conducting functional groups and enhanced connectivity within the polymer matrix, creating more efficient pathways for proton transport [94]. These materials can also increase the membrane's ionic exchange capacity, further boosting conductivity. Uniform distribution of inorganic nanoparticles in the Polymeric Membrane has been recognized as a substantial practice to lessen the fuel passing through the membrane [31, 41]. The proton migration way in Nafion-Metal Oxide nanoparticles composite membrane is shown in Fig. 3.

4.1.2. *Silica based filler*

The silica surface contains numerous hydrophilic –SiOH groups that enhance the water retention capability at high temperatures [95]. But at elevated temperatures, the water in the membrane starts evaporation, which causes a contraction in the water pathways of the membrane and provides low water content for proton transfer, resulting in a decrease in proton transport [96]. The low-priced SiO_2 was usually synthesized in situ from alkoxide tetraethyl orthosilicate (TEOS) via a sol-gel process. The synthesized silica powders possessed a 3D structure and desired porous and hygroscopic properties. The ordered nanophase-separation

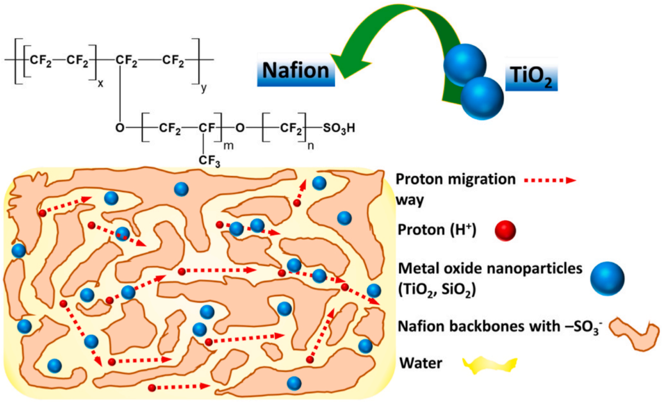

Fig. 3. The proton migration pathway in the nafion-metal oxide nanoparticles composite membrane [51].

and well-dispersion maintenance were also important for better water uptake, which was shown by Xu et al. [97] simply by swelling the Nafions with SiO_2. The introduction of Silica reduced the swelling degree with a higher water uptake relative to the pristine membrane. The SiO_2 obtained from TEOS hydrolysis was self-anchored inside the $–SO_3H$ ionic cluster and –OH groups on the silica surface were further sulfonated inherently by $–SO_3H$ groups. However, to improve the poor miscibility of blend hybrid membranes, Di et al. [98] fixed the lower content of superior proton conductive Nafion particles into largely porous SiO_2 networks and then added them to the base membrane. The additive Nafion-SiO_2exhibitedbetter flexibility and higher tensile strength than pristine SPEEK membrane at the same measurement condition. Table 1 shows electrochemical and mechanical properties of Polymer Electrolyte Membranes with Silica based Fillers.

The proton transfer mechanisms for silica-based fillers are shown in Table 2. The sulfonated silica/Nafion composite primarily employs the Grotthuss mechanism, enhanced by additional sulfonic acid groups that promote proton hopping, particularly under high humidity [109]. In contrast, phosphonated silica/Nafion membranes demonstrate superior conductivity in low-humidity conditions due to stable proton dissociation from phosphonic acid groups [110]. Polydopamine-modified silica supports both Grotthuss and vehicular mechanisms through catechol groups, ensuring stable proton conduction even in dry environments [111]. Phosphotungstic acid-doped silica forms continuous proton-conducting channels, providing high conductivity across various temperatures. Additionally, ionic liquid-functionalized silica enhances proton migration via the vehicular mechanism, maintaining stable conductivity under low-humidity conditions [112].

Functionalization of the silica particles may reduce or solve the problems of severe aggregation due to excessive filler contents, which reduces the active surface area of the fillers and causes a decrease in the water uptake of the hybrid membrane. Du et al. [117] reported that the better dispersion of sulfonated SiO_2 was due to the decreased number of silanol groups on SiO_2 particles which restricted agglomeration in the membrane, thereby ionic clusters would be obtained which resulted in more dense hydrophilic cluster networks in the hydrated state. The proton conducting pathways containing inorganic hygroscopic materials held more water strongly resulting in increased proton conductivity and also leading to improved thermal and mechanical properties. Boutsika et al. [118] demonstrated the high diffusion coefficients for many hours at temperatures as high as 130 °C without any external humidification. $–SO_3H$ groups on the particles increased the acidity of the sulfonated SiO_2 nanofillers and resulted in higher ion exchange capacities of the nanocomposite membrane. The water molecules and the acid sites on the silica surface strongly interact to enhance the water uptake and it improved proton conductivity in all relative humidity conditions of the nanocomposite membranes. Oh et al. [119] demonstrated that at 80^{0}Cand under 25 % relative humidity, the sulfonated silica-Nafion(1 wt%) hybrid membrane showed a greater maximum power density (454 mw cm^{-2}) and current density (2062 mA cm^{-2}) relative to the pure Nafion. Kim et al. [120] added that the hydrophilic functionalized silica ($FSiO_2$) particles filled the pores in the membrane which rendered better resistance against permeation of H_2 gas and decreased significantly the hydrophobic cluster size of the sulfonated fluorinated block copolymer.

The interfacial hydrogen bonding between the polar groups in sulfonated fluorinated block copolymer and functionated silica particles effectively increased the thermal and mechanical stabilities of the composite membrane. Similar results were obtained by the phosphonation of silica particles as reported by Sharma et al. [107], which was employed in sulfonated poly ether sulfone (SPES). The additional functional groups of SiO_2 and POH by incorporating phosphosilicate into SPEEK membranes enhanced water absorption to provide pathways for proton transfer and increased the conductivity of composite membrane at high temperature, as shown by Tung & Hwang [121]. In addition, the phosphonation of both, the filler and base polymer matrix significantly enhances the membrane performance for HTPEMFCs as reported by Elumalai [122]. They found that the mesoporous silica (SBA-15) with a higher surface area and larger volume of ordered mesopores contain active sites to be functionalized by acid groups, providing dynamic H-bonded networks when incorporated into Nafion and facilitated anhydrous proton transfer above 100 °C. This higher temperature tolerance of the composite membrane was attributed to the greater bond energy of the C–P bond compared with the C–S bond as in sulfonation. Recently, amino-functionalized hollow mesoporous SiO_2 was utilized as an excellent filler due to its superior biocompatibility along with its enhanced conductivity (11 times more than pure Nafion at 80 °C and low RH), but having the major drawback of poor durability when operated at elevated temperatures, as investigated by Zhang et al. [123].

The incorporation of phosphotungstic acid (PWA) impregnated mesoporous SiO_2 remarkably enhanced the stability at 200^{O}C of PES-

Table 1

Electrochemical and Mechanical properties of PEMs with Silica based Fillers.

Filler	Polymer	Operating condition (Temperature°C), Relative humidity, RH %	Proton conductivity (S/cm)	Power Density (mW/cm^2)	Mechanical strength (MPa)	Ref.
3 % silica	Nafion	110 °C, 60 %	0.033	113	18	[97]
Sulfonated silica	Nafion	110 °C, 60 %	0.07	140	–	[96]
Sulfonated silica	SSA- Nafion (1 wt% SSA)	80 °C, 100 %	0.2301	454	18.4	[99]
14.3 wt% SiO_2-PWA	Recast Nafion	110 °C, 70	0.0267	540 mA/cm^2	–	[100]
15 wt% SiO_2 (polydopamine modified silica nanoparticles)	SPEEK	120 °C, anhydrous	0.00452	–	–	[101]
SiO_2 glass powders combined with small portion of Nafion	SPEEK	80 °C, 90 %	0.018	–	–	[98]
20 wt % meso-SiO_2/HPW	SPEEK	120 °C, 30 %	0.0019	–	–	[102]
10 wt% SiO_2 with 5 wt% SiWA	SPEEK	–	0.0696	–	–	[103]
5 wt% SiO_2, acid doping level 10	PBI	180 °C and 0 %	0.1027	240	–	[104]
Mesoporous silica (MCM-41, SBA-15)	5 wt % PA-doped ABPBI	150 °C	0.0674	–	–	[105]
10 wt% MCM-41, acid doping level 2–9	PBI	150 °C	–	310	45.36	[106]
Phosphonated silica	SPES	–	5.42	–		[107]
8.7 % silica	SSt- AGE	70 °C, 75 %	0.421	70		[108]

Table: 2
Comparison of silica-based fillers for proton transfer mechanism in composite membranes.

Filler Type	Functional Groups/ Modification	Dominant Proton Transfer Mechanism	Composite Membrane	Performance Characteristics	References
Sulfonated silica (SiO_2–SO_3H)	Sulfonic acid (-SO_3H) groups	Grotthuss mechanism (proton hopping via hydrogen bonds)	Sulfonated SiO_2/ Nafion	High proton conductivity under high humidity due to increased proton hopping sites	[113]
Phosphonated silica (SiO_2-PO_3H_2)	Phosphonic acid (-PO_3H_2) groups	Grotthuss mechanism, enhanced at low humidity	Phosphonated SiO_2/Nafion	Improved conductivity under low-humidity conditions, maintaining proton dissociation	[114]
Polydopamine-modified silica (SiO_2-PDA)	Catechol groups from polydopamine	Combination of Grotthuss and vehicular mechanisms	SiO_2-PDA/Nafion	Enhanced water retention and stable proton conduction in dry conditions	[115]
Phosphotungstic acid-doped silica (SiO_2-PWA)	Heteropoly acids (PWA)	Superprotonic conductivity via continuous proton-conducting channels	SiO_2-PWA/Nafion	High conductivity across a wide temperature range, improved thermal stability	[116]
Ionic liquid-functionalized silica (ILS)	Ionic liquids (ILs)	Vehicular mechanism (proton migration via ion pairs)	ILS/Nafion	Effective in low-humidity conditions, supporting proton migration through electrostatic interactions	[105]

PVP polymer matrix without external humidification. Li et al. [124] exhibited in their investigation that the PWA was immobilized in Silica gel as well as in sulfonated Nafion because of their crosslinking with thermally durable silica frameworks in the composite; which rendered improved thermal stability and water uptake, besides reserving its intrinsic property. Chia et al. [103] in their experiments with 10 wt% of SiO_2 and 5 wt% of silicotungstic acid (SiWA) into SPEEK matrix, showed electrochemical stability of the membrane. Li et al. [125] demonstrated that ionic liquids which is conductive at higher temperatures and zero humidity condition were used to form highly ion conductive channels in the membrane matrix. The thermal stability of the –SO_3H groups in the membrane was improved upon the addition of SiO_2 particles, which not only decreased the loss of ionic liquids but also mitigated the problem of excessive swelling. Kuo & Lin [106] noticed that the pore size of mesoporous silica particles remarkably influences the proton transport of hybrid membranes, as it is very much comparable to absorb and retain phosphoric acid (PA) level in the polybenzimidazole (PBI)-based hybrid membranes.

The higher loadings of mesoporous SiO_2(MCM-41 and SBA- 15) additives in the composite membrane increased the phosphoric acid doping level as well as the number of H-bonding between phosphoric acid and the –OH groups of the fillers, which prevented acid leakage from the membranes. A similar result was reported when Kurdakova et al. [126] utilized mesoporous SiO_2 (MCM-4)which increased the thermal stability of the Polybenzimidazole-based PEM and rendered twenty percent higher maximum power densities compared with pristine PBI-5N PEMs. Subsequently, Seo et al. [127] introduced an Al-substituted hexagonally ordered mesoporous silica channel into a poly(2,2′-m-(phenylene)-5,5′-bibenzimidazole) membrane, which provided not only increased proton conductivity but also rendered stable operation under the non-humid condition at 150 °C for 600 h. These channel scans retain more phosphoric acid resulting in increased proton transport and good MEA performance.

An interesting technique was explored by Chesnokova et al. [108] to increase the mechanical strength and chemical resistance of composite membranes by combining the base polymer matrix with one or more organic materials that possess plasticizing properties. Afterward, the composite was blended with silica nanoparticle filler at a higher operating temperature. It was found that the introduction of unsaturated Glycidyl Ethers with TEOS into the sulfonated hybrid membrane appreciably increases the mechanical strength and thermal strength as well. It was also observed that TEOS can be easily incorporated into the membrane structure when polyvinyl alcohol (PVA) was additionally incorporated into the membrane. The presence of the modifiable –OH group in PVA induces remarkable improvements in thermal and mechanical strength because of its effective crosslinking with aldehydes, as shown by Sahin [128]. A similar result was observed when Therese et al. [129], incorporated poly (Amide-Imide) into the sulphonated poly(ether ketone) to enhance the mechanical potency and chemical resilience at elevated operating temperatures. Afterward the composite was blended with hydrophilic sulfonated silica (s-SiO_2) nanofillers which increases the amorphous phase, because the filler and the matrix very nicely interacted interracially, as the hygroscopic nature of sulfonated SiO_2 increased the homogeneous distribution in the matrix. The progress in proton conductivity of silica-based fillers into various polymeric matrices is shown in Fig. 4.

4.1.3. TiO_2 based fillers

TiO_2 has drawn attention to be utilized as a filler material in fuel cell membranes because of its low cost and availability in nature. Similar modifications of SiO_2 particles can be applied to TiO_2. The higher surface area of titania facilitates the improvement of the electrochemical performance of a composite membrane. In addition, due to its inherent stability, nonflammability, poor solubility, high resistance to corrosion, and nonhazardous nature, it is suitable to be used for high operating temperatures [131]. The naturally occurring polymorphs are rutile, anatase, and brookite. It was determined by Solanki et al. [132] through the thermal stability analyses of titanium oxide-filled sulfonated polyvinyl alcohol membranes that, increasing TiO_2 to a certain extent (up to 20 %) enhanced the thermal stability appreciably, which increased the membrane crystallinity, thereby restrains the motion of the chain portion of the polymer. In addition, the membrane absorbs more water due to the hygroscopic properties of TiO_2; which induces more H-bondage between the water molecules and facilitates in higher proton mobility in polymeric matrices. Table 3 shows the electrochemical and mechanical properties of polymer electrolyte membranes with titania-based fillers.

The proton transfer mechanisms in composite membranes containing TiO_2-based fillers are primarily influenced by the functional groups attached to the TiO_2 particles. Fillers functionalized with amino acids promote proton hopping through carboxyl and amine groups, enhancing water retention and facilitating the Grotthuss mechanism [142]. Similarly, Polyacrylamide (PAMPS)-grafted TiO_2 introduces sulfonic acid groups, improving proton conductivity in low-humidity conditions [143]. Polystyrene sulfonic acid (PSSA)-*g*-TiO_2 membranes exhibit high conductivity through a dense distribution of sulfonic acid groups, effectively retaining water [144]. The rGONR@TiO_2 fillers utilize both Grotthuss and vehicular mechanisms, leveraging the catalytic properties of TiO_2 and the water retention of reduced graphene oxide nanoribbons [145]. Sulfonated TiO_2 and sulphophenylated TiO_2 enhance proton transfer via the Grotthuss mechanism, increasing proton-donating sites and offering thermal stability. The sGO-SiO_2 composite further combines the benefits of graphene oxide and silica, facilitating proton transfer even under low-humidity conditions. The comparison of TiO_2-based fillers for proton transfer mechanisms in composite membranes is shown in Table 4.

Saccà et al. [150] reported that the functionalized titanium oxide in composite membranes exhibited enhanced mechanical property, and

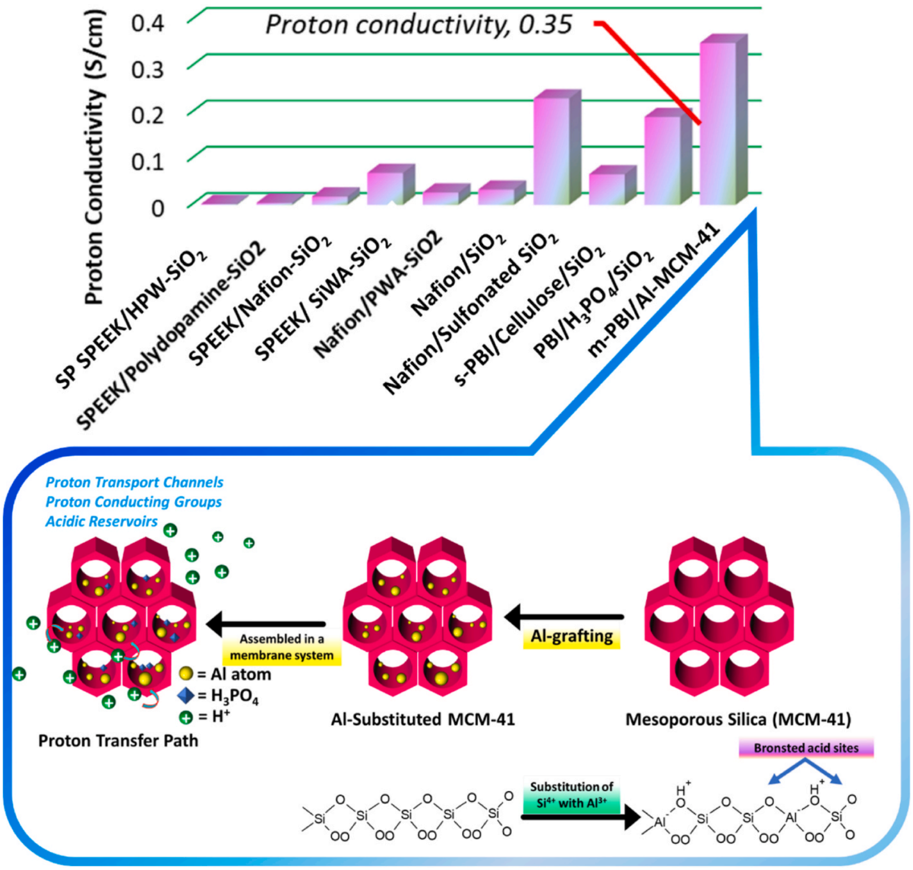

Fig. 4. The advancement of proton conductivity using SiO_2-based fillers in various polymeric membranes [97–103,130,119,127].

Table 3
Comparative study of Electrochemical and Mechanical properties of Polymer Electrolyte Membranes with Titania based Fillers.

Filler	Polymer	Operating condition (Temperature °C), Relative humidity, RH%	Proton conductivity (S/cm)	Power Density (mW/cm^2)	Mechanical strength (MPa)	Ref.
15 wt% amino acid functionalized TiO_2	SPEEK	20 °C, 100 %	0.00737	–	–	[133]
10 wt% organic functionalized TiO_2 (nano-particles)	SPEEK	100 °C, 100 %	0.04	–	–	[134]
7.5 wt% PAMPS-g TiO_2	SPEEK	80 °C	0.16	283	49.5	[135]
7.5 wt% PSSA-g TiO_2	SPEEK	80 °C	0.146	245	48	[135]
1 wt% rGONR@ TiO_2	SPEEK	100 °C	1.79	–	64.46	[136]
0.75 wt % $sTiO_2$	B-SPAES/5 % PES	80 °C, 100 %	0.1734	620	45.2	[137]
2 wt% TiO_2	PBI	150 °C	0.043	450	–	[138]
5 wt% TiO_2,	PA-doped PBI	180 °C	~0.08	–	–	[139]
2 wt% TiO_2, Acid doping level 15.3	PBI	150 °C, 10 %	0.13	800	–	[140]
2 wt% sulphophenylated TiO_2, acid doping level 12.1	PBI	150 °C	0.096	621	–	[141]

improved proton transport i.e., better electrochemical performance compared to an unfilled Nafion as observed in an investigation of the Nafion matrix modified by a commercially treated anatase titania. The cross-linking of the titanium dioxide particles with the Nafion chains increases the glass transition temperature (Tg) at a lower relative humidity level for composite membranes. In practice, the proton conductivity of the composite Nafion-TNT (tubular titania) membranes was higher than that of the pure membrane in all humidity ranges. Haragirimana et al. [137] studied the proton conductivity of sulfonated polymer blend membranes when sulfonated inorganic fillers were incorporated into them. In recent years, notable enhancements in the performance of hydrogen fuel cells have been achieved through the incorporation of inorganic fillers into polymer matrices, particularly within polymer electrolyte membranes (PEMs). However, the interfacial compatibility between these components has been identified as a critical limitation. Poor interfacial adhesion has been associated with phase separation, diminished mechanical integrity, and reduced proton conductivity under fuel cell operating conditions [151]. To mitigate these issues, various strategies have been employed. Surface functionalization of inorganic fillers has been widely implemented, wherein groups such as sulfonic acid ($-SO_3H$), phosphonic acid ($-PO_3H_2$), and amine ($-NH_2$) have been introduced onto the filler surfaces of SiO_2, TiO_2, ZrO_2, and

Table 4
Comparison of TiO_2-Based fillers for proton transfer mechanisms in composite membranes.

Filler Type	Functional Groups/ Modification	Dominant Proton Transfer Mechanism	Composite Membrane	Performance Characteristics	References
Amino acid functionalized TiO_2	Carboxyl (-COOH) and amine (-NH_2) groups	Grotthuss mechanism (proton hopping via hydrogen bonding)	Amino acid-TiO_2/ SPEEK	Enhanced water retention, stable proton conductivity at various humidity levels	[146]
PAMPS-g-TiO_2 (Poly(2-acrylamido-2-methyl-1-propanesulfonic acid))	Sulfonic acid (-SO_3H) groups	Grotthuss mechanism through sulfonic acid sites	PAMPS-TiO_2/SPEEK	High proton conductivity at low humidity, improved ion channel formation	[147]
PSSA-g-TiO_2 (polystyrene sulfonic acid)	Sulfonic acid (-SO_3H) groups	Grotthuss mechanism with continuous proton hopping	PSSA-TiO_2/SPEEK	Increased structural integrity and water retention, efficient conduction across humidity levels	[147]
rGONR@TiO_2 (reduced graphene oxide nanoribbons on TiO_2)	Sulfonated nanoribbons	Hybrid of Grotthuss and vehicular mechanisms	rGONR-TiO_2/SPEEK	Enhanced catalytic activity, stable conductivity with mixed mechanisms	[145]
Sulfonated TiO_2 (sTiO_2)	Sulfonic acid (-SO_3H) groups	Grotthuss mechanism through sulfonic groups and water molecules	sTiO_2/SPEEK	High proton conductivity at elevated temperatures due to structural water retention	[148]
Sulphophenylated TiO_2	Sulphophenyl (-$C_6H_4SO_3H$) groups	Grotthuss mechanism with high proton dissociation	Sulphophenylated TiO_2/SPEEK	Improved conductivity and thermal stability	[148]
sGO-SiO_2 (sulfonated graphene oxide functionalized silica)	Sulfonic acid (-SO_3H) groups	Dual Grotthuss and vehicular mechanisms	sGO-SiO_2/SPEEK	Enhanced water retention and conductivity in low-humidity conditions	[149]

graphene oxide (GO), thereby enhancing compatibility with sulfonated polymer matrices [152]. Consequently, improved filler dispersion and stronger interfacial interactions have been observed, contributing to mechanical reinforcement and enhanced ion transport. Additionally, it has been demonstrated that the intrinsic properties of the polymer matrix play a significant role in interfacial dynamics. Sulfonated polymers such as SPEEK and SPSU, despite their chemical robustness, have exhibited issues related to hydrophilic–hydrophobic phase separation [153]. To address this, amphiphilic and block copolymers have been synthesized, facilitating more uniform filler distribution and promoting continuous proton conduction pathways [154]. The efficacy of such approaches has been validated through morphological and electrochemical characterization techniques, including TEM, AFM, and EIS, which have confirmed the formation of well-integrated interfaces with reduced resistance and increased conductivity. Furthermore, proton-conducting interfaces have been proposed, wherein active fillers form conduction bridges rather than passive reinforcement phases, as shown with heteropoly acids and functionalized silica [41]. Nonetheless, interfacial degradation under thermal and chemical stress remains a concern, and efforts are ongoing to develop covalently bonded and dynamic cross-linked interfaces to enhance long-term stability. The proton conductivity was found to reduce as a result of dilution of free –SO_3H groups in sulfonated poly arylene ether sulfone/poly ether sulfone (SPAES/PES) blend PEM. The decrease in free –SO_3H groups was compensated by the addition of sulfonated titanium oxide fillers, which rendered better hydrophilicity to the blend system and demonstrated the improved proton conductivity (223.2 mS cm^{-1}) when the SPAES/PES/sTiO_2 membrane is fully hydrated.

In PEMFCs operated at higher temperatures (HTPEMFC), Phosphoric acid (H_3PO_4) is employed in lieu of water to overcome its short extent of operating temperature. Polybenzimidazole (PBI) possesses some necessary properties such as improved thermal stability and mechanical potency, lower fuel permeability, and barrier to chemical degradation, though having relatively low proton conductivity for use in HT-PEMFC. Usually, the best practice to increase the proton conductivity is the application of functionalized metal oxide fillers as suggested by Sharma et al. [87]; Haragirimana et al. [137]; Bonis et al. [134]; Wu et al. [133]. A nanocomposite membrane with functionalized $TiO_2$was developed by Lee et al. [141], which helped in improving the proton transport of the membrane by preventing agglomeration. The acidic sites of sulfo-phenylated titania strongly interacted with the basic groups of the PBI matrix. Then the membranes were doped with H_3PO_4 for HT-PEMFC application. It was observed that the PEMs were not only insoluble but also kept their shape in various testes owing to their higher degree of crosslinking and more homogenous structure compared with thermally cured pure PBI membrane.

Roy et al. [136] reported an excellent observation in their review that, wrapping the nanofillers TiO_2 with reduced graphene oxides hydrophobic nanoribbons (-rGONR) may prevent both the formation of $(-SO_3^-)_n$ ionic clusters and/or agglomeration of nanofillers in the matrix. It was noticed that excessive incorporation of metal oxides nanoparticles reduced the dimensional and mechanical stability of Polymer Electrolyte Membranes [97,155]. The strong hydrophilic property of filler nanoparticles in Polymer Electrolyte Membranes probably takes out some water from ionic groups resulting in the degradation in H^+ transport. Wrapped nanoparticles of special geometry modified the nano-cracks in between the interface of base polymeric material and the nanofillers employed. The homogeneously dispersed ionic clusters create well-attachment of H_2/H^+ linking bridges as micro-pathways. Consequently, higher proton conduction could be achieved under non-hydrous and low-humidified conditions. Again, amino-functionalized nanoparticles with sulfonated nanoparticles were excellent additives for enhancing the proton conductivity of PEMs as shown recently by Salarizadeh et al. [135]in an investigation. Here poly sodium styrene sulfonate and poly (2- acrylamide-2-methyl-1-propane sulfonic acid) polymers act as an emulsifier and create core-shell nanoparticles with TiO_2 to render the uniform distribution of hybrid nanoparticles into the polymer matrix which increases the availability of proton transport sites. Polymeric chains are connected to the periphery of the nanomaterials and hinder the nanofillers from gathering in the membrane. Therefore, the water uptake, proton conductivity, ion exchange capacity, and mechanical characteristics of the nanohybrid membrane became improved and thereby exhibited good potential for PEMFC application.

4.2. Carbon-based filer

Carbonaceous nanofiller materials render some special properties to polymer membranes due to their different structure, dimension, porous nature, and surface reactive groups. Carbonaceous substances of several dimensions and forms, e.g., spherical carbon nanoparticles, carbon nanotubes, and layered carbon material [79,156]. Carbon nanotubes (CNTs), composed of graphene materials with single or multiple layers have a hollow cylindrical structure with open or closed ends. Different types of carbon nanotubes, based on their specific diameter are single-layer carbon nanotubes (SWNTs), double-walled carbon nanotubes (DWNTs), and multi-walled carbon nanotubes (MWNTs) with a length usually smaller than 100 nm [157]. Electrochemical and mechanical properties of PEMs with carbonaceous materials-based Fillers have been shown in Table 5. Carbon nanotubes generally interact with other additives easily to give the polymer some advantages as good morphological and electrical properties [158]. Recently graphene oxide (GO) is a very strong candidate, as the inclusion of these filler materials [156,159] enhanced the mechanical potency of the hybrid membranes appreciably because of its affluent oxygen-containing surface functional groups, e.g., hydroxyl, epoxy, and carboxyl groups. Chen et al. [160] showed that Graphene oxide, in general, can balance between the properties of proton conductivity and the swelling nature of the membrane. GO incorporated into the SPAES matrix checked the swelling of composite membranes and promoted the aggregation of –SO_3H groups of SPAES molecular chain (large ionic clusters) to increase proton transfer as it was dispersed throughout the matrix. The special two-dimensional structure of GO assisted to improve the proton conduction and the dimensional stability of the composite membrane. In another investigation, Li et al.[161]noticed that embedding of GO nanosheets with comparatively lower oxidation degree induced the lowest interference on nanophase separation in Nafion, which effectively assisted the distinct nanophase separation. Again, at a higher oxidation degree of graphene oxide, the disturbance in nanophase separation was not apparent, but a significant enhancement of water uptake was observed. Therefore, GO as a structure modifier can make highly efficient hybrid membranes by controlled incorporation of functional water sorption sites and slightly tuning the phase separation process of the polymer matrix. The progress in proton conductivity using carbonaceous material-based fillers into various polymeric membranes has been shown in Fig. 5.

The incorporation of carbon-based fillers in polymer electrolyte membranes (PEMs) significantly enhances proton transfer mechanisms, leading to improved conductivity and durability. Sulfonated graphene oxide (sGO) facilitates proton transport via the Grotthuss mechanism, establishing a continuous network of proton donors [183]. Phosphotungstic acid-doped reduced graphene oxide (HPW/rGO) employs a hybrid mechanism that combines Grotthuss and vehicle pathways, enhancing conductivity, especially under low-humidity conditions [184]. Similarly, sulfonated carbon nanotubes (sCNTs) provide tubular channels for proton hopping, while TiO_2@CNTs composites leverage the synergy between TiO_2 and CNTs to improve both conductivity and water retention [185]. These enhancements contribute to the overall performance of PEMs in fuel cells under varying operational conditions. The comparison of carbon-based fillers for proton transfer mechanisms in composite membranes is presented in Table 6. The Nafion-GO composite membranes also exhibited a reduced swelling degree when water uptake was improved. Sun et al. [168] reported that the SPEEK membranes doped with two-dimensional nanosheets of graphene oxide improved efficiency compared with carbon nanotubes doped membranes. The greater specific surface area of the flake structure in contact with SPEEK favors the proton transport effectively. The experimental results suggested that the two-dimensional nanosheets GO (rGO) doped with the same loading of phosphotungstic acid were more uniformly dispersed in the membrane than the carbon nanotubes doped with the same content and showed sufficient thermal stability to enhance mechanical strength and rendered superior oxidation resistance [186].

The inclusion of SWCNTs into the polymer matrix can increase the thermal durability of the composite PEMs as was reported by Sivasubramanian et al. [188]. Since smaller pores in the nanocomposite membranes dispersed over the surface of the membranes than that of the pristine membrane, it could hold more water molecules that enhanced the proton transport of the membrane. However, carbon nanotubes with an increased concentration lower the sulfonic acid content and reduce the swelling behavior of the composites, which improved the tensile strength of polymer nanocomposites and retarded the oxidative degradation of SPEEK. Similarly, sulfonated SWCNT increased the compatibility between the filler and Nafion polymeric materials and increased the mechanical and thermal steadiness of the Nafion-s SWCNT composite membranes. The prepared membranes were a better option for fuel cell applications due to their superior thermal and mechanical steadiness and comparatively increased proton conductivity. Accordingly, Steffy et al. [176] incorporated sulfonated multiwalled carbon nanotube (sMWCNT) as a potential additive into the Nafion matrix to make a hybrid PEMFC for applications at lower humidity conditions. Sulfonated MWCNT acted as a hygroscopic filler and increased proton transport of composite membranes, especially at lower humidity conditions. Sulfonic acid groups of sulfonated multi-walled carbon nanotube increased the compatibility between the filler and polymeric

Table 5
Electrochemical and mechanical properties of PEMs with carbonaceous materials-based Fillers.

Filler (content in wt%)	Polymer	Operating condition Temperature °C, Relative humidity, RH%	Proton conductivity (S/cm)	Power Density (W/cm^2)	Mechanical strength (MPa)	Ref.
sGO (10 %)	Nafion	120**°C**	0.047	0.15	–	[162]
0.8 % sGO-SiO2	Nafion	50**°C**	0.0481	–	–	[163]
IL-H_2PO_4/GO	Nafion	110 °C	0.061	0.02	–	[164]
Pt-G/SiO2 (1.5–3.0)%	Nafion	–	0.0925	–	–	[165]
sGO	SPEEK	80**°C**	0.1405	0.0425	–	[166]
5 wt% s-GO	SPEEK	80 °C, 30 %	0.055	0.378	–	[167]
HPW/rGO	c-SPEEK	80 °C, 100 %	0.11904	0.876	21.62	[168]
5 wt% sGO/Fe_3O_4	SPEEK/PVA	25**°C**	0.084	0.1227	51.2	[169]
2 wt% GO	PBI	165 °C, 0 %	0.1297	0.378	–	[170]
3 wt% GO	SPAES	120 °C,100 %	0.183	–	25.17	[160]
1 wt% VGO	SPAES90	80 °C, 50 %	0.0338	–	32.2	[171]
2 wt% SATS-GO	SPAES	80 °C, 90 %	0.1314	–	65.2	[172]
1 wt% SPTA-GO	SPAES	80 °C, 100 %	0.4125	1.58	56.4	[173]
sCNT	Nafion	152 °C	~0.33	–	~40	[174]
0.05 wt% MWCNT	Nafion	80**°C**	0.112	0.65	16	[175]
Sulfonated MWCNT	Nafion	60**°C**	0.023	0.549	11.4	[176]
s-SWCNTs (0.05 wt%)	Nafion	100 °C. 100 %	0.0155	0.650	–	[175]
0.25 wt% SMWCNT	Nafion	60 °C, 80 %	0.198	0.867	11.4	[176]
PABS-SWCNT	SPEEK	80**°C**	0.0678	0.15	35.3	[177]
5 wt% TiO_2@CNTs	SPEEK	80 °C	0.104	–	47.1	[178]
Sulfonated CNT (3 wt%)	SPEN	80 °C	0.275	–	42.35	[179]
MWCNT-SO_3H (3 %)	SPEN	80**°C**	0.052	–	97.48	[180]
CNT (1 wt%)	PBI	180**°C**	0.074	0.1735	106	[181]
1 wt% *p*-MWCNTs,Acid doping level 12.4	PBI	160 °C, 0 %	0.11	0.780	–	[182]

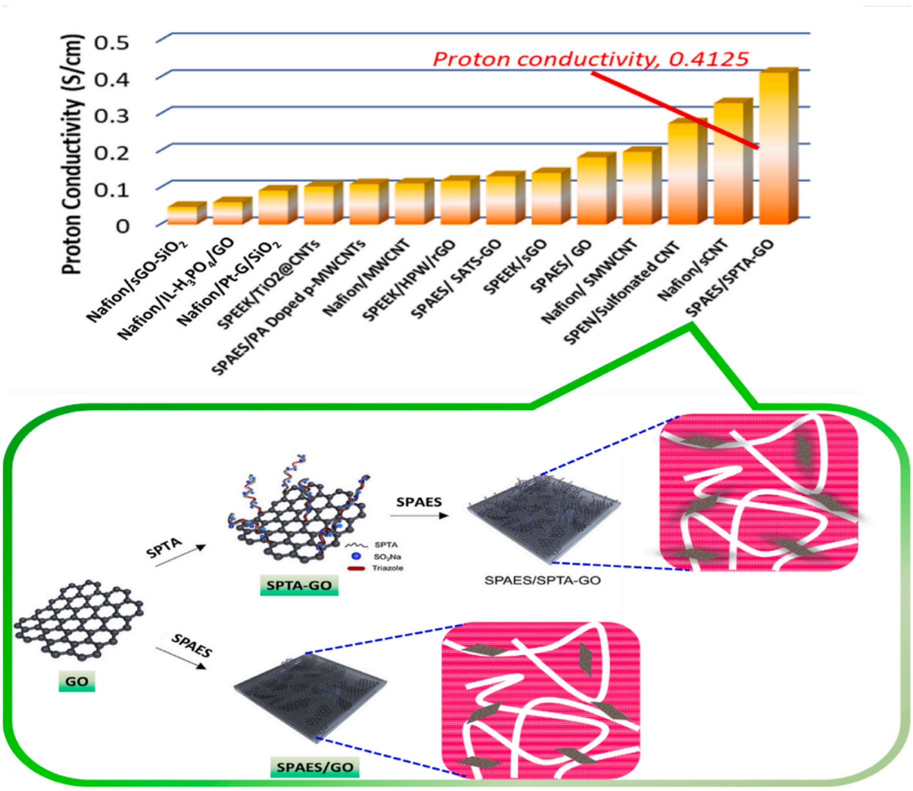

Fig. 5. The progress in proton conductivity using carbonaceous material-based fillers into various polymeric membranes and the formation of the highly proton conductive composite membrane SPAES/SPTA-GO and its characterization [113,117,121,123,127,128,143,133–137,141,145].

Table 6
Comparison of carbon-based fillers for proton transfer mechanisms in composite membranes.

Filler Type	Functional Groups/ Modification	Dominant Proton Transfer Mechanism	Composite Membrane	Performance Characteristics	References
Sulfonated graphene oxide (sGO)	Sulfonic acid (-SO_3H) groups	Grotthuss mechanism (proton hopping along sulfonic acid sites and water molecules)	sGO/SPEEK	Increased water retention, improved proton conductivity, and mechanical strength	[183]
HPW/rGO (phosphotungstic acid-doped reduced graphene oxide)	Phosphotungstic acid (HPW) and rGO	Grotthuss and vehicle mechanisms (proton hopping and diffusion along HPW network and rGO surface)	HPW/rGO/PBI	Enhanced proton conductivity under low-humidity conditions, high-temperature stability	[184]
SATS-GO (sulfonated Poly (arylene thioether sulfone) grafted graphene oxide)	Sulfonic acid and sulfone groups	Grotthuss mechanism (proton hopping via sulfonic acid groups)	SATS-GO/SPES or PBI	Improved water retention, chemical stability, and mechanical strength	[172]
SPTA-GO (sulfonated polytriazole grafted graphene oxide)	Sulfonic acid and triazole rings	Grotthuss and vehicle mechanisms (proton hopping and water-assisted diffusion)	SPTA-GO/ SPEN	Increased proton conductivity and resistance to chemical degradation	[173]
Sulfonated carbon nanotubes (sCNT)	Sulfonic acid (-SO_3H) groups	Grotthuss mechanism (proton hopping through tubular CNT pathways)	sCNT/PBI or SPES	Enhanced proton mobility, mechanical reinforcement, and conductivity	[185]
Multiwalled carbon nanotubes (MWCNT)	Limited surface functionalization	Vehicle mechanism (water-mediated proton diffusion)	MWCNT/PBI or SPES	Mechanical reinforcement with moderate proton conductivity	[185]
TiO_2@CNTs	Hydroxyl (-OH) groups from TiO_2 and CNT structure	Grotthuss mechanism (hydroxyl groups) and extended pathways along CNTs	TiO_2@CNTs/ SPEEK	Improved water retention, proton mobility, and mechanical stability under low-humidity conditions	[187]

materials as well, thus increasing the mechanical and thermal steadiness of the Nafion-sMWCNT composite membranes. Again phosphonic acid functionalized MWCNTs as the nanofiller materials were incorporated by Kannan et al. [189] into the PBI matrix (1 % filler loading) at 140 °C in dry conditions from the composite membrane, which achieved the proton conductivity better than both the pristine PBI membrane and that contained non-functionalized nanotubes. Afterward, the effect of sulfonated MWCNT on the ionic conductivities of a Sulfosuccinic acid (SSA) crosslinked PVA blend membrane was investigated by Kakati et al. [190], which also showed an enhancement of the ionic conductivity for the blend and the nanocomposite membrane as compared to the pristine polymer.

Liu et al. [191] explored that the insulating property and hydrophilicity of the SiO_2 layer, coated on CNTs eliminated the risks of electronic short-circuiting. The interaction between single-layer CNTs and chitosan decreased the effective number of the amino functional groups of chitosan and thereby reduced the water absorption of the chitosan/SCNTs membrane, which ensured the homogenous dispersion of SCNTs. The electrostatic interaction and H-bonds between single layer CNTs and chitosan assisted the formation of the continuous ion transporting channels. Therefore, the CS/SCNTs composite membrane showed improved thermal stability and oxidative resilience, mechanical potency, and proton conductivity. Again, Tsen [178] prepared a new nano-filler TiO_2 coated CNTs and exhibited similar results when incorporated into the SPEEK matrix. Due to the insulation in the denser TiO_2 coating layer, it also overcomes the danger of electronic short-circuiting created for carbon nanotubes effectively. At the same time, the polar difference between carbon nanotubes and SPEEK can be reduced by the hydrophilicity of $TiO_{2,}$ hence promoting the uniform distribution of carbon nanotubes in the membrane. Therefore, the composite membranes exhibited simultaneously increased strength and proton conductivity.

Lee et al. [192] reported on Platinum/graphene filler in Nafion membrane for application at lower humidity polymer electrolyte membrane fuel cells as platinum provided the reaction site for self-humidifying the membrane. The Pt/Graphene filler exhibited a decrease in water absorption due to the less hydrophilicity of platinum and showed a higher proton transport under anhydrous conditions relative to the pristine Nafion and Nafion/GO PEMs. Afterward, Lee et al. [165] demonstrated in another experiment that, below 1.5 wt % loading of Platinum/Graphene, the cell performance was enhanced with silica. At higher loading of Pt/Graphene filler, excessive inorganic content hindered the proton transport, resulting in reduced cell performance. Therefore, both Pt/Graphene and silica loadings should be optimized in the membrane to get better cell performance. Very interestingly, Yang et al. [193]conducted a similar experiment by developing a hybrid membrane using Pt-deposited titania and graphene oxide(GO) into Nafion. With the increase of GO until 20 wt %, the membranes showed an improved ion exchange capacity concerning the recast Nafion. The Pt–TiO2 filler exhibited improved membrane performance with varying levels of relative humidity but was not satisfactory at 0 % relative humidity. Incorporating the graphene oxide afterward improved the cell polarization to a greater extent at zero percent relative humidity compared to Nafion/Pt–TiO_2composite at the same relative humidity (RH).

Rajput et al. [194] demonstrated the effect of functionalization of graphene by varying the amount of sulfonated graphene oxide (sGO) content into polyvinyl chloride (PVC) based composite proton exchange membrane (PEMs). The functionalization of polymers has been recognized as a critical strategy for tailoring the physicochemical properties of membrane materials used in electrochemical devices. Through the incorporation of specific functional groups, ion conductivity, chemical stability, mechanical strength, and selectivity can be significantly enhanced [195]. In the context of fuel cell membranes, such functionalization plays a vital role in facilitating efficient ion transport, improving durability under operational conditions, and enabling compatibility with various electrochemical environments. Therefore, the design and synthesis of functionalized polymers are considered essential for the advancement of high-performance ion exchange membranes. Sulfonation has decreased the hydrophobicity of the graphene, therefore dispersed well in the membrane as water uptake increased. The improvement in thermal and mechanical properties of composite membrane was attributed to the uniform distribution of sGO in polymeric matrices. The composite membrane was found to drastically increase proton exchange capacity with the addition of sGO, as more functional groups provided more active sites for the transfer of protons. The good mechanical stability was due to the formation of H-bonds of sGO with polymeric backbone, which favored keeping up the intrinsic properties of the membrane. The vinyl functionalized graphene oxide (VGO) was incorporated by Kim et al. [171] into thiolate terminated sulfonated poly(arylene ether sulfone) membranes with a higher degree of sulfonation (DS) as a cross-linkable polymer matrix. The reinforcement effect of GO filler was due to its two-dimensional geometry with its higher surface area. The composite membrane showed better dimensional steadiness even at higher temperatures since the crosslinked structure hindered the water absorption. The end-group crosslinking also rendered the benefits of retaining higher proton transport of sulfonated poly(arylene ether sulfone) membranes. Lee et al. [172] introduced a highly DS of 100 on graphene oxide with the thiolate group in sulfonated poly(arylene thioether sulfone) for use as filler materials. The GO units being the scavenger of the oxidative radicals improve the oxidative durability of the composite PEM compared to the pristine sulfonated poly(arylene ether sulfone) membrane. Highly sulfonated SATS-GO as a hydrophilic material can enhance the water uptake capability of the membrane and thereby enhance the proton conductivity. In addition, the sulfonic acid groups improved the compatibility between inorganic filler materials and matrix polymer as well as improved thermochemical and mechanical properties of the polymer electrolyte membrane. The effect of sulfonated polytriazole grafted graphene oxide (SPTA-GO) on sulfonated poly(arylene ether sulfone) (SPAES) based polymer membrane was explored by Han et al. [173].

The intrinsic radical scavenging capability and hydrophilic character of GO can increase the mechanical strength as well as oxidative durability of the membrane but deteriorates the proton conductivity easily by resisting the proton transport pathways due to agglomeration. The ability of H_2 transport" refers to the membrane's permeability to molecular hydrogen gas. While PEMs are primarily designed to selectively conduct protons (H^+) from the anode to the cathode in a fuel cell, a certain degree of hydrogen gas diffusion through the membrane known as hydrogen crossover. Therefore, hydrogen permeability becomes an important membrane parameter. High hydrogen crossover is undesirable because it leads to fuel loss, reduces energy efficiency, and can accelerate membrane degradation by facilitating the formation of reactive oxygen species through undesired reactions at the cathode [196]. Additionally, excessive H_2 crossover can pose safety risks by promoting direct recombination of hydrogen and oxygen gases, potentially resulting in localized heating or membrane failure. Therefore, SPTA-GO containing both acid and basic functional groups can improve the physicochemical stabilities without deteriorating the proton transport by the increased hydrophilicity.

A recent investigation was conducted by Lim & Kim [197], where they utilized perfluoropolyether grafted GO (PFPE-GO) as an additive. The oxygen-containing functional groups in GO were reduced when PFPE-GO was prepared. The hydrophobic character of PFP and reduced graphene oxide combinedly affect to reduce the proton conductivity of the membrane. The reduced GO also disconnected the hydrophilic channels. It was observed that when the perfluoropolyether grafted GO loading in SPAES/PFPE-GO was greater than 1 wt%, the PFPE-GO was not uniformly distributed, because of which the membrane performance deteriorated. The good dispersion of PFPE-GO could probably lessen the barrier which originated from the aggregation of fillers and also prevented over swelling at higher relative humidity. The incorporation of PFPE-GO further improved both the mechanical potency and dimensional steadiness of PEMs. The incorporation of antioxidant grafted GO increased the chemical stability of SPAES more effectively than graphene oxide without the antioxidant as stated by Kim et al. [198]. The combining effects of radical scavenging property of 4-amino-2,2,6,6-tetramethylpiperidinegrafted onto GO surface and the implicit antioxidant characteristic of graphene oxide appreciably improved the chemical and oxidative resilience of SPAES/HA-GO hybrid membrane. The excellent dimensional and mechanical potency of SPAES/HA-GO PEMs was obtained due to the acid-base interaction between the –SO_3H groups of SPAES and the amine groups of amines grafted graphene oxide compared to the pristine matrix and SPAES/GO composite membranes.

Abouzari-Lotf et al. [199] proposed an extensively dispersible phosphonated graphene oxide (PGO) into 2,6-Pyridine functionalized polybenzimidazole matrix for hosting phosphoric acid (PA) moiety at different levels to develop a highly conductive and stable high-temperature PEM. The inclusion of PGO enhanced the acid doping level which rendered durable performance under anhydrous conditions at elevated temperature and remarkably enhanced the proton transport of the composite membranes. Oh et al. [200] utilized graphene oxide (GO), embellished with phosphotungstic acid into sulfonated poly(arylene ether ketone) block copolymer at 80 °C under the whole extent of relative humidity, which showed higher proton conductivity, current density, and better oxidative stability relative to the NRE-212 membrane and pristine SPAEK at the same operating condition. Maiti et al. [164] synthesized a dihydrogen phosphate imidazolium IL functionalized hydrophilic additive of GO, IL/GO and was incorporated into Nafion 117 solution to avoid the proton conduction dependency on water at higher temperatures under anhydrous conditions. The incorporation of this additive increased the thermal stability. The proton conductivity was increased with temperature and the content of IL-H_2PO_4. Functionalized graphite oxide by 3-aminopropyl triethoxy silane ionic liquid ILGO in PBI were used by Xu et al. [201] for high temperature PEMFCs, Here, the imidazole species acted as a base to create acid-base pairs within the membrane to promote proton conductivity following the Grotthuss mechanism [202]. It similarly exhibited an exact level of proton transport when imbibed with H_3PO_4 at lower H_3PO_4 content. Hence, these composite membranes may be an efficient candidate for HTPEMFCs.

4.3. Metal-organic framework (MOF)

In the Metal-Organic Frameworks, the permeable crystalline solid substances comprise metallic clusters with organic linkers in such an ordered arrangement where the designed cages and porous holes can specifically absorb gaseous as well as different other species [203]. The appropriate choice of the precursors and balancing of the states of the combination-the molar proportion of reagents, temperature, and so forth by post-synthetic chemical changes can effectively control the composition and cavity size of metal-organic frameworks. The high porosity and surface area of MOFs in combination with their tunable functionality make them attractive for association with guest species [204]. This potential application of MOFs for PEMFC was because of the improved proton conduction (for some cases identical to Nafion) in extensive ranges of humidity and temperatures and higher chemical resilience in severe conditions. Among MOF-based fillers, GO@UiO-66-NH_2 is identified as the most effective, offering superior mechanical reinforcement through graphene oxide and excellent electrochemical durability. The amino-functionalized UiO-66 ensures high proton conductivity and structural stability over extended operation. Although UiO-66-SO_3H and HPW@MIL101 enhance conductivity, their mechanical strength is comparatively lower. ZIF-8 and ZIF-67 exhibit limited conductivity and durability, reducing their suitability for high-performance fuel cells. The mechanical and electrochemical properties of these composite membranes are detailed in Table 7.

Metal-organic structures (MOFs) with high crystallinity spanned from metal and ligand units make specified proton transport channels by forming H-bonded networks or functional groups contained in holes, through which protons can move. Again, the sulfonated polymers as a decent medium construct uninterrupted pathways for proton transport. Incorporation of Fe-MIL-101-NH_2 into sulfonated poly (2, 6-dimethyl-1, 4-phenylene oxide) results in a hybrid membrane with proton conduction of 0.10 Scm^{-1}, 25 % greater than that of the pure matrix (0.08 Scm^{-1}) at room temperature. ZIF-8 was made by blending poly (2-acrylamido-2-methylpropane sulfonic acid with poly(vinyl alcohol), which formed a ternary composite membrane that showed higher proton conductivity (0.134 S/cm at 80 °C under 100 % relative humidity) compared to that of Nafion-117 [215]. Zr-MOFs have attracted considerable interest very recently, because of their higher robustness and easy tunable structure. UiO-66 (UiO: University of Oslo) which was made from octahedral $Zr_6O_4(OH)_4$ by 12-fold linkages with the organic ligand 1,4-benzene-dicarboxylate (BDC), is a highly crystalline zirconium-based Metal-Organic Frameworks. However, proton transport pathways between metal-organic framework particles were not consecutive within the membrane matrix. Thus, it is a great challenge to make continuous proton transport pathways of metal-organic frameworks. However, the progress in proton conductivity using Metal-Organic Frameworks based fillers is shown in Fig. 6.

Anahidzade et al. [230] increased the bulk conductivity of MIL(101) at low RH and high temperatures using controlled impregnation of the Metal-Organic Frameworks with H_3PO_4 and H_2SO_4 respectively. Remarkably the MOF containing the highest amount of H_2SO_4 displayed an excellent proton conductivity at 70 °C was 1.82 Scm^{-1} and 40 °C was 0.92×10^{-2} Scm^{-1} at 90 % RH, which surpassed Nafion and other MOF based proton conductors value. The result of the inclusion of sulfonated MIL-101(Cr) on PEM efficiency was also investigated by Li et al. [216]. At 75 °C and 100 % relative humidity, the proton conductivity was improved almost twice by 0.306 S/cm, compared with the pure polymer membranes. MIL(101) is a metal-organic framework material consisting of highly crystalline materials having metal coordination nodes and connected organic linkers to produce an infinite multi-dimensional polymer network with large spaces within the framework. Among MOFs, Chromium terephthalate MIL(101) has been widely investigated due to having some specific properties like 3D structure, high surface

Table 7
Mechanical and electrochemical durability of metal-organic framework (MOF) composite membranes.

MOF Filler	Mechanical Durability	Electrochemical Durability	Comments
UiO-66-NH_2 (amino-functionalized UiO-66)	High mechanical stability due to strong Zr–O bonds [205].	Excellent proton conductivity due to the presence of amino groups, which enhance proton transport pathways [206].	Overall good balance of mechanical and electrochemical properties. It can maintain long-term durability in fuel cells.
UiO-66-SO_3H (sulfonic acid functionalized UiO-66)	Good mechanical durability, although slightly lower than UiO-66-NH_2 due to increased water uptake [207].	Enhanced proton conductivity due to sulfonic acid groups (SO_3H), but the membrane can swell under hydrated conditions, reducing mechanical stability [208].	Suitable for high-proton conductivity but may suffer from swelling under high humidity.
GO@UiO-66-NH_2 (graphene oxide doped amino-functionalized UiO-66)	Excellent mechanical durability as graphene oxide reinforces the membrane structure [209].	High electrochemical stability and proton conductivity due to the synergy between graphene oxide and UiO-66-NH_2 [210].	Superior durability and performance, combining the advantages of both GO and UiO-66.
ZIF-8 (zeolitic-imidazolate frameworks)	Moderate mechanical durability, weaker Zn–N bonds make it less stable under stress compared to UiO-66 [211].	Moderate proton conductivity, lower than ZIF-8 based fillers, but maintains chemical stability [211].	Less suitable for fuel cell applications due to weaker mechanical and electrochemical performance.
ZIF-67 (zeolitic-imidazolate frameworks)	Similar to ZIF-8, it exhibits moderate mechanical strength due to Co–N coordination bonds [212].	Lower proton conductivity than UiO-66-based fillers, though it offers good chemical stability [212].	Limited suitability for fuel cells due to lower proton conductivity.
Sul-MIL101 (sulfonated Chromium terephthalate-MIL101)	Moderate mechanical durability, slightly weaker than UiO-66 due to higher water uptake [213].	High proton conductivity due to sulfonic acid groups but may suffer from swelling under hydrated conditions [213].	Provides high proton conductivity but needs careful hydration control to maintain mechanical durability.
HPW@MIL101 (phosphotungstic acid doped MIL101)	Good mechanical stability with some reinforcement from phosphotungstic acid [214].	Excellent proton conductivity due to HPW doping, enhancing electrochemical performance [214].	Highly suitable for fuel cell applications with strong electrochemical durability.

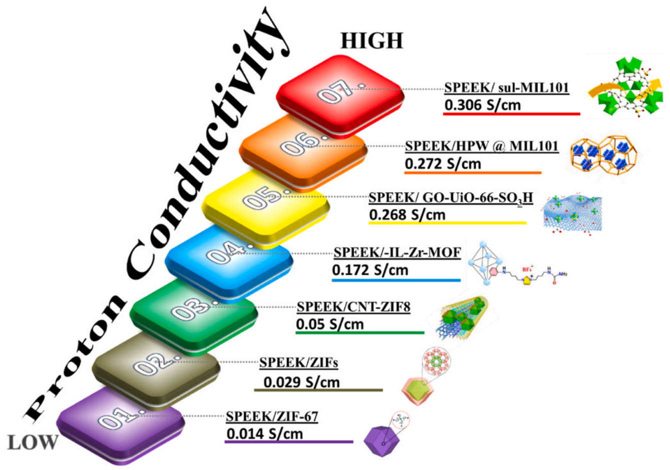

Fig. 6. Performance of proton conductivity under optimum protocol based on metal-organic framework fillers of different forms of polymeric membranes [216–229].

area with enormous active sites, tunable pore sizes, and better thermal durability [218].

Functionalization of ligand in the metal-organic framework as an effective way to enhance proton transport was investigated by Li et al. [216] on different UiO-66, which contain functionalized ligands such as –SO$_3$H, –CO$_2$H, –NH$_2$. UiO-66 containing two –SO$_3$H groups connected to the double carboxylate bearing 1,4-benzene-dicarboxylate (bdc) ligand showed excellent performance. The free –SO$_3$H groups formed strong H-bond networks and induced an enhanced proton conductivity in the framework when tethered onto GO surfaces and added to the SPEEK matrix [220]. The Schematic illustration of the enhanced transport properties of the GO@UiO-66-SO$_3$H is shown in Fig. 7(a). Again, amino-functionalized UiO-66 (UiO- 66-NH$_2$) nanoparticles, a noted Zirconium based Metal-Organic Framework, were introduced into the SPEN polymer matrix by Zheng et al. [231] to prepare a PEM with higher output, where the amino and carboxyl/sulfonic acid groups are covalent-ionically crosslinked to increase the methanol barrier and dimensional stability of polymer electrolyte membranes effectively. Rao et al. [232] also reported on the usage of UiO-66-NH$_2$, when tethered onto GO surfaces and added to the Nafion matrix. The strong metal-ligand bonding UiO-66-NH$_2$ [233] makes it relatively more stable than those of amino functionalized MIL-53 and MIL-101 [203]. It possessed both the octahedral and tetrahedral cages. Its micropores were slight bigger, compared with amino functionalized MIL-53 (one dimensional micropores) and amino functionalized MIL-101, some other metal organic frameworks [234,235]. Therefore, the hindrance for proton transport through greater three-dimensional micropores was comparatively smaller. The interaction of amino group of UiO-66-NH$_2$ with –SO$_3$H group of Nafion favors the proton transport at lower humidity or zero humidity condition. The polymer electrolyte membrane exhibited the proton conductivity of 0.303 S/cm at 90 °C, 95 % relative humidity, and 3.403×10^{-3} S/cm at anhydrous condition, both the values are more than that of the pure Nafion, respectively [232]. Furthermore, the composite PEM showed superior durability of proton transport even after 3250 min, ascribed to the excellent water retention, thermal durability, and higher dimensional stability of UiO-66-NH$_2$. This work provided a remarkable reference to design optimized metal organic framework structure as proton conductor. MIL(101) consists of terephthalic acid (1,4-benzene dicarboxylate, 1,4-bdc) linker with Cr-MOFs, which had a solid cubic structure with pentagonal and hexagonal types of extra-large pore windows with rigid cavities [236]. The

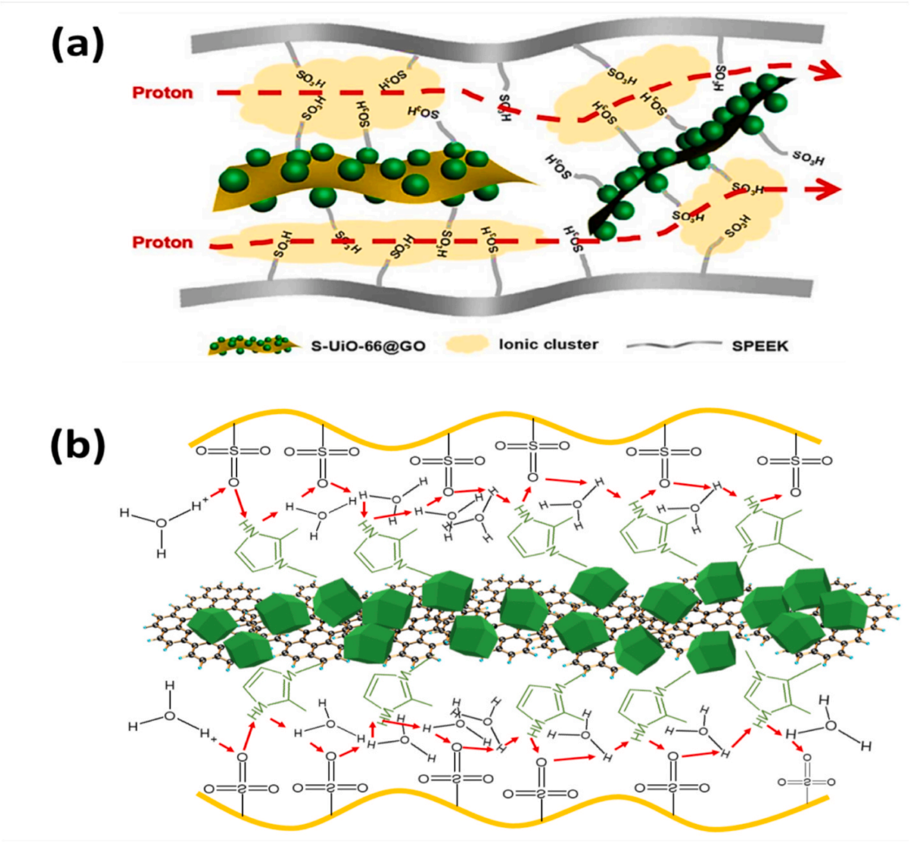

Fig. 7. (a) Schematic illustration of the enhanced transport properties of the GO@UiO-66-SO3H. [220]; (b) SPEEK/CNT-ZIF8 Composite membrane formation and proton transport in the membrane [224].

filler molecules such as HPW are loaded into these cavities and then used to prepare nanocomposite membrane by doping it into SPEEK matrix. Additional proton transporting nanochannels were fabricated in the cavities of HPW@MIL(101) and within the interface of HPW@MIL(101) and SPEEK, that facilitated the improvement of proton conduction property. Meanwhile, due to the hygroscopic nature of HPW, the membrane dehydration was reduced or eliminated at higher temperatures. The proton transport under lower RH condition was significantly increased [218].

The incorporation of Metal-Organic Frameworks with imidazole and histamine is a novel strategy to ensure improved proton conduction within medium temperature limits and lower humidity [237]. Covalent Organic Framework (COF)-based fillers have emerged as a highly promising class of materials for enhancing the performance of composite membranes used in electrochemical applications. Due to their intrinsic properties such as high surface area, tunable pore size, and structural regularity COFs can be designed to facilitate selective ion transport while minimizing undesired crossover of fuel or gases. When incorporated into polymer matrices, COF-based fillers contribute to improved mechanical strength, thermal stability, and chemical resistance. Moreover, functional groups can be precisely introduced into the COF structure, enabling synergistic interactions with the polymer backbone and enhancing ion conductivity [238]. These features make COFs particularly suitable for application in advanced membrane systems, where both structural integrity and ion-selective transport are critical to overall device performance. As a result, COF-based composite membranes are increasingly being explored for use in fuel cells, batteries, and other energy conversion technologies.

Due to the impregnation of nano-tunnels of Al-naphthalene-dicarboxylate (ndc), imidazole@Al-MOF showed the conductivity of 10^{-5} Scm^{-1} at 120 °C, whereas the histamine@Al-MOF had the value as high as 10^{-3} Scm^{-1} in the same RH and at 150 °C, which was due to the presence of more protons in histamine and a more effectively packed nano tunnel compared to imidazole favored the more effective transport of H^+. Again, Escorihuela et al. [31] noticed that Fe-based Metal--Organic Framework containing coordinated imidazole (Im-Fe-MOF) demonstrated a proton conductivity three times greater, as compared to physically absorbed Imidazole at Fe-MOF at 60 °C and 98 % relative humidity. The consistency in the proton transport property was also explained by the presence of imidazole coordination in Im-Fe-MOF. Trindade et al. [222] investigated the encapsulating effect of sulfonated metal ionic liquids, namely 1-butylimidazolium hydrogen sulfate ($BIm.HSO_4$), 1-butyl-3-methylimidazolium hydrogensulfate ($BMI.HSO_4$), and 3-triethylammonium propane sulfonic hydrogensulfate ($TEA-PS.HSO_4$) ILs in Zr-MOF. TEA-PS. HSO_4 Ionic Liquid contains a sulfonic acid group and an SO_4H group, which dissociates to yield more hydrogen ions, thus contributing to the enhancement of proton conduction. In addition, water molecules are aggregated due to H-bonding within the pores of highly crystalline Zirconium-based MOF, which increased the proton transport in the SPEEK matrix, but in prolonged contact with water, excess swelling causes membrane dissolution. ILs provide consistency to the PEM since ILs prevent the membrane from absorption of higher amounts of water. But a higher concentration of ionic liquids generates agglomeration and reduces proton transport in the membranes. Another class of MOFs is zeolitic-imidazolate frameworks (ZIFs), as reported [204,239]. Owing to its large surface and thermal durability up to 550 °C, the MOFs exhibited better uniformity with polymers, when overloaded to make composite-matrix PEM. ZIF-8, a notable Zinc-based MOFs was extensively investigated as shown in Fig. 7(b), in which the complicated Zinc–Nitrogen coordinate bond provides 11.6 Å sized larger pores to render low barrier migration of molecules through these pores, at the same time 0.34 nm sized smaller nominal pores aperture enables outstanding exclusion of molecules.

4.4. *Acid dopant, phosphonic acid, HPA, other acids and ILs fillers*

The highly conductive PEM materials at fully anhydrous conditions are highly desirable for their development, because of their simple water management system, as reported by Zhang et al. [240] in the case of Phosphoric acid-doped polybenzimidazole membranes at higher temperatures (in the extent of 140–180 °C). Hou et al. [241] showed the availability of nanostructure and functional groups –N = in the imidazole ring of the polybenzimidazole film help to form H-bonds as a connection to proton transport. Therefore, the PA-PBI composite membranes retain better proton conductivity under low relative humidity conditions (lower than 10 % relative humidity). Severe performance degradation can take place in presence of moisture to the above level, as it causes the leakage of the doped H_3PO_4 from the membranes [240,242]. Suzuki et al. [243] stated that two approaches may be utilized to overcome this issue, physically pouring the phosphoric acids into the nanoporous holes of SiO_2, zeolites, etc., or by chemical bonding of Phosphoric acids with basic sites of imidazoles and pyridine [244]. Kuo and Lin [106] stated that the phosphoric acid doping level was promoted with the increase of mesoporous silica- MCM-41 or SBA-15 contents in the polybinzimidazole-epoxy matrices of the hybrid membranes, which was attributed to the more H-bonding of phosphoric acid molecules with the hydroxyl groups of the filler materials. The Silica nanoparticles in the PBI/MCM-41 and PBI/SBA-15 membranes retained a larger amount of acid molecules since they prevented acid from leaching from the membranes.

A quick decrease in conductivity was noticed in most of the polymer electrolyte membranes because of the resistance caused by the water loss of the membrane. Even a faint transport resistance can remarkably decrease the proton conductivity [245]. The term “faint transport resistance” in the context of polymer electrolyte membranes (PEMs) refers to a small but significant hindrance to proton movement through the membrane. Scientifically, this resistance arises due to factors such as partial dehydration, microstructural changes, or interruption in the continuous water network required for efficient proton conduction [246]. Proton conductivity in PEMs, such as Nafion, heavily depends on the presence of hydrated ionic clusters within the membrane structure. Protons are primarily transported via two mechanisms: the Grotthuss mechanism (proton hopping through a hydrogen-bonded water network) and the vehicle mechanism (protons associated with water molecules moving together). Both mechanisms require a sufficient level of membrane hydration conduction [246]. Even a slight loss of water content can disrupt the continuity of proton-conducting pathways, thereby introducing a “faint” or minimal resistance that still significantly impedes proton transport.

Amphoteric proton species, for example, H_3PO_4 allow anhydrous proton transport because of their intrinsic properties like higher proton-solvation, higher self-ionization, and stronger intermolecular hydrogen bonding network, which is applicable in a fuel cell. By enhancing the Phosphoric Acid content up to 100 wt%, the proton transport of the membrane also enhances above 100 times [201,247]. Dang et al. [248] reported, that doped PAs with imidazole microcapsules (ImMCs) of tunable lumen size and shell thickness was added to the SPEEK matrix for its excellent adsorption ability, and the resulting membrane provides the desirable conducting groups of ImMCs with high acid retention ability to boost the proton conductivity at higher temperature and anhydrous condition. Mecerreyes et al. [249] synthesized a porous polybenzimidazole (PBI) membrane in which the PA content can be enhanced more than three times and the proton conductivity jumped from 1.5 to 50 mS cm^{-1}. Ou et al. [250] demonstrated that the dense and porous layers of poly [2,20-(*p*-oxydiphenylene)- 5,50-benzimidazole] (OPBI) membrane were effectively useable for higher temperature operation in PEMFCs and also provided additional free volume for PA absorption, thereby resulted in high proton conductivity of the membrane. The high molecular OPBI as the membrane matrix material provided good mechanical strength and toughness for the resultant membranes. Imidazolium ILs containing PO_4^{3-}ion were utilized by Maity et al. [251] to modify SiO_2 nanofillers and then added into the polybenzimidazole matrix as shown in Fig. 8 to increase phosphoric acid absorption and retention capability. The obtained PEM exhibited a 58 % decrease in phosphoric acid loss and a nearly2-fold increase in proton transport relative to the pristine polybenzimidazole membrane. Li et al. [252] demonstrated that the incorporation of 1-methylimidazole ionic liquids to the benzyl position of PAEK resulted in stable conjugate nitrogen heterocycle that provided acid adsorption sites to promote PA doping rate and proton transport. The grafted PBI membranes containing additional benzimidazole pendants improved the H-bond interaction between polymeric chains. Tian et al. [253] successfully utilized 3-Glycidoxypropyltrimethoxysilane (KH560) with 2-chloromethyl benzimidazole, grafted onto the Polybenzimidazole main chain. The benzimidazole side chains rendered high content of H_3PO_4 uptakes with retaining the mechanical properties of the membrane. The imidazole rings containing the side chain assisted the proton transport and lowered the activation energy. Meanwhile, 3-Glycidoxypropyltrimethoxysilane could hydrolysis resulting in a Si–*O*–Si network structure, which absorbed more H_3PO_4 and efficiently improved the stability of phosphoric acid. Therefore, the proton conductivity was enhanced, as well as exhibited outstanding thermal and chemical resilience and adequate mechanical potency. However, the retention of phosphoric acids as earlier mentioned was usually transitory in most cases, when investigated in the durable operation.

Phosphoric acid-Polybenzimidazole (PA-PBI) composite membranes containing inorganic additives, such as silica, zirconium oxide, titanium oxide, and zirconium hydrogen phosphates have superior relative humidity toleration [139,255]. However, the creation of non-homogeneous membranes and aggregation of filler materials has remained a challenge. The operational gap between Nafion® (below 100 °C and above 80 % relative humidity) and PA-PBI (at 140–180 °C and less than 10 % RH) was recovered by incorporating a phosphoric acid doped polyphenylene-based ion-pair coordinated membrane QAPOH, which showed static proton transport up to 40 % relative humidity at 80 °C [256]. The increased relative humidity toleration of QAPOH was ascribed to the robust interaction between quaternary ammonium (QA) cations and dihydrogen phosphate anions, which resisted leakage of phosphoric acid from the polymer composite at higher relative humidity. Mechanical features of the membranes suggested that they grew entirely flexible when doped with phosphoric acid [257–259].

In recent years, the functional modification of polybenzimidazole membrane was focused to enhance the superior properties of polymer electrolyte membranes. Cross-linking grafting, blending, sulfonating and inorganic doping are the methods generally used to improve PA doping levels. Wang et al. [260] showed, that amino-modified polybenzimidazole with ethyl phosphonic acid side chains (PBI–N-H_2-EPA-X) assisted PA sorption and thereby showed long-term conduction stability. Again, more phosphoric acid absorbed resulted in higher proton conductivity but also decreased the mechanical potency. The presence of several pyridine groups increased the mechanical durability of the PA-doped membrane, as investigated by Singh et al. [261] for HT-PEMFCs. The superior performance of the Radel-based membranes containing 4-hydroxy pyridine side chains and imidazole cross-links (HP-IM) was due to their remarkable PA doping in the matrix and exhibited a much higher potential as indicated from the ex-situ conductivity test. Bai et al. [262] utilized poly (arylene piperidine)s as H_3PO_4 (PA) absorbing matrix, which was suitable for PEMFCs application operated at a higher temperature. The poly (arylene piperidine) exhibited superior thermal stability. Among the poly (arylene piperidine)s, PA doped poly (N-methyl-piperidine-*co*-*p*-terphenyl) showed a higher proton transport at the anhydrous condition and improved tensile strength, which originated due to the creation of micro-phase separation in phosphoric acid doped poly (N-methyl-piperidine-*co*-*p*-terphenyl) membrane. A similar experiment was conducted by Berber & Nakashima [263]in which the characterization of bipyridine-based polybenzimidazole polymers was reported for fuel cell (FC) application. The addition of extra aromatic nitrogen into the PBI backbone for the potential loading of H_3PO_4 was supposed to increase the proton transport while retaining a high thermal and mechanical stability.

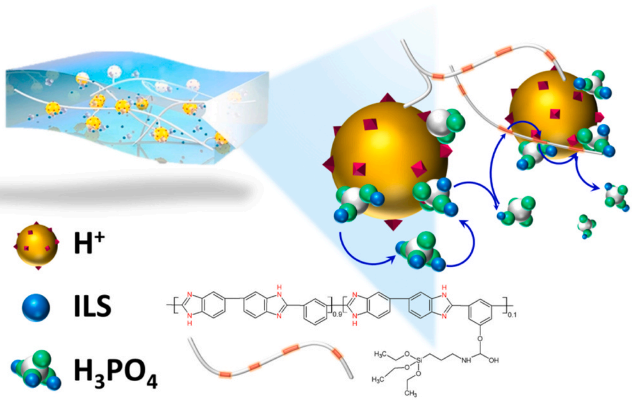

Fig. 8. Imidazolium ILs containing PO_4^{3-} ion into Polybenzimidazole matrix [254].

Again, the long-term stability of the fuel cell was decreased with the increase in the loading of H_3PO_4, which resulted in free acid leakage, poor mechanical characteristics, and deterioration of the membrane. Vinyl phosphonic acid (VPA) at different content proportions was added with N-vinyl-2-pyrrolidone (NVP)to form the copolymer, in which phosphonic acid acted as a proton donor and imidazole groups as proton acceptor; thereby, obtained higher proton conductivity of polybenzimidazole membrane under lower content of PA dopant condition [264,265]. A strategy devised by Teixeira et al. [266] to modify the Nafion properties, where various aryl- and azahetero aromatic bisphosphonic acid derivatives were incorporated as dopants. The amphoteric character of nitrogen in azahetero cycles enhanced the proton-conductivity of the membrane. In addition, the presence of the–SO_3H group in Nafion and the phosphonic acid group of dopants increase the performance i.e., water absorption, ion exchange capacity, and hydration number in the new composite membrane significantly.

Tanaka et al. [267] first utilize phytic acid doped polybenzimidazole nanofibers (PBINf) to form an efficient proton transport channel in the through-plane direction of the composite membrane. The void space of the nanofiber framework was loaded with a typical proton transporting perfluoro sulfonate polymer, which provided3-D network nanostructures to transport proton and water successfully through an acid-condensed layer in between the acid-doped PBI nanofiber and the polymeric matrix. In addition, the strong nanofiber network structures inhibited gas pervasion and over swelling in the polymer matrix domain at higher RH. The mechanical robustness of nanofiber frameworks allowed the formation of an ultra-thin polymer electrolyte membrane of thickness, less than 5 mm which decreases the membrane impedance significantly and subsequently causes a decrease in cost. Taherkhani et al. [268] showed, that poly(acrylic acid), due to its weak acidity property played an interesting role as a polybenzimidazole dopant to prevent leaching of the low molecular weight acid. The superior proton conductivity with average molecular weight and molar proportion of poly(acrylic acid) was due to the existence of pores, which increased the WU in membranes and formed new channels for proton transport. In addition, –COOH groups resulted in more H-bond networks between polybenzimidazole and poly(acrylic acid), which in turn increased the tensile strength.

4.4.1. *Heteropolyacids*

Heteropolyacids (HPAs), in most cases, are encompassed by an enormous number of water molecules, which display strong acidity and high conductivity and are suitable for operating under anhydrous conditions [269]. The HPAs, e.g., silicotungstic acids ($H_3SiW_{12}O_{40}$, SWA), phosphotungstic acid ($H_3PW_{12}O_{40}$, PWA), and phosphomolybdic acid ($H_3PMo_{12}O_{40}$, PMA) most often utilized as filler materials in proton-conduction systems.

Chia et al. [270] incorporated silicotungstic acid, a crystalline material with the highest proton conductivity among other heteropoly acids and thermal stability, and silica was used as supporting material in SPEEK polymer to immobilize SiWA, which improved the thermal property of SPEEK/SiO_2-SiWA composite membrane. The weight proportion of SiO_2 to SiWA (2:1) resulted in an increased proton conductivity of porous membranes, on the other hand, a reduction in the silica ratio provided a denser structure with higher thermal durability. However, insufficient support may cause leakage of silicotungstic acid from the membranes. Afterward, Chia et al. [103] also proved the fact that the optimum content of the fillers in the SPEEK matrix containing a 2:1 ratio of silica and SiWA has the best performance. The coupling agents (3-aminopropyl)triethoxysilane and carbonyldiimidazole were incorporated to improve the consistency of the organic phase (SPEEK polymer) and inorganic phase (SiO_2 and SiWA).

Xu et al. [271] modified HPAs to increase their surface acidity by partially substituting them with cesium to form CsHPA, which decreased the water solubility of the salt and enhanced its surface area, therefore the interaction with the polymer matrix increased remarkably. This also improves the PEM conductivity, whereas the SiO_2-based salt strengthens the mechanical features of the PEM. Ooi et al. [272] incorporated organic solid acid cesium hydrogen sulfate-silicotungstic acid composite (CHS-WSiA) into PBI containing hexafluoropropylene groups with various loading values. A newly formed hydrogen interaction between phosphoric acid and CHS allowed faster proton transfer and improved the durability of the composite membrane. Ya et al. [273] demonstrated that the mechanical milling of composite materials assisted to make irreversible super protic phases nano-interface of a complex H-bonding network between $CsHSO_4$ and $H_4SiW_{12}O_{40}$, which exhibited increased conductivities. Wang et al. [274] intercalated phosphotungstic acid into layered ferric sulfophenyl phosphate (FeSPP), to form an insoluble organic-inorganic proton conducting composite membrane which possessed layered structures that assisted the construction of an orderly arranged proton transport channel. The P–*O*–Fe σ bond and Fe–*O*–W σ bond in the proton-conducting FeSPP-PWA network facilitated render immobilization of rigidity and hindrance to the leaching of PWA at higher RH.

4.4.2. Ionic liquids

The Ionic liquids (ILs) doped membranes are extensively used in fuel cells because clean ionic liquids offer high ionic conductivity and exhibit excellent thermal stability at high temperatures (∼200 °C). Electrochemical and mechanical properties of polymer electrolyte membranes with acid dopants, heteropoly acids and ionic liquids at different operating conditions have been shown in Table 8.

Zhang et al. [240] chose Imidazole-type ionic liquid (IL) owing to its enormous dehydrated hopping sites which facilitated the enhanced proton conduction within the composite membrane. Methacrylic acid polyelectrolyte microcapsules (PMCs) were used to increase the ionic liquid uptake and retain significantly in the composite membrane. In addition, the crosslinked shells of polyelectrolyte microcapsules

Table 8
Electrochemical and mechanical properties of PEMs with acid dopants, heteropoly acids and ionic liquids at different operating conditions.

Filler	Polymer	Operating condition (Temp.°C), Relative humidity, RH%	Proton conductivity (S/cm)	Power Density (mW/cm^2)	Mechanical strength (MPa)	Ref.
19 wt% $H_3PW_{12}O_{40}$	meso-Nafion	80 °C, 50 %	0.072	541	–	[275]
Phosphosilicate sol ((6SPEEK/4(P–Si)) wt %)	SPEEK	70 °C, 95 %	0.138	–	–	[276]
70 wt% solidacid(CsH_2PO_4) and phospho silicatesol	SPEEK	230 °C	0.0018	–	–	[277]
15 wt% Imidazolemicro-capsule/HPW	SPEEK	Room temperature, 100 %	0.0316	–	–	[278]
10 wt% SiO_2 with 5 wt% SiWA	SPEEK	–	0.0480	–		[270]
30 wt% CsPOMo, acid doping level 4.5	PBI	150 °C, 0 %	0.12	600	–	[271]
CHS-WSiA, PA doping level 8	F_6PBI	150 °C, 0 %	0.0021	498	–	[272]
PWA-IL	SPAEKS[b]	80 °C, 100 %	0.127	–	–	[279]
8 wt% PWA	Sulfonated bisphenol-A-poly- sulfone	80 °C	0.0597	–	–	[280]
PWA(15 wt%)	Ferric sulfophenyl phosphate	180 °C, 100 %	0.140 (1.65 × 10^{-2} at 0 % RH)	–	–	[274]
10 wt% imidazole micro-capsule	PAdoped SPEEK	150 °C,anhydrous	0.0347	–	–	[248]
2 wt% IL	SPEEK	170 °C, anhydrous	0.0104	–	–	[281]
IL 1,6-di (3-methyl imidazolium)hexanebis(hexafluoro-phosphate) and 1-butyl-3-methyl imidazolium hexafluorophosphate	PA-dopedPBI	180 °C, anhydrous	0.078	–	–	[282]
15 wt% 1-(3-trimethoxy silyl propyl)-3-methylimidazolium chloride IL	PA-dopedPBI	180 °C, anhydrous	0.061	–	–	[283]
5 % ionic liquid functional silica, PA doping level 9.65	PBIOH	170 °C	0.106	–	–	[254]
1-Methyl imidazole (ILs), PA doping level 19.2	PAEK	170 °C	0.091	–	–	[252]
PA	OPBI	180 °C, anhydrous	0.072	393 at 160 °C	–	[250]
PA doping level 85 % at 60 °C	PBI-Sc-5	170 °C, anhydrous	0.104	411.7	103	[257]
PA doping level 10.5	Bipyridine based polybenzimidazole	120 °C	0.0375	779	24.50	[263]
PA	PBI:PAA blend (1:4)	150 °C	0.005	–	82.84	[268]
PA doping level 14.4	QAPOH	180 °C, RH > 90 %	0.06	800	–	[256]
PA doping level 82 %	Poly(N-methylpiperidine-*co*-terphenyl)	180 °C, anhydrous	0.096	1220.2	12	[262]
PA doping level 253.3 %	15 wt% EPA grafted PBI-NH_2-EPA	170 °C	0.062	–	–	[260]

hindered the ionic liquid leakage, which rendered the dimensional stability of PEM. The PMCs bearing –CO_2H groups generated strong electrostatic interactions with the ionic liquids, resulting in elevated anhydrous proton conductivity. Thanganathan and Nogami [284] showed that an increase in ILs fraction can enhance the compact nature of membranes by increasing crosslinking density, which resists the proton transport in the membrane, whereas the thermal durability of the membrane was increased by the presence of both 1-ethyl-3-methyl imidazolium tetrafluoro borate (IL-EMI-BF_4) and silica. In the case of PVA-based hybrid membranes, the conductivity depends on the concentration of ILs. These hybrid membranes exhibited less water uptake with increasing the content of the ionic liquid.

Tian et al. [283] prepared the Si–*O*–Si networks by combining 1-(3-trimethoxysilylpropyl)-3-methylimidazolium chloride ionic liquid with Polybenzimidazole to form a potential hybrid membrane for PEMFCs application. ILs became hydrolyzed forming a Si–*O*–Si network structure under the acidic condition in the composite membranes and increased the theH_3PO_4 doping level and proton conductivity simultaneously. Due to this, the obtained Polybenzimidazole/ionic liquid hybrid membrane displayed remarkable thermal and chemical durability as well as increased mechanical potency for higher temperature (above 200 °C) PEMFCs. Liu et al. [254] synthesized –OH groups bearing polybenzimidazole (PBIOH)/IL-functionalizedSiO_2 (ILS) hybrid membrane for application in higher temperature PEMFCs. The IL-functionalizedSiO_2nanomaterials were produced from the polymeric chain of silane monomers3-(triethoxysilyl) propyl isocyanate in the membrane which improved the efficiency of composite membranes by the formation of the Si–*O*–Si network in the membrane. Therefore, the PBIOH-ILS hybrid membrane was found to exhibit superior thermal and oxidative stability as well as enhanced mechanical strength. The proton transport was increased remarkably since the ionic liquids with a higher specific area absorbed more H_3PO_4 in the membrane.

5. Crosslinking agent

In the cross-linking process, the polymeric chains bind other materials involving covalent or ionic bonds. The density of the crosslinker influences the properties of the membranes, such as lower compactness decreases the melting point of the polymer, moderate compactness alters the sticky property of the elastomer, and higher potency and higher compactness make it very rigid or glassy. The **e**lectrochemical and mechanical properties of polymer electrolyte membranes with different crosslinking agents at different operating conditions have been shown in Table 9.

Sulfosuccinic acid (SSA) has a comparatively larger chemical structure, with two –COOH groups and one –SO_4H group as cross-linkable sites with strong hydrophilicity, which renders biodegradable properties to the polymer matrix. Therefore, two types of the cross-linked network were shown by Li et al. [147] in the PVA-PAMPS Cross-linked membrane, in which SSA as a crosslinking agent reacted with sulfonated Poly Vinyl Alcohol to create the first crosslinked network, and *N*,N^{I} methylene bis (acrylamide), another crosslinking agent was added to react with 2-Acrylamido-2-methyl-1-propanesulfonic acid (AMPS) monomer to create the second Crosslinked network. The crosslinked interpenetrating network structure improved both the mechanical properties and hydrolytic stability and also reduced the swelling ratio of the composite PEMs significantly. Poly(vinyl alcohol) (PVA), as a polyhydroxy polymer was chosen as a polymer matrix by Tutgun et al. [292] owing to its hydrophilic characters and higher density functions, favorable for treatments chemically with crosslinking agent sulfosuccinic acid (SSA) to obtain crosslinked PVA–SSA esters. Hexagonal boron nitride hBN-doped PVA–SSA membrane may be undisturbedly utilized in higher temperature applications up to 150 °C. Altaf et al. [285] reported that sulfonated PVA (SPVA) also contains a sulfonic(SO_3^-) ionic group for proton conduction. The carboxyl groups in the sulfosuccinic acid crosslinking agent react with the –OH group in polyvinyl alcohol leading to a reduction in the number of a hydroxyl group (-OH group) which decreases the hydrophilicity of the membranes, whereas the number of sulfonic and carboxyl groups is increased. The SO_3H groups can block some water-absorbing sites, resulting in a reduction in swelling of the PVA-crosslinked PEMs. Zhou et al. [293] utilized KN–B (a type of reactive dyes that contain reactive vinyl sulfone groups that bonded covalently to sulfonic groups to enhance the water solubility) as a charge carrier to blend with PVA to form PVA/KN–B composite membrane. The covalent bond between KN-type reactive dyes and PVA possessed excellent chemical stability under acidic conditions. A three-dimensional network structure was constructed under the cross-linking action of diethylenetriamine penta acetic acid (DE) to form the compact inner structure. Therefore, the PVA/KN–B membrane had higher proton conductivity at room temperature, while the PVA/KN–B/DE membrane had better anti-oxidative stability during 168 h of evaluation.

Tian et al. [253] successfully utilized 3-Glycidoxypropyl trimethoxy silane (KH560) as a cross-linker into a PBI-based polymer matrix which hydrolysis to form Si–*O*–Si networks structure as shown in Fig. 9(a), that absorbed more H_3PO_4. Therefore, outstanding thermal and chemical durability and sufficient mechanical strength with enhanced proton conductivity were achieved from the composite membrane. Wang et al. [286] observed that the N–H sites in H_3PO_4-doped polybenzimidazole membrane can easily be reacted with crosslinking agent di-functional

Table 9

Electrochemical and mechanical properties of polymer electrolyte membranes with different crosslinking agents at different operating condition.

Crosslinking agent	Membrane	Operating condition (Temp.° ^0C) Relative humidity, RH%	Proton conductivity (S/cm)	Power Density (MW/cm^2)	Mechanical strength (MPa)	Ref.
Sulfosuccinic acid(SSA)	PA doped ABPBI-MMT/SPVA	140 °C, 100 %	0.157	1100	–	[285]
SSA and N, N' methylene bis(acrylamide)	SPVA/PAMPS-40 %	100 °C	0.146	–	29.23	[147]
3-Glycidoxy propyl trimethoxy silane	PA/CPBIm-5	180 °C	0.092	–	101.4	[253]
bis(3-phenyl-3,4-dihydro-2H-1,3-benzoxazinyl) isopropane	PA doped PBI	160 °C, anhydrous	0.073	690	–	[286]
Polyethylene glycole	$SPEEK/SiO_2$ (10 %)	80 °C,100 %	0.185	379	25	[287]
0.5 wt% Divinyl benzine	Poly(Styrene sulfonic acid grafted PEEK	120 °C	0.10	–	–	[288]
bis(2-methacryloxy ethyl) phosphate	VPA-SPAES	120 °C, 40 %	0.015	187	–	[289]
5 Vol% Triallyl cyanurate	PA doped 4VP Grafted ETFE	120 °C	0.039	–	43.6	[290]
3, $3'$ diaminobenzidine	sIPN-SPAEK-SPI	80 °C	0.128	–	64	[291]

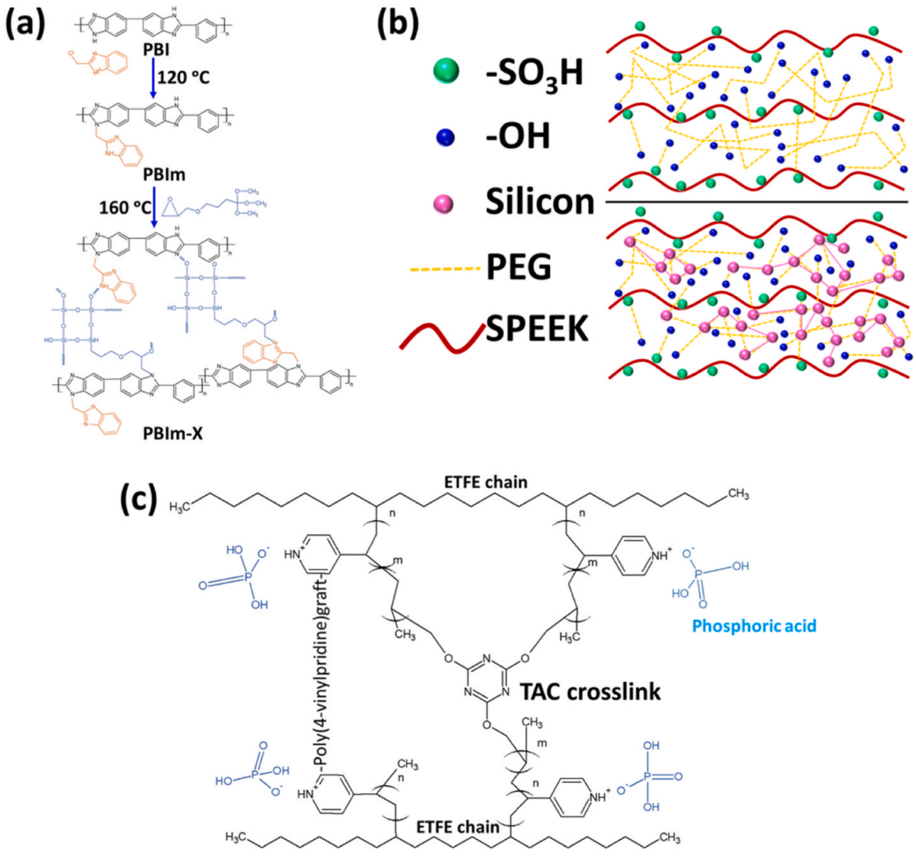

Fig. 9. (a)Si–*O*–Si networks structure by 3-Glycidoxypropyl trimethoxy silane (KH560) as a cross-linker into PBI based polymer matrix [253], (b)Cross-linked sulfonated poly (ether ether ketone)-poly ethylene glycol/silica organic–inorganic nanocomposite membrane [287], (c)Tentative molecular structure of crosslinked PA doped membrane based on 4-VP grafted ETFE film [290].

benzoxazine, which resulted in a decrease in proton transport; but at the same time, the greater free volume of crosslinked membrane further increased the Phosphoric Acid absorption and exhibited improved proton conductivity with mechanical performance and excellent oxidative stability. Kumari et al. [287] incorporated Poly Ethylene Glycol (PEG) as a cross-linking agent and dispersant, uniformly dispersing the SiO_2 nano-particles in the SPEEK/SiO_2 nanocomposite membrane as shown in Fig. 9(b), which showed excellent electrochemical and mechanical properties with superior hydrophilic-hydrophobic phase separation.

Hasegawa et al. [288] utilized divinyl benzene (DVB) < 1 wt% as a crosslinker into poly (styrene sulfonic acid)– grafted PEEK and investigated the influence of crosslinking on thermal resilience at 120^0 C for 500 h which suggested that very smaller content of crosslinkers may increase the hydrothermal stability at the higher temperature while decreasing the conductivity and WU tendency slightly. Ramly et al. [294] utilized Benzoin Ether Ether (BEE) as photoinitiated in case of UV crosslinking of SPEEK with Methyl Cellulose MC to form a more compact network, therefore improving the membrane dimensional stability. Dimensional stability, in the context of fuel cell membranes, was defined as the ability of the membrane to resist changes in its physical dimensions during hydration and dehydration cycles, which are common during fuel cell operation. This stability was deemed crucial, as excessive swelling during hydration could lead to mechanical deformation, reduced proton conductivity, and, eventually, membrane failure. The incorporation of Benzoin Ether Ether (BEE) as a photoinitiator in the crosslinking of sulfonated poly(ether ether ketone) (SPEEK) with methyl cellulose (MC) was shown to improve the dimensional stability of the membrane by forming a robust crosslinked network [295]. This crosslinking limited excessive water uptake, thereby reducing swelling and shrinkage during hydration-dehydration cycles, which enhanced mechanical durability and mitigated membrane deformation [296]. The methyl cellulose component provided mechanical reinforcement and flexibility, while covalent bonds formed via Benzoin Ethyl Ether (BEE) restricted the mobility of the polymer chains, preventing volumetric changes that could compromise proton conductivity [297]. Membranes with such crosslinking demonstrated superior proton conductivity under high-humidity conditions compared to non-crosslinked SPEEK membranes, as the compact structure minimized sulfonic group dilution and gas crossover [298]. The C–C group from BEE was introduced to form a crosslink that prevented the water swelling tendency of MC. The greater extent of water molecules was bound within the narrow holes of the crosslinked SPEEK-MC, relative to the membrane that was not cross-linked. With the enhancement of methyl cellulose concentration at the higher temperature, the proton transport enhances, since the internal pressing between SPEEK and methyl cellulose contributed to the migration of the charge carrier.

Kim et al. [289] explored a novel crosslinking agent bis(2-(methacryloyloxy) ethyl) phosphate, that reduces the rigidity of crosslinked Vinyl Phosphonic Acid-based polymer networks by the flexible oxyethylene connections and the phosphate group in bis(2-(methacryloyloxy) ethyl) phosphate structure, to make it more ductile. The crosslinking agent bis(2-(methacryloyloxy) ethyl) phosphate refrained the reduction of the mechanical and chemical stabilities by the poly (vinyl phosphonic acid) chains in the semi-Interpenetrating network membranes. Sithambaranathan et al. [290] reported on triallyl cyanurate (TAC) as a suitable crosslinker to improve the mechanical strength and thermal durability of radiation grafted poly(ethylene-*co*-tetrafluoroethylene) ETFE/poly4-vinylpyridine (4-VP)/PA membranes. The tentative molecular structure of crosslinked PA doped membrane based on 4-VP grafted ETFE film is shown in Fig. 9(c).

Wang et al. [291] developed a series of novel Semi-interpenetrating polymer networks from cross-linkable SPAEKs and sulfonated polyimides SPIs with 3,3′-diaminobenzidine (DAB) as crosslinkers. Most researchers used glutaraldehyde [30,299,300]and formaldehyde [301]**,** as crosslinking agents to prepare the chitosan-based biomaterials and studied their physical properties. Most recently Munavalli & Karidurganavar [302] reported on two different types of crosslinkers, polystyrene sulfonic acid-*co*-maleic acid (PSSA-MA) and sulphothalic acid (SPTA), which were employed in sulfonated poly(arylene ether ketones) copolymer to produce different hybrid PEMs. These crosslinkers demonstrate both the features of cross-linkable property and proton conductivity, which was primarily because of the availability of hydrophilic groups (-SO_3H and –COOH) in the membranes that incredibly increased both proton conductivity and thermal durability. The progress in proton conductivity of crosslinkers into various polymeric membranes is shown in Fig. 10. The improved crosslinking density due to the hydrogen bonding and ionic interaction favors the tensile strength and limits the passage of free radicals to arrive at the polymer backbone in both the series of membranes, which is liable for achieving the long-time durability of PEMs.

The various fillers and crosslinking agents, along with their primary advantages and disadvantages regarding hydrogen fuel cell performance, have been summarized in Table 10. Fillers within proton exchange membranes (PEMs) can undergo leaching under high-temperature and acidic conditions, potentially leading to membrane degradation and ion contamination. In PEM fuel cells, proton exchange membranes are employed, through which protons (H^+) are selectively conducted from the anode to the cathode. In contrast, AEM fuel cells utilize anion exchange membranes, by which hydroxide ions (OH^-) are transported from the cathode to the anode. These membranes differ not only in the type of charge carrier but also in the pH environment under which they operate. PEMs are generally operated under acidic conditions, while AEMs function in alkaline environments [306]. As a result, different catalyst materials are required, with precious metals such as platinum typically being used in PEM systems, whereas non-precious metal catalysts may be used in AEM systems due to their enhanced stability under alkaline conditions. Furthermore, the membrane materials themselves differ chemically. PEMs are commonly based on perfluorosulfonic acid polymers, such as Nafion, which provide high proton conductivity and chemical stability. AEMs, on the other hand, are typically composed of quaternary ammonium-functionalized polymers, designed to conduct anions and maintain chemical integrity in alkaline media.

Silica-based fillers, despite their inherent chemical stability, were found to be susceptible to leaching at elevated temperatures due to interactions between their functional groups, such as sulfonic and phosphonic acids, with water and protons in the membrane matrix [307]. Phosphotungstic acid (PWA)-doped silica was reported to leach under harsh conditions, introducing contaminants that degraded proton conductivity [307]. In comparison, titania (TiO_2)-based fillers exhibited greater thermal and chemical resilience, attributed to the stability of Ti–O bonds. However, functionalized TiO_2, such as sulfonated TiO_2, weakened filler-membrane interactions, increasing the risk of leaching [307]. Carbonaceous fillers, including sulfonated carbon nanotubes (sCNT), demonstrated thermal stability but underwent gradual hydrolysis of sulfonic acid groups, leading to the release of carbon particles over time [325]. Metal-organic frameworks (MOFs), like UiO-66-NH_2, provided high chemical stability, though functionalized variants, such as UiO-66-SO_3H, partially leached, reducing performance [319,326] Therefore, achieving a balance between filler stability and proton conductivity was considered essential for preventing degradation and ensuring the long-term efficiency of fuel cells.

6. Perspectives

The sulfonic group density on polymer surfaces may increase the protonic conductivity at low relative humidity (RHs) for a sustainable fuel cell. It could be innovative to develop chemical molecules with better proton conductivities than sulfonic groups. It might be possible to use the linkages between two aromatic rings in tetraamines or, and in dicarboxylic acids to improve proton conductivity. In order to create a flexible film with improved proton conductivity, N or O or other groups can be introduced into the main chain. A radiation-induced sulfonic group grafting to perfluorinated polymers might be a feasible strategy for making high temp/low RH PEMs. A polybenzimidazole (PBI) based membrane has been found to be the most feasible and can be used as a commercial PEM due to its excellent chemical properties at temperatures ranging from 100 °C to 250 °C without humidification.

The use of SPEEK and acid-base blends as Nafion substitutes under high-temperature conditions can be investigated. In order to prepare high temperature/low RH electrodes at a commercial scale, a modification of Nafion is suggested, since Nafion-modified PEMs are compatible with catalyst layers on electrode surfaces. Nafion continues to serve as the benchmark for PEM applications due to its superior proton

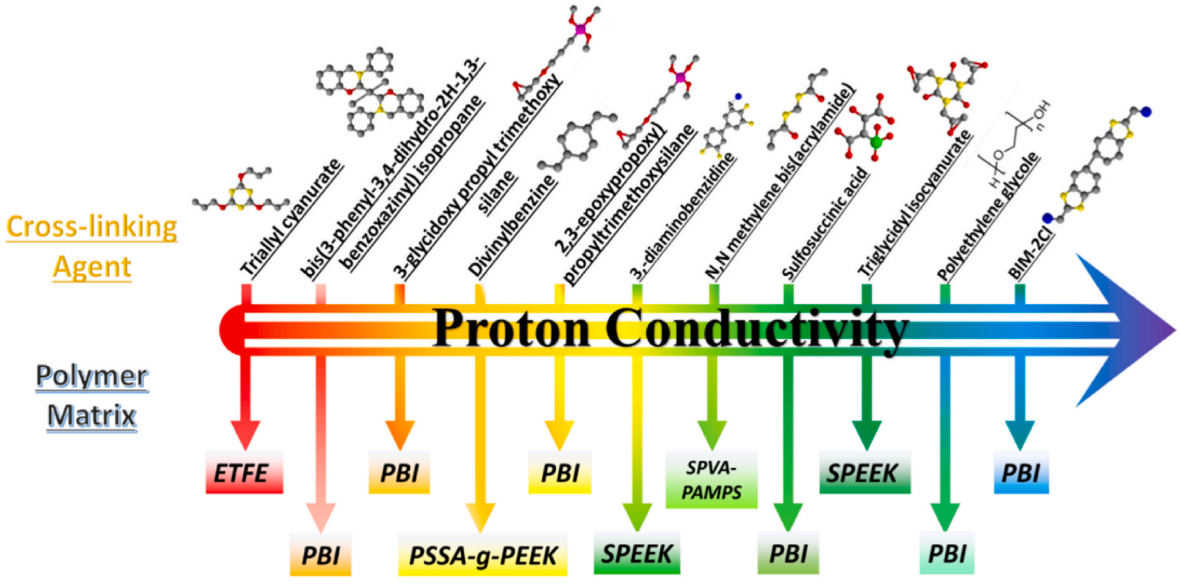

Fig. 10. The progress in proton conductivity using different cross-linking agents to polymeric membranes [147,253,260,285–288,290,303–305].

Table 10

Advantages and disadvantages of fillers and crosslinking agents in hydrogen fuel cell performance.

Type	Filler/Crosslinking Agent	Advantages	Disadvantages	Performance Impact on Hydrogen Fuel Cells
Silica (SiO_2) based fillers	Sulfonated silica	High proton conductivity, excellent water retention, chemical stability	Possible agglomeration reducing effective surface area	Enhances proton conductivity, improves durability under humid conditions [307]
	Phosphonated silica	Good chemical stability, promotes proton conduction	Limited mechanical strength compared to other fillers	Provides enhanced proton transport under low humidity conditions [308]
	Polydopamine-modified silica	Improved adhesion to polymer matrices, good thermal stability	Synthesis complexity, high cost	Enhances both mechanical properties and proton conductivity [309]
	Phosphotungstic acid doped silica	High proton conductivity due to acid doping	Vulnerable to leaching in humid environments	Enhances high proton conductivity under low-humidity conditions [309]
	Ionic liquid functionalized silica (ILS)	Superior ion transport, high conductivity under anhydrous conditions	Expensive, synthesis complexity	Enhances proton conductivity under anhydrous conditions [155]
Titania (TiO_2) based fillers	Amino acid functionalized TiO_2	Improves proton conductivity and chemical stability	Limited conductivity enhancement compared to other fillers	Enhances chemical stability and proton transport [146]
	2-Acrylamido-2-methyl-1-propane sulfonic acid) (PAMPS)-g TiO_2	High proton conductivity due to sulfonic acid group	Poor mechanical strength	Improves proton transfer while being susceptible to reduced mechanical durability [135]
	Poly sodium styrene sulfonate (PSSA)-*g* TiO_2	Good thermal and chemical stability, high proton transport	Limited flexibility, synthesis complexity	Enhances fuel cell performance by improving proton transport and thermal stability [135]
	Reduced graphene oxides nanoribbons (GONR)@ TiO_2	Enhanced surface area for proton transfer	High cost, synthesis complexity	Improves proton conductivity and mechanical strength [136]
	Sulfonated TiO_2 ($sTiO_2$)	Improved proton conductivity, good thermal and chemical stability	Possible agglomeration	Enhances proton conductivity, improves mechanical strength [310]
	Sulphophenylated TiO_2	High proton conductivity, improved chemical stability	Expensive synthesis	Enhances proton conductivity and durability under humid conditions [311]
Carbonaceous materials-based fillers	Sulfonated graphene oxide (sGO)	Excellent conductivity and large surface area	Poor dispersion in polymer matrix	Improves conductivity and durability [312]
	Phosphotungstic acid doped reduced graphene oxide (HPW/rGO)	High proton conductivity due to acid doping	Leaching of phosphotungstic acid in humid environments	Improves proton transfer and high-temperature performance [168]
	SATS-GO (sulfonated Poly(arylene thioether sulfone) grafted GO)	Enhanced chemical stability, high proton conductivity	Expensive, synthesis complexity	Improves proton conductivity, good chemical stability [172]
	SPTA-GO (sulfonated polytriazole grafted GO)	Good chemical stability, high ion conductivity	Limited improvement in mechanical strength	Enhances proton transfer and durability in humid conditions [173]
	Sulfonated carbon nanotube (sCNT)	High conductivity, increased mechanical strength	Agglomeration tendency, costly	Enhances both mechanical properties and proton transfer [313]
	Multiwalled carbon nanotube (MWCNT)	Increases mechanical strength, moderate conductivity	Poor dispersion, lower proton conductivity than sCNT	Enhances durability, moderate improvement in proton conductivity [314]
	Sulfonated MWCNT	High proton conductivity, improved mechanical properties	Expensive synthesis	Significant improvement in conductivity and strength [315]
	TiO_2@CNTs	Enhances proton transfer, excellent thermal stability	Synthesis complexity	Enhances proton transfer efficiency, especially under low-humidity conditions [178]
Metal-organic framework (MOF) based fillers	UiO-66-NH_2	Excellent thermal stability, high surface area for proton conduction	Expensive, synthesis complexity	Enhances proton transfer, improves chemical stability [316]
	UiO-66-SO_3H	High proton conductivity, good chemical stability	Possible acid leaching	Significantly improves proton transfer [317]
	GO@UiO-66-NH_2	High surface area, enhanced chemical stability	High cost, difficult synthesis	Enhances proton conductivity and mechanical strength [318]
	ZIF-8	Excellent thermal and chemical stability	Low proton conductivity	Primarily enhances mechanical stability with limited impact on proton conductivity [319]
	ZIF-67	Good chemical stability, moderate conductivity	Synthesis complexity	Improves durability with moderate proton transport improvements [320]
	Sul-MIL101	High proton conductivity, good chemical stability	High cost, possible leaching	Enhances proton conductivity under high-temperature conditions [216]
Crosslinking agents	Sulfosuccinic acid (SSA)	Enhances water retention, improves proton conductivity	Prone to degradation under extreme conditions	Improves conductivity and durability in PEMs [321]
	3-Glycidoxy propyl trimethoxy silane (GPTMS)	Enhances mechanical strength, improves filler dispersion	Requires complex synthesis	Improves mechanical stability with moderate conductivity improvements [322]
	Polyethylene glycol (PEG)	Enhances flexibility and water uptake	Low thermal stability	Improves membrane flexibility and water management but reduces thermal durability [323]
	Divinyl benzene (DVB)	Improves crosslinking density, enhances mechanical strength	Limits flexibility of membranes	Enhances mechanical properties but may reduce ion transport [324]

Table 11
Comparison of different polymer membranes.

Property	Nafion	SPEEK (Sulfonated Polyether Ether Ketone)	PBI (Polybenzimidazole)	SPES/SPAES-PES (Sulfonated Poly(ether sulfone)	Compare performance	References
Proton conductivity	>0.1 S/cm under hydrated conditions	0.01–0.05 S/cm	0.02–0.03 S/cm at high temperatures	0.05–0.08 S/cm	The perfluorosulfonic acid (PFSA) structure of Nafion enables well-defined ion channels for proton hopping, outperforming the weaker ion-conducting pathways in SPEEK and PBI. Composite membranes with fillers (e.g., sGO/SPEEK) still exhibit lower conductivity than Nafion, particularly under low humidity.	[327,328]
Chemical stability	High, with resistance to oxidative and acidic degradation	Prone to hydrolysis and desulfonation at high temperatures	Moderate chemical stability, but susceptible to oxidative degradation	Prone to chemical degradation under acidic conditions	The perfluorinated backbone of Nafion ensures superior chemical resilience, maintaining proton conductivity over long-term operation. Chemical modifications, such as UiO-66-NH_2/SPEEK, improve stability but still do not match Nafion's performance.	[329,330]
Mechanical strength	Durable under hydration-dehydration cycles and mechanical stresses	Suffers from brittle failure at low hydration	Brittle at high temperatures without hydration	Limited durability under stress and hydration cycles	Nafion retains mechanical integrity across varying temperatures and hydration levels. Alternative membranes tend to shrink, swell, or crack, with fillers like TiO_2/PBI enhancing strength but compromising conductivity.	[331,332]
Water retention	High, with excellent hydration even at low humidity	Dehydrates under low humidity, causing conductivity loss	Requires high hydration for optimal performance	Moderate water retention but unstable under fluctuating humidity	Nafion's hydrophilic sulfonic acid groups ensure effective water uptake, which promotes continuous proton transport. SPEEK-based membranes suffer from dehydration, resulting in significant performance decline.	[333,334]
Thermal stability	Operates effectively up to 80 °C and beyond	Degrades at elevated temperatures	Operates above 100 °C but faces mechanical failure	Limited thermal stability, with degradation under extended high-temperature exposure	Although PBI membranes are designed for high-temperature use, their mechanical durability declines over time. Nafion's thermal performance remains consistent under both high and low temperatures, which is unmatched by alternatives.	[335,336]

conductivity, chemical stability, mechanical durability, and water retention under varied conditions. Although alternatives like SPEEK and PBI demonstrate specific advantages, they often exhibit limitations in conductivity, stability, or mechanical integrity, preventing them from fully matching Nafion's performance. The Comparison of different crosslinking agents is shown in Table 11. Considering their outstanding stability at high operating temperatures, acid-base membranes are promising candidates for HT-PEMFCs; however, they need much more extensive testing before they can be applied practically. It may be possible to design PEMs for HT-PEMFC by incorporating inorganic particles modified by ionic liquid (ILs). It is, however, necessary to conduct more research into ways of immobilizing ILs on inorganic particles so that the leaching of ILs can be prevented. An ILs/PBI ion pair with the proper and appropriate design could provide a membrane electrolyte for future PEMFCs that can replace conventional membranes and provide a robust electrochemical application.

Most crosslinking agents form three-dimensional networks in the composite membrane, which act as reinforcements. PBI matrices may be optimized by using suitable crosslinking agents and crosslinking agents with their contents. In addition to providing a base for the membrane, carbon nanotubes or graphite are helpful for increasing its durability and stability. The fuel cell properties can be improved by a number of treatment processes, as shown in Fig. 11. Functionalized particles can be tested as a potential candidate for fabricating membranes with enhanced mechanical properties from inorganic particles. In order to make membranes stronger and more thermally resistant, polymer blending may be a promising procedure. To enhance desirable thermal and mechanical stability with PVA membranes, additional modification methods including copolymerization, cross-linking, polymer blending, and mixed methods that employed multiple modifications could be further investigated. The lack of oxygen absorption from phosphoric acid, phosphate ion adsorption on the catalyst surface, and electrolyte movement within the cells pose significant challenges for PBI-based membranes. The free electrolyte conducts ions in the electrode, which is crucial for the performance of the cell. A greater amount of research is needed to determine the optimal doping level required to reduce acid loss in cell membranes based on PBI.

7. Conclusions

Several novel PEMs with improved properties have been investigated in this article and have shown that they can be used as substitutes for Nafion. In order for PEMs to be effective in fuel cell applications, additives play an essential role in improving their mechanical and electrical properties. A polymer composite membrane operating at high temperatures can be improved by incorporating metal oxide, multi-walled carbon nanotubes, and reduced graphene oxide. However, the inclusion of higher loading of spherical metal oxide (silica, titania) particles with higher surface area resulted in a reduction in water uptake. It can blockade the proton conduction pathways or form more tortuous proton conductive pathways. In the case of nanotube metal oxides, the existing water molecules within the nanotube increase the water uptake. Composite membranes fabricated by sulfonation, carboxylation, silanisation, crosslinking, and functionalization with acid-based groups are capable of achieving optimal fuel cell performance for automotive applications. High-temperature problems caused by dehydration can easily be resolved with better proton conductors, including heteropolyacids and ionic liquids. Acid and ionic liquid leaching limit their feasible application as a viable candidate. Although ionic liquids are widely used, their adverse environmental impact still raises concerns. In low-temperature PEMs, additives like sulfonated graphite oxide can improve performance. The complicated manufacturing process and the high price of graphene-based materials restrict their use for commercialization. PEMs face changes in

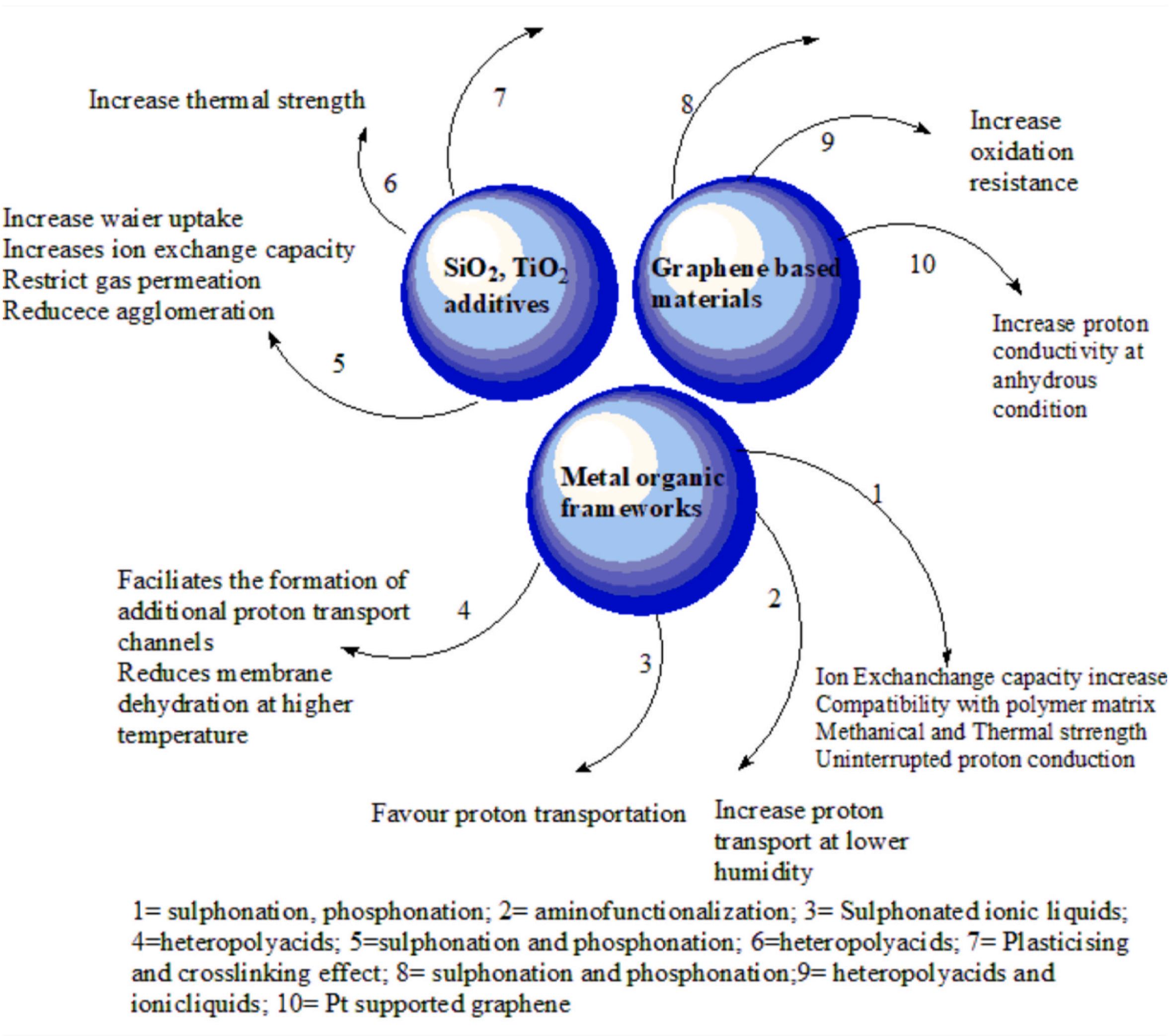

Fig. 11. Materials used to enhance the properties of fuel cell membranes.

temperature, humidity, and reactant activity, which can deteriorate the overall performance of the membrane. Cross-linking agent and their structural modification by functionalization significantly enhance the mechanical durability and proton conductivity at a time. In most cases, the synthesized membranes display poor performance due to some problems such as agglomeration and swelling. Balancing the states of combination i.e, the proportion of matrix material and additive materials, temperature, and so on effectively controls the target properties of the composite membrane and hinders aggregation of additive materials. The uniform dispersion impacts positively in terms of electrochemical properties, mechanical stability, and flexibility of composite membranes. Good dimensional and mechanical potency, high proton conductivity, optimum water retaining capability, and improved compatibility of additives with polymer matrices result in an excellent proton exchange membrane. Reviewing in detail, it was observed that the potential application of metal-organic frameworks into the PBI membrane matrix resulted in excellent proton conduction in extensive ranges of humidity and temperatures and higher chemical resilience in severe conditions. The highly porous surface area with tunable functionality of metal-organic frameworks makes it attractive to be associated with membrane matrices and guest species. HT-PEMFC applications can use commercial PEMs based on PBI membranes because they are the most practical ones. Metal-organic frameworks (MOFs), particularly UiO-66-NH_2 and UiO-66-SO_3H, along with sulfonated graphene oxide (sGO), have been identified as the most promising fillers for fuel cell membranes. These materials enhance proton conductivity, thermal stability, and mechanical strength by promoting robust filler-matrix interactions and providing effective proton transport pathways, essential for long-term fuel cell performance. In fact, the development of a low-priced sustainable proton exchange membrane can assist the feasible usage of fuel cell in portable devices, power generators, and in automobile applications. The mechanism analysis and design development of novel hybrid polymer electrolyte membranes should be the focal point of research in the field of materials science and an in-depth investigation needs to be conducted before any practical action is taken.

CRediT authorship contribution statement

Aminul Islam: Writing – review & editing, Writing – original draft, Supervision, Funding acquisition, Conceptualization. **Mamun Shahriar:** Writing – original draft, Resources, Methodology. **Md. Tarekul Islam:** Writing – original draft, Resources, Conceptualization. **Siow Hwa Teo:** Writing – original draft, Software, Resources, Formal analysis, Data curation. **M. Azizur R. Khan:** Writing – original draft, Validation, Resources, Conceptualization. **Yun Hin Taufiq-Yap:** Resources, Methodology, Investigation. **Suman C. Mohanta:** Writing – original draft, Resources, Methodology. **Ariyan Islam Rehan:** Writing – original draft, Resources, Investigation. **Adiba Islam Rasee:** Writing – original draft, Resources, Methodology, Formal analysis. **Khadiza Tul Kubra:** Writing – original draft, Resources, Methodology, Investigation, Data curation.

Md. Munjur Hasan: Writing – original draft, Formal analysis, Data curation. **Md. Shad Salman:** Writing – original draft, Resources, Conceptualization. **R.M. Waliullah:** Writing – original draft, Software, Resources, Formal analysis, Data curation. **Md. Nazmul Hasan:** Writing – original draft, Methodology, Formal analysis, Data curation. **Md. Chanmiya Sheikh:** Writing – original draft, Validation, Resources, Conceptualization. **Tetsuya Uchida:** Validation, Resources, Conceptualization. **Mrs Eti Awual:** Writing – original draft, Methodology, Data curation. **Mohammed Sohrab Hossain:** Writing – original draft, Software, Resources. **Hussein Znad:** Resources, Methodology, Formal analysis. **Md. Rabiul Awual:** Writing – review & editing, Writing – original draft, Supervision, Funding acquisition, Conceptualization.

Declaration of competing interest

The authors declare that they have no known competing financial interests or personal relationships that could have appeared to influence the work reported in this paper.

Acknowledgements

This research was supported by the Bangladesh Energy and Power Research Council (BEPRC) and carried out at the Hydrogen Energy and CO_2 Conversion Laboratory, Department of Petroleum and Mining Engineering, Jashore University of Science and Technology, Jashore 7408, Bangladesh.

References

[1] Tang H, Geng K, Wu L, Liu J, Chen Z, You W, Li N. Fuel cells with an operational range of–20° C to 200° C enabled by phosphoric acid-doped intrinsically ultramicroporous membranes. Nat Energy 2022;7(2):153–62.

[2] Wang B, Ling Z, Liu Y, Hu S, Liu Q, Fu X, Yang J. Side-chain vertical imidazole backbone enhances phosphoric acid uptake in Poly (2, 5-benzimidazole) membranes for high-temperature PEMFCs. Int J Hydrogen Energy 2024;84: 959–67.

[3] Ling Z, Wang B, Zhou Y, Liu Q, Fu X, Zhang R, Hu S, Li X, Zhao F, Bao X. Fabricating rapid proton conduction pathways with sepiolite nanorod-based ionogel/Nafion composites via electrospinning. Polymer 2024;306:127211.

[4] Liu Q, Wang X, Zhang X, Ling Z, Wu W, Fu X, Bao X. Polyethyleneimine-filled sepiolite nanorods-embedded poly (2, 5-benzimidazole) composite membranes for wide-temperature PEMFCs. J. Cleaner Prod 2022;359:131977.

[5] Zhang X, Fu X, Yang S, Zhang Y, Zhang R, Hu S, Bao X, Zhao F, Li X, Liu Q. Design of sepiolite-supported ionogel-embedded composite membranes without proton carrier wastage for wide-temperature-range operation of proton exchange membrane fuel cells. J. Mater. Chem. A. 2019;7(25):15288–301.

[6] Wang B, Ling Z, Wang X, Dong X, He J, Liu Q, Fu X, Zhang R, Hu S, Yang J. Amination modification of halloysite nanotubes for the in-situ synthesis of polybenzimidazole-based composite proton exchange membranes. Mater Lett 2024;377:137355.

[7] Xiong C, Ling Z, Wang B, Yu Y, Liu Q, Fu X, Wu C, Zhang R, Hu S, Bao X, Yang J. Electrospinning-assisted construction of rapid proton conduction channels in halloysite nanotube-encapsulated ionic liquid-embedded sulfonated poly (ether ether ketone) proton exchange membranes. Fuel (Guildf) 2024;362:130814.

[8] Liu Q, Xiong C, Shi H, Liu L, Wang X, Fu X, Zhang R, Hu S, Bao X, Li X, Zhao F. Halloysite ionogels enabling poly (2, 5-benzimidazole)-based proton-exchange membranes for wide-temperature-range applications. J Membr Sci 2023;668: 121192.

[9] Wang B, Ling Z, Li N, Liu Q, Fu X, Zhang R, Hu S, Meng Z, Zhao F, Li X. Graphene oxide-intercalated montmorillonite layered stack incorporated into poly (2, 5-benzimidazole) for preparing wide-temperature proton exchange membranes. ACS Appl Nano Mater 2023;6(21):20355–66.

[10] Meng Z, Zou Y, Li N, Wang B, Fu X, Zhang R, Hu S, Bao X, Li X, Zhao F, Liu Q. Graphene oxide-intercalated microbial montmorillonite to moderate the dependence of nafion-based PEMFCs in high-humidity environments. ACS Appl Energy Mater 2023;6(3):1771–80.

[11] Mogg L, Hao GP, Zhang S, Bacaksiz C, Zou YC, Haigh SJ, Peeters FM, Geim AK, Lozada-Hidalgo M. Atomically thin micas as proton-conducting membranes. Nat Nanotechnol 2019;14(10):962–6.

[12] Liu Q, Sun Q, Ni N, Luo F, Zhang R, Hu S, Bao X, Zhang F, Zhao F, Li X. Novel octopus shaped organic–inorganic composite membranes for PEMFCs. Int J Hydrogen Energy 2016;41(36):16160–6.

[13] Liu Q, Ni N, Sun Q, Wu X, Bao X, Fan Z, Zhang R, Hu S, Zhao F, Li X. Poly (2, 5-benzimidazole)/trisilanolphenyl POSS composite membranes for intermediate temperature PEM fuel cells. J Wuhan Univ Technol -Materials Sci Ed 2018;33: 212–20.

[14] Liu Q, Luo Y, Yang S, Xiong Y, Wang R, Fu X, Zhang R, Hu S, Bao X, Xu C. Transfer-free in-situ synthesis of high-performance polybenzimidazole grafted graphene oxide-based proton exchange membrane for high-temperature proton exchange membrane fuel cells. J Power Sources 2023;559:232666.

[15] Ling Z, Wang B, Liu Q, Fu X, Zhang R, Li X, Zhao F, Bao X, Hu S, Yang J. In-situ strategies for melamine-functionalized graphene oxide nanosheets-based nanocomposite proton exchange membranes in wide-temperature range applications. J Colloid Interface Sci 2025;678:388–99.

[16] Ling Z, Wang B, Liu Q, Fu X, Zhang R, Hu S, Li X, Zhao F, Bao X, Yang J. Amination modification of graphene oxide for the in-situ synthesis of sulfonated polyimide-based composite proton exchange membranes. Eur Polym J 2024;215: 113223.

[17] Zhou Y, Wang B, Ling Z, Liu Q, Fu X, Zhang Y, Zhang R, Hu S, Zhao F, Li X, Bao X. Advances in ionogels for proton-exchange membranes. Sci Total Environ 2024; 921:171099.

[18] Liu L, Zhu L, Wang Y, Guan X, Zhang Z, Li H, Wang F, Zhang H, Zhang Z, Yang Z, Ma T. Starfish-inspired solid-state Li-ion conductive membrane with balanced rigidity and flexibility for ultrastable lithium metal batteries. Angew Chem Int Ed 2025;64(7):e202420001.

[19] Cheng T, Liu Q, Jiang G, Yang B, Wang X, Wang P. Numerical study of proton exchange membrane fuel cells with airfoil cross flow field. J Power Sources 2025; 631:236232.

[20] Tian Y, Cai Y, Chen Y, Jia M, Hu H, Xie W, Li D, Song H, Guo S, Zhang X. Accessing the O Vacancy with anionic redox chemistry toward superior electrochemical performance in O3 type Na-ion oxide cathode. Adv Funct Mater 2024;34(32):2316342.

[21] Xia J, Gao L, Cao M, Zhang C, Tan M, Wang Q, Lv F, Tao L. Mn incorporated BiOCl anode for high performance sodium ion batteries. Appl Surf Sci 2025;695: 162888.

[22] Zhao C, Song Y, Chen H, Chen H, Li Y, Lei A, Wu Q, Zhu L. Improving the performance of microbial fuel cell stacks via capacitive-hydrogel bioanodes. Int J Hydrogen Energy 2025;97:708–17.

[23] Zhu L, Song Y, Chen H, Wang M, Liu Z, Wei X, Zhao C, Ai T. Optimization of power generation and sewage treatment in stacked pulsating gas-liquid-solid circulating fluidized bed microbial fuel cell using response surface methodology. Int J Hydrogen Energy 2025;101:161–72.

[24] Fu L, Wang J, Fu X, Zhao G. Finite-time Pade-based adaptive FNN controller implementation for microbial fuel cell with delay and multi-disturbance. Int J Hydrogen Energy 2025;98:1034–43.

[25] Cao M, Chen W, Ma Y, Huang H, Luo S, Zhang C. Cross-linked K2Ti4O9 nanoribbon arrays with superior rate capability and cyclability for lithium-ion batteries. Mater Lett 2020;279:128495.

[26] Chen X, Wei S, Wang J, Tong F, Söhnel T, Waterhouse GI, Zhang W, Kennedy J, Taylor MP. Lithium insertion/extraction mechanism in Mg2Sn anode for lithium-ion batteries. Intermetallics 2024;169:108306.

[27] Zhan Y, Ren X, Zhao S, Guo Z. Enhancing prediction of electron affinity and ionization energy in liquid organic electrolytes for lithium-ion batteries using machine learning. J Power Sources 2025;629:235992.

[28] Chu JY, Kim AR, Nahm KS, Lee HK, Yoo DJ. Synthesis and characterization of partially fluorinated sulfonated poly (arylene biphenylsulfone ketone) block copolymers containing 6F-BPA and perfluorobiphenylene units. Int J Hydrogen Energy 2013;38(14):6268–74.

[29] Kim B, Kannan R, Nahm KS, Yoo DJ. Development and characterization of highly conducting nonfluorinated di and triblock copolymers for polymer electrolyte membranes. J Dispersion Sci Technol 2016;37(9):1315–23.

[30] Rosli NA, Loh KS, Wong WY, Yunus RM, Lee TK, Ahmad A, Chong ST. Review of chitosan-based polymers as proton exchange membranes and roles of chitosan-supported ionic liquids. Int J Mol Sci 2020;21(2):632.

[31] Escorihuela J, Narducci R, Compañ V, Costantino F. Proton conductivity of composite polyelectrolyte membranes with metal-organic frameworks for fuel cell applications. Adv. Mater. Interfaces 2019;6(2):1801146.

[32] Liu Y, Liu S, Lai X, Miao J, He D, Li N, Luo F, Shi Z, Liu S. Polyoxometalate-modified sponge-like graphene oxide monolith with high proton-conducting performance. Adv Funct Mater 2015;25(28):4480–5.

[33] Yagiz M, Çelik S, Topcu A. Performance comparison of bio-inspired flow field designs for direct methanol fuel cell and proton exchange membrane fuel cell. Int J Hydrogen Energy 2024;75:200–10.

[34] Liu N, Bi S, Liu J, Ye Q, Liu G, Ou Y, Liu H, Gong C. PA-doped nanofiber composite proton exchange membranes with ultrahigh proton conductivity and methanol barrier performance for direct methanol fuel cells. Sep Purif Technol 2025;358:130313.

[35] Li X, Faghri A. Review and advances of direct methanol fuel cells (DMFCs) part I: design, fabrication, and testing with high concentration methanol solutions. J Power Sources 2013;226:223–40.

[36] Matos BR, Dresch MA, Santiago EI, Moraes LP, Carastan DJ, Schoenmaker J, Velasco-Davalos IA, Ruediger A, Tavares AC, Fonseca FC. Nafion membranes annealed at high temperature and controlled humidity: structure, conductivity, and fuel cell performance. Electrochim Acta 2016;196:110–7.

[37] Safronova EY, Lysova AA, Voropaeva DY, Yaroslavtsev AB. Approaches to the modification of perfluorosulfonic acid membranes. Membranes 2023;13(8):721.

[38] Maiti TK, Singh J, Dixit P, Majhi J, Bhushan S, Bandyopadhyay A, Chattopadhyay S. Advances in perfluorosulfonic acid-based proton exchange membranes for fuel cell applications: a review. Chem Eng J Adv 2022;12:100372.

[39] Abdullah RF, Rashid U, Taufiq-Yap YH, Ibrahim ML, Ngamcharussrivichai C, Azam M. Synthesis of bifunctional nanocatalyst from waste palm kernel shell and its application for biodiesel production. RSC Adv 2020;10(45):27183–93.

[40] Syazwani ON, Ibrahim ML, Kanda H, Goto M, Taufiq-Yap YH. Esterification of high free fatty acids in supercritical methanol using sulfated angel wing shells as catalyst. J Supercrit Fluids 2017;124:1–9.

[41] Esmaeili N, Gray EM, Webb CJ. Non-fluorinated polymer composite proton exchange membranes for fuel cell applications–A review. ChemPhysChem 2019;20(16):2016–53.

[42] Park JS, Shin MS, Kim CS. Proton exchange membranes for fuel cell operation at low relative humidity and intermediate temperature: an updated review. Curr Opin Electrochem 2017;5(1):43–55.

[43] Choi SR, Kim DY, An WY, Choi S, Park K, Yim SD, Park JY. Assessing the degradation pattern and mechanism of membranes in polymer electrolyte membrane fuel cells using open-circuit voltage hold and humidity cycle test protocols. Mater Sci Energy Technol 2022;5:66–73.

[44] Ishimoto T, Koyama M. A review of molecular-level mechanism of membrane degradation in the polymer electrolyte fuel cell. Membranes 2012;2(3):395–414.

[45] Wang D, Yao D, Wang Y, Wang F, Xin Y, Song S, Zhang Z, Su F, Zheng Y. Carbon nanotubes and graphene oxide-based solvent-free hybrid nanofluids functionalized mixed-matrix membranes for efficient CO2/N2 separation. Sep Purif Technol 2019;221:421–32.

[46] Agmon N. The grotthuss mechanism. Chem Phys Lett 1995;244(5–6):456–62.

[47] Deamer DW. Proton permeation of lipid bilayers. J Bioenerg Biomembr 1987:457–79.

[48] Gagliardi GG, Ibrahim A, Borello D, El-Kharouf A. Composite polymers development and application for polymer electrolyte membrane technologies—a review. Molecules 2020;25(7):1712.

[49] Wong CY, Wong WY, Ramya K, Khalid M, Loh KS, Daud WR, Lim KL, Walvekar R, Kadhum AA. Additives in proton exchange membranes for low-and high-temperature fuel cell applications: a review. Int J Hydrogen Energy 2019;44(12):6116–35.

[50] Karimi MB, Mohammadi F, Hooshyari K. Recent approaches to improve Nafion performance for fuel cell applications: a review. Int J Hydrogen Energy 2019;44(54):28919–38.

[51] Yin C, Li J, Zhou Y, Zhang H, Fang P, He C. Phase separation and development of proton transport pathways in metal oxide nanoparticle/nafion composite membranes during water uptake. J Phys Chem C 2018;122(17):9710–7.

[52] Kuwertz R, Kirstein C, Turek T, Kunz U. Influence of acid pretreatment on ionic conductivity of Nafion® membranes. J Membr Sci 2016;500:225–35.

[53] Junoh H, Jaafar J, Nordin NA, Ismail AF, Othman MH, Rahman MA, Aziz F, Yusof N. Performance of polymer electrolyte membrane for direct methanol fuel cell application: perspective on morphological structure. Membranes 2020;10(3):34.

[54] Phonyiem M, Chaiwongwattana S, Lao-Ngam C, Sagarik K. Proton transfer reactions and dynamics of sulfonic acid group in Nafion®. Phys Chem Chem Phys 2011;13(23):10923–39.

[55] Marx D, Tuckerman ME, Hutter J, Parrinello M. The nature of the hydrated excess proton in water. Nature 1999;397(6720):601–4.

[56] Kreuer KD. Proton conductivity: materials and applications. Chem Mater 1996;8(3):610–41.

[57] Paul DK, McCreery R, Karan K. Proton transport property in supported Nafion nanothin films by electrochemical impedance spectroscopy. J Electrochem Soc 2014;161(14):F1395.

[58] Tang H, Geng K, Hu Y, Li N. Synthesis and properties of phosphonated polysulfones for durable high-temperature proton exchange membranes fuel cell. J Membr Sci 2020;605:118107.

[59] Lazanas AC, Prodromidis MI. Electrochemical impedance spectroscopy— a tutorial. ACS Meas. Sci. Au. 2023;3(3):162–93.

[60] Heimerdinger P, Rosin A, Danzer MA, Gerdes T. A novel method for humidity-dependent through-plane impedance measurement for proton conducting polymer membranes. Membranes 2019;9(5):62.

[61] Al-Madani G, Kailani MH, Al-Hussein M. Test system for through-plane conductivity measurements of hydrogen proton exchange membranes. Int J Electrochem Sci 2015;10(8):6465–74.

[62] Choi Y, Platzek P, Coole J, Buche S, Fortin P. The influence of membrane thickness and catalyst loading on performance of proton exchange membrane fuel cells. J Electrochem Soc 2024;171(10):104507.

[63] Saidin NU, Jehan OS, Leong KS, Choo TF, Wong WY, Loh KS, Yunus RM. Influence of ionomer concentration and membrane thickness on membrane electrode assembly in alkaline fuel cell performance. Asia Pac J Chem Eng 2024;19(2):3024.

[64] Shi N, Wang G, Wang Q, Wang L, Li Q, Yang J. Acid doped branched poly (biphenyl pyridine) membranes for high temperature proton exchange membrane fuel cells and vanadium redox flow batteries. Chem. Eng. J. 2024;489:151121.

[65] Li Y, Liao J, Lu Y, Shen J. High-performance ether-free branched poly (isatin terphenyl fluorene) with sulfonated pendant side chains for proton exchange membrane fuel cells. J Power Sources 2024;615:235079.

[66] Lai W, Haile SM. Impedance spectroscopy as a tool for chemical and electrochemical analysis of mixed conductors: a case study of ceria. J Am Ceram Soc 2005;88(11):2979–97.

[67] Gervillié-Mouravieff C, Bao W, Steingart DA, Meng YS. Non-destructive characterization techniques for battery performance and life-cycle assessment. Nat Rev Electr Eng 2024;1(8):547–58.

[68] Hunsom M. Electrochemical impedance spectroscopy (EIS) for PEM fuel cells. Spectroscopic properties of inorganic and organometallic compounds: techniques. Materials and Applications 2011;42:196–247.

[69] Müller F, Ferreira CA, Azambuja DS, Aleman C, Armelin E. Measuring the proton conductivity of ion-exchange membranes using electrochemical impedance spectroscopy and through-plane cell. J Phys Chem B 2014;118(4):1102–12.

[70] Germer W, Harms C, Tullius V, Leppin J, Dyck A. Comparison of conductivity measurement systems using the example of nafion and anion exchange membrane. Solid State Ionics 2015;275:71–4.

[71] Guo JW, Wang JL, Jiang SK, Li L. To Measure In-plane conductivity of Nafion membrane with general electrochemical approach. Mater Chem Phys 2023;303:127824.

[72] De León SE, Pupovac A, McArthur SL. Three-Dimensional (3D) cell culture monitoring: opportunities and challenges for impedance spectroscopy. Biotechnol Bioeng 2020;117(4):1230–40.

[73] Bertok T, Lorencova L, Chocholova E, Jane E, Vikartovska A, Kasak P, Tkac J. Electrochemical impedance spectroscopy based biosensors: mechanistic principles, analytical examples and challenges towards commercialization for assays of protein cancer biomarkers. Chemelectrochem 2019;6(4):989–1003.

[74] Santana J, Espinoza-Andaluz M, Villon G, Qi Y, Li T, Andersson M. Temperature impact on the internal resistance of a polymer electrolyte fuel cell considering the electrochemical impedance spectroscopy diagnosis. ECS Trans 2020;96(1):183.

[75] Cabello SP, Mollá S, Ochoa NA, Marchese J, Giménez E, Compañ V. New bio-polymeric membranes composed of alginate-carrageenan to be applied as polymer electrolyte membranes for DMFC. J Power Sources 2014;265:345–55.

[76] Orazem ME, Tribollet B. A tutorial on electrochemical impedance spectroscopy. ChemTexts 2020;6(2):12.

[77] Fuentes I, Andrio A, García-Bernabé A, Escorihuela J, Viñas C, Teixidor F, Compañ V. Structural and dielectric properties of cobaltacarborane composite polybenzimidazole membranes as solid polymer electrolytes at high temperature. Phys Chem Chem Phys 2018;20(15):10173–84.

[78] Zuo Z, Fu Y, Manthiram A. Novel blend membranes based on acid-base interactions for fuel cells. Polymers 2012;4(4):1627–44.

[79] Shaari N, Kamarudin SK. Recent advances in additive-enhanced polymer electrolyte membrane properties in fuel cell applications: an overview. Int J Energy Res 2019;43(7):2756–94.

[80] Lade H, Kumar V, Arthanareeswaran G, Ismail AF. Sulfonated poly (arylene ether sulfone) nanocomposite electrolyte membrane for fuel cell applications. A review Int. J. Hydrogen Energy. 2017;42(2):1063–74.

[81] de Azpiazu Nadal, Ignasi. Proton-conducting (blend) membranes based on sulfonated/phosphonated and basic polymers. Diss. Université de Pau et des Pays de l'Adour 2023. Universität Stuttgart (Allemagne).

[82] Zhai S, Lu Z, Ai Y, Liu X, Wang Q, Lin J, He S, Tian M, Chen L. Highly selective proton exchange membranes for vanadium redox flow batteries enabled by the incorporation of water-insoluble phosphotungstic acid-metal organic framework nanohybrids. J Membr Sci 2022;645:120214.

[83] Sarirchi S, Rowshanzamir S, Mehri F. Simultaneous improvement of ionic conductivity and oxidative stability of sulfonated poly (ether ether ketone) nanocomposite proton exchange membrane for fuel cell application. Int J Energy Res 2020;44(4):2783–800.

[84] Matos BR, Santiago EI, Rey JF, Ferlauto AS, Traversa E, Linardi M, Fonseca FC. Nafion-based composite electrolytes for proton exchange membrane fuel cells operating above 120 C with titania nanoparticles and nanotubes as fillers. J Power Sources 2011;196(3):1061–8.

[85] Zakaria Z, Shaari N, Kamarudin SK, Bahru R, Musa MT. A review of progressive advanced polymer nanohybrid membrane in fuel cell application. Int J Energy Res 2020;44(11):8255–95.

[86] Shi G, Tryk DA, Iwataki T, Yano H, Uchida M, Iiyama A, Uchida H. Unparalleled mitigation of membrane degradation in fuel cells via a counter-intuitive approach: suppression of H_2O_2 production at the hydrogen anode using a Pt skin–PtCo catalyst. J. Mater. Chem. A. 2020;8(3):1091–4.

[87] Trogadas P, Parrondo J, Mijangos F, Ramani V. Degradation mitigation in PEM fuel cells using metal nanoparticle additives. J Mater Chem 2011;21(48):19381–8.

[88] Mohammed M, Jawad AJ, Mohammed AM, Oleiwi JK, Adam T, Osman AF, Dahham OS, Betar BO, Gopinath SC, Jaafar M. Challenges and advancement in water absorption of natural fiber-reinforced polymer composites. Polym Test 2023;124:108083.

[89] Cazan C, Enesca A, Andronic L. Synergic effect of TiO2 filler on the mechanical properties of polymer nanocomposites. Polymers 2021;13(12):2017.

[90] Islam SS, Jose T, Seikh AH, Karim MR, Alnaser IA, Bose S. Shear-aligned graphene oxide nanosheets incorporated PVDF composite membranes for selective dye rejection with high water flux. RSC Adv 2024;14(38):27852–61.

[91] Trisno ML, Dayan A, Lee SJ, Egert F, Gerle M, Kraglund MR, Jensen JO, Aili D, Roznowska A, Michalak A, Park HS. Reinforced gel-state polybenzimidazole hydrogen separators for alkaline water electrolysis. Energy Environ Sci 2022;15(10):4362–75.

[92] Soleimani B, Asl AH, Khoshandam B, Hooshyari K. Enhanced performance of nanocomposite membrane developed on sulfonated poly (1, 4-phenylene ether-ether-sulfone) with zeolite imidazole frameworks for fuel cell application. Sci Rep 2023;13(1):8238.

[93] Burye T. Effect of elevated PEM fuel cell operating temperature (120° C and 140° C) and membrane thickness on proton conductivity for combat vehicle use. ECS Trans 2020;97(7):685.

[94] Subianto S, Pica M, Casciola M, Cojocaru P, Merlo L, Hards G, Jones DJ. Physical and chemical modification routes leading to improved mechanical properties of perfluorosulfonic acid membranes for PEM fuel cells. J Power Sources 2013;233:216–30.

[95] Kumar PS, Carolin CF. Polymer electrolyte membranes. Diffus Found 2019;23:82–9.

[96] Xu G, Wei Z, Li S, Li J, Yang Z, Grigoriev SA. In-situ sulfonation of targeted silica-filled Nafion for high-temperature PEM fuel cell application. Int J Hydrogen Energy 2019;44(56):29711–6.

[97] Xu G, Wu Z, Wei Z, Zhang W, Wu J, Li Y, Li J, Qu K, Cai W. Non-destructive fabrication of Nafion/silica composite membrane via swelling-filling modification strategy for high temperature and low humidity PEM fuel cell. Renew Energy 2020;153:935–9.

[98] Di Z, Xie Q, Li H, Mao D, Li M, Zhou D, Li L. Novel composite proton-exchange membrane based on proton-conductive glass powders and sulfonated poly (ether ether ketone). J Power Sources 2015;273:688–96.

[99] Esmaielzadeh S, Ahmadizadegan H. Construction of proton exchange membranes under ultrasonic irradiation based on novel fluorine functionalizing sulfonated polybenzimidazole/cellulose/silica bionanocomposite. Ultrason Sonochem 2018;41:641–50.

[100] Shao ZG, Xu H, Li M, Hsing IM. Hybrid Nafion–inorganic oxides membrane doped with heteropolyacids for high temperature operation of proton exchange membrane fuel cell. Solid State Ionics 2006;177(7–8):779–85.

[101] Wang J, Bai H, Zhang H, Zhao L, Chen H, Li Y. Anhydrous proton exchange membrane of sulfonated poly (ether ether ketone) enabled by polydopamine-modified silica nanoparticles. Electrochim Acta 2015;152:443–55.

[102] Song JM, Woo HS, Sohn JY, Shin J. 12HPW/meso-SiO2 nanocomposite CSPEEK membranes for proton exchange membrane fuel cells. J Ind Eng Chem 2016;36:132–8.

[103] Chia MY, San Thiam H, Leong LK, Koo CH, Saw LH. Study on improvement of the selectivity of proton exchange membrane via incorporation of silicotungstic acid-doped silica into SPEEK. Int J Hydrogen Energy 2020;45(42):22315–23.

[104] Devrim Y, Devrim H, Eroglu I. Polybenzimidazole/SiO2 hybrid membranes for high temperature proton exchange membrane fuel cells. Int J Hydrogen Energy 2016;41(23):10044–52.

[105] Mishra AK, Kim NH, Lee JH. Effects of ionic liquid-functionalized mesoporous silica on the proton conductivity of acid-doped poly (2, 5-benzimidazole) composite membranes for high-temperature fuel cells. J Membr Sci 2014;449:136–45.

[106] Kuo YJ, Lin HL. Effects of mesoporous fillers on properties of polybenzimidazole composite membranes for high-temperature polymer fuel cells. Int J Hydrogen Energy 2018;43(9):4448–57.

[107] Sharma PP, Gupta H, Kulshrestha V. Phosphorylated hybrid silica-sulfonated polyethersulfone composite proton-exchange membranes: magnetic resonance investigation for enhanced proton-exchange dynamics. Int J Hydrogen Energy 2020;45(34):16955–64.

[108] Chesnokova A, Lebedeva OV, Malakhova EA, Raskulova TV, Kulshrestha V, Kuzmin AV, Pozdnyakov AS, Pozhidaev YN. New non-fluoridated hybrid proton exchange membranes based on commercial precursors. Int J Hydrogen Energy 2020;45(37):18716–30.

[109] Xu G, Dong X, Xue B, Huang J, Wu J, Cai W. Recent approaches to achieve high temperature operation of nafion membranes. Energies 2023;16(4):1565.

[110] Zhang H, He Y, Zhang J, Ma L, Li Y, Wang J. Constructing dual-interfacial proton-conducting pathways in nanofibrous composite membrane for efficient proton transfer. J Membr Sci 2016;505:108–18.

[111] Zeng J, Jiang SP. Characterization of high-temperature proton-exchange membranes based on phosphotungstic acid functionalized mesoporous silica Nanocomposites for fuel cells. J Phys Chem C 2011;115(23):11854–63.

[112] Wu W, Li Y, Chen P, Liu J, Wang J, Zhang H. Constructing ionic liquid-filled proton transfer channels within nanocomposite membrane by using functionalized graphene oxide. ACS Appl Mater Interfaces 2016;8(1):588–99.

[113] Sivasankaran A, Sangeetha D. Influence of sulfonated SiO2 in sulfonated polyether ether ketone nanocomposite membrane in microbial fuel cell. Fuel (Guildf) 2015;159:689–96.

[114] Joseph J, Tseng CY, Hwang BJ. Phosphonic acid-grafted mesostructured silica/Nafion hybrid membranes for fuel cell applications. J Power Sources 2011;196(18):7363–71.

[115] Muchtar S, Yusuf M, Mulyati S, Syamsuddin Y, Fathanah U, Takagi R. Membrane modification with polydopamine to improve performances—a mini review. J Rekayasa Kimia Lingkungan 2023;18(1):53–68.

[116] Xu G, Xue S, Wei Z, Li J, Qu K, Li Y, Cai W. Stabilizing phosphotungstic acid in Nafion membrane via targeted silica fixation for high-temperature fuel cell application. Int J Hydrogen Energy 2021;46(5):4301–8.

[117] Du L, Yan X, He G, Wu X, Hu Z, Wang Y. SPEEK proton exchange membranes modified with silica sulfuric acid nanoparticles. Int J Hydrogen Energy 2012;37(16):11853–61.

[118] Boutsika LG, Enotiadis A, Nicotera I, Simari C, Charalambopoulou G, Giannelis EP, Steriotis T. Nafion® nanocomposite membranes with enhanced properties at high temperature and low humidity environments. Int J Hydrogen Energy 2016;41(47):22406–14.

[119] Oh K, Kwon O, Son B, Lee DH, Shanmugam S. Nafion-sulfonated silica composite membrane for proton exchange membrane fuel cells under operating low humidity condition. J Membr Sci 2019;583:103–9.

[120] Kim AR, Vinothkannan M, Yoo DJ. Artificially designed, low humidifying organic–inorganic (SFBC-50/FSiO2) composite membrane for electrolyte applications of fuel cells. Compos B Eng 2017;130:103–18.

[121] Tung SP, Hwang BJ. Synthesis and characterization of hydrated phosphor–silicate glass membrane prepared by an accelerated sol–gel process with water/vapor management. J Mater Chem 2005;15(34):3532–8.

[122] Elumalai V, Rathinavel S, Annapooranan R, Ganapathikrishnan M, Sangeetha D. Phosphonated mesoporous silica based composite membranes for high temperature proton exchange membrane fuel cells. J Solid State Electrochem 2019;23:1837–50.

[123] Zhang J, Liu J, Lu S, Zhu H, Aili D, De Marco R, Xiang Y, Forsyth M, Li Q, Jiang SP. Ion-exchange-induced selective etching for the synthesis of amino-functionalized hollow mesoporous silica for elevated-high-temperature fuel cells. ACS Appl Mater Interfaces 2017;9(37):31922–30.

[124] Li J, Xu G, Luo X, Xiong J, Liu Z, Cai W. Effect of nano-size of functionalized silica on overall performance of swelling-filling modified Nafion membrane for direct methanol fuel cell application. Appl Energy 2018;213:408–14.

[125] Li Y, Zhang M, Wang X, Li Z, Zhao L. Anhydrous conducting composite membranes composed of SPEEK/silica/ionic liquids for high-temperature proton exchange. Electrochim Acta 2016;222:1308–15.

[126] Kurdakova V, Quartarone E, Mustarelli P, Magistris A, Caponetti E, Saladino ML. PBI-based composite membranes for polymer fuel cells. J Power Sources 2010;195(23):7765–9.

[127] Seo K, Nam KH, Han H. Proton transport in aluminum-substituted mesoporous silica channel-embedded high-temperature anhydrous proton-exchange membrane fuel cells. Sci Rep 2020;10(1):10352.

[128] Sahin A. The development of Speek/Pva/Teos blend membrane for proton exchange membrane fuel cells. Electrochim Acta 2018;271:127–36.

[129] Therese JA, Gayathri R, Selvakumar K, Prabhu MR, Sivakumar P. Incorporation of sulfonated silica nano particles into polymer blend membrane for PEM fuel cell applications. Mater Res Express 2019;6(11):115336.

[130] Zhang J, Aili D, Lu S, Li Q, Jiang SP. Advancement toward polymer electrolyte membrane fuel cells at elevated temperatures. 2020. Research.

[131] Cozzi D, de Bonis C, D'Epifanio A, Mecheri B, Tavares AC, Licoccia S. Organically functionalized titanium oxide/Nafion composite proton exchange membranes for fuel cells applications. J Power Sources 2014;248:1127–32.

[132] Solanki JN, Mishra PS, Murthy ZV. In situ prepared Tio 2 nanoparticles cross-linked sulfonated pva membranes with high proton conductivity for dmfc. Quim Nova 2016;39:704–11.

[133] Wu H, Cao Y, Shen X, Li Z, Xu T, Jiang Z. Preparation and performance of different amino acids functionalized titania-embedded sulfonated poly (ether ether ketone) hybrid membranes for direct methanol fuel cells. J Membr Sci 2014;463:134–44.

[134] de Bonis C, Simari C, Kosma V, Mecheri B, D'Epifanio A, Allodi V, Mariotto G, Brutti S, Suarez S, Pilar K, Greenbaum S. Enhancement of proton mobility and mitigation of methanol crossover in sPEEK fuel cells by an organically modified titania nanofiller. J Solid State Electrochem 2016;20:1585–98.

[135] Salarizadeh P, Javanbakht M, Pourmahdian S, Hazer MS, Hooshyari K, Askari MB. Novel proton exchange membranes based on proton conductive sulfonated PAMPS/PSSA-TiO2 hybrid nanoparticles and sulfonated poly (ether ether ketone) for PEMFC. Int J Hydrogen Energy 2019;44(5):3099–114.

[136] Roy T, Wanchoo SK, Pal K. Novel sulfonated poly (ether ether ketone)/rGONR@TiO2 nanohybrid membrane for proton exchange membrane fuel cells. Solid State Ionics 2020;349:115296.

[137] Haragirimana A, Li N, Ingabire PB, Hu Z, Chen S. Multi-component organic/inorganic blend proton exchange membranes based on sulfonated poly (arylene ether sulfone) s for fuel cells. Polymer 2020;210:123015.

[138] Pinar FJ, Cañizares P, Rodrigo MA, Ubeda D, Lobato J. Titanium composite PBI-based membranes for high temperature polymer electrolyte membrane fuel cells. Effect on titanium dioxide amount. RSC Adv 2012;2(4):1547–56.

[139] Özdemir Y, Üregen N, Devrim Y. Polybenzimidazole based nanocomposite membranes with enhanced proton conductivity for high temperature PEM fuel cells. Int J Hydrogen Energy 2017;42(4):2648–57.

[140] Lobato J, Cañizares P, Rodrigo MA, Úbeda D, Pinar FJ. A novel titanium PBI-based composite membrane for high temperature PEMFCs. J Membr Sci 2011;369(1–2):105–11.

[141] Lee S, Seo K, Ghorpade RV, Nam KH, Han H. High temperature anhydrous proton exchange membranes based on chemically-functionalized titanium/polybenzimidazole composites for fuel cells. Mater Lett 2020;263:127167.

[142] Wang G, Kang J, Yang S, Lu M, Wei H. Influence of structure construction on water uptake, swelling, and oxidation stability of proton exchange membranes. Int J Hydrogen Energy 2024;50:279–311.

[143] Erkartal M, Aslan A, Erkilic U, Dadi S, Yazaydin O, Usta H, Sen U. Anhydrous proton conducting poly (vinyl alcohol)(PVA)/poly (2-acrylamido-2-methylpropane sulfonic acid)(PAMPS)/1, 2, 4-triazole composite membrane. Int J Hydrogen Energy 2016;41(26):11321–30.

[144] Li C, Song Y, Wang X, Zhang Q. Synthesis, characterization and application of S-TiO2/PVDF-g-PSSA composite membrane for improved performance in MFCs. Fuel (Guildf) 2020;264:116847.

[145] Shawky AM, Kotp YH, Mousa MA, Aboelfadl MM, Hekal EE, Zakaria K. Effect of titanium oxide/reduced graphene (TiO2/rGO) addition onto water flux and reverse salt diffusion thin-film nanocomposite forward osmosis membranes. Environ Sci Pollut Res 2024;31(16):24584–98.

[146] Wu H, Shen X, Xu T, Hou W, Jiang Z. Sulfonated poly (ether ether ketone)/amino-acid functionalized titania hybrid proton conductive membranes. J Power Sources 2012;213:83–92.

[147] Li HQ, Liu XJ, Wang H, Yang H, Wang Z, He J. Proton exchange membranes with cross-linked interpenetrating network of sulfonated polyvinyl alcohol and poly (2-acrylamido-2-methyl-1-propanesulfonic acid): excellent relative selectivity. J Membr Sci 2020;595:117511.

[148] Devrim Y, Erkan S, Bac N, Eroğlu I. Preparation and characterization of sulfonated polysulfone/titanium dioxide composite membranes for proton exchange membrane fuel cells. Int J Hydrogen Energy 2009;34(8):3467–75.

[149] Peressut AB, Latorrata S, Stampino PG, Dotelli G. Development of self-assembling sulfonated graphene oxide membranes as a potential proton conductor. Mater Chem Phys 2021;257:123768.

[150] Sacca A, Carbone A, Gatto I, Pedicini R, Freni A, Patti A, Passalacqua E. Composites Nafion-titania membranes for Polymer Electrolyte Fuel Cell (PEFC) applications at low relative humidity levels: chemical physical properties and electrochemical performance. Polym Test 2016;56:10–8.

[151] Yang D, Tan Y, Li B, Ming P, Xiao Q, Zhang C. A review of the transition region of membrane electrode assembly of proton exchange membrane fuel cells: design, degradation, and mitigation. Membranes.;12(3):306.

[152] Vengatesan MR, Mittal V. Surface modification of nanomaterials for application in polymer nanocomposites: an overview. Surface modification of nanoparticle and natural fiber fillers. 2015. p. 1–28.

[153] Shukla AK, Alam J, Alhoshan M. Recent advancements in polyphenylsulfone membrane modification methods for separation applications. Membranes 2022;12(2):247.

[154] Zhang C, Peng Z, Huang C, Zhang B, Xing C, Chen H, Cheng H, Wang J, Tang S. High-energy all-in-one stretchable micro-supercapacitor arrays based on 3D laser-induced graphene foams decorated with mesoporous ZnP nanosheets for self-powered stretchable systems. Nano Energy 2021;81:105609.

[155] De Araujo CC, Kreuer KD, Schuster M, Portale G, Mendil-Jakani H, Gebel G, Maier J. Poly (p-phenylene sulfone) s with high ion exchange capacity: ionomers with unique microstructural and transport features. Phys Chem Chem Phys 2009;11(17):3305–12.

[156] Zhao Y, Zhang Y, Wang Y, Cao D, Sun X, Zhu H. Versatile zero-to three-dimensional carbon for electrochemical energy storage. Carbon Energy 2021;3(6):895–915.

[157] Taufiq Musa M, Shaari N, Kamarudin SK. Carbon nanotube, graphene oxide and montmorillonite as conductive fillers in polymer electrolyte membrane for fuel cell: an overview. Int J Energy Res 2021;45(2):1309–46.

[158] Akbari E, Buntat Z. Benefits of using carbon nanotubes in fuel cells: a review. Int J Energy Res 2017;41(1):92–102.

[159] Wallace GG, Chen J, Li D, Moulton SE, Razal JM. Nanostructured carbon electrodes. J Mater Chem 2010;20(18):3553–62.

[160] Chen R, Xu F, Fu K, Zhou J, Shi Q, Xue C, Lyu Y, Guo B, Li G. Enhanced proton conductivity and dimensional stability of proton exchange membrane based on sulfonated poly (arylene ether sulfone) and graphene oxide. Mater Res Bull 2018;103:142–9.

[161] Li P, Wu W, Liu J, Shi B, Du Y, Li Y, Wang J. Investigating the nanostructures and proton transfer properties of Nafion-GO hybrid membranes. J Membr Sci 2018;555:327–36.

[162] Zarrin H, Higgins D, Jun Y, Chen Z, Fowler M. Functionalized graphene oxide nanocomposite membrane for low humidity and high temperature proton exchange membrane fuel cells. J Phys Chem C 2011;115(42):20774–81.

[163] Feng K, Tang B, Wu P. Sulfonated graphene oxide–silica for highly selective Nafion-based proton exchange membranes. J Mater Chem A 2014;2(38):16083–92.

[164] Maiti J, Kakati N, Woo SP, Yoon YS. Nafion® based hybrid composite membrane containing GO and dihydrogen phosphate functionalized ionic liquid for high temperature polymer electrolyte membrane fuel cell. Compos Sci Technol 2018;155:189–96.

[165] Lee DC, Yang HN, Park SH, Park KW, Kim WJ. Self-humidifying Pt–graphene/SiO2 composite membrane for polymer electrolyte membrane fuel cell. J Membr Sci 2015;474:254–62.

[166] Prapainainar P, Pattanapisutkun N, Prapainainar C, Kongkachuichay P. Incorporating graphene oxide to improve the performance of Nafion-mordenite composite membranes for a direct methanol fuel cell. Int J Hydrogen Energy 2019;44(1):362–78.

[167] Sadakiyo M, Okawa H, Shigematsu A, Ohba M, Yamada T, Kitagawa H. Promotion of low-humidity proton conduction by controlling hydrophilicity in layered metal–organic frameworks. J Am Chem Soc 2012;134(12):5472–5.

[168] Sun F, Qin LL, Zhou J, Wang YK, Rong JQ, Chen YJ, Ayaz S, Hai-Yin YU, Liu L. Friedel-Crafts self-crosslinking of sulfonated poly (etheretherketone) composite proton exchange membrane doped with phosphotungstic acid and carbon-based nanomaterials for fuel cell applications. J Membr Sci 2020;611:118381.

[169] Beydaghi H, Javanbakht M, Bagheri A, Salarizadeh P, Ghafarian-Zahmatkesh H, Kashefi S, Kowsari E. Novel nanocomposite membranes based on blended sulfonated poly (ether ether ketone)/poly (vinyl alcohol) containing sulfonated graphene oxide/Fe_3O_4 nanosheets for DMFC applications. RSC Adv 2015;5(90):74054–64.

[170] Üregen N, Pehlivanoğlu K, Özdemir Y, Devrim Y. Development of polybenzimidazole/graphene oxide composite membranes for high temperature PEM fuel cells. Int J Hydrogen Energy 2017;42(4):2636–47.

[171] Kim J, Kim K, Han J, Lee H, Kim H, Kim S, Sung YE, Lee JC. End-group cross-linked membranes based on highly sulfonated poly (arylene ether sulfone) with vinyl functionalized graphene oxide as a cross-linker and a filler for proton exchange membrane fuel cell application. J Polym Sci 2020;58(24):3456–66.

[172] Lee H, Han J, Kim K, Kim J, Kim E, Shin H, Lee JC. Highly sulfonated polymer-grafted graphene oxide composite membranes for proton exchange membrane fuel cells. J Ind Eng Chem 2019;74:223–32.

[173] Han J, Lee H, Kim J, Kim S, Kim H, Kim E, Sung YE, Kim K, Lee JC. Sulfonated poly (arylene ether sulfone) composite membrane having sulfonated polytriazole grafted graphene oxide for high-performance proton exchange membrane fuel cells. J Membr Sci 2020;612:118428.

[174] Yin C, Xiong B, Liu Q, Li J, Qian L, Zhou Y, He C. Lateral-aligned sulfonated carbon-nanotubes/Nafion composite membranes with high proton conductivity and improved mechanical properties. J Membr Sci 2019;591:117356.

[175] Liu YL, Su YH, Chang CM, Wang DM, Lai JY. Preparation and applications of Nafion-functionalized multiwalled carbon nanotubes for proton exchange membrane fuel cells. J Mater Chem 2010;20(21):4409–16.

[176] Steffy NJ, Parthiban V, Sahu AK. Uncovering Nafion-multiwalled carbon nanotube hybrid membrane for prospective polymer electrolyte membrane fuel cell under low humidity. J Membr Sci 2018;563:65–74.

[177] Shukla A, Dhanasekaran P, Sasikala S, Nagaraju N, Bhat SD, Pillai VK. Nanocomposite membrane electrolyte of polyaminobenzene sulfonic acid grafted single walled carbon nanotubes with sulfonated polyether ether ketone for direct methanol fuel cell. Int J Hydrogen Energy 2019;44(50):27564–74.

[178] Tsen WC. Hydrophilic TiO2 decorated carbon nanotubes/sulfonated poly (ether ether ketone) composite proton exchange membranes for fuel cells. Polym Eng Sci 2020;60(8):1832–41.

[179] Feng M, You Y, Zheng P, Liu J, Jia K, Huang Y, Liu X. Low-swelling proton-conducting multi-layer composite membranes containing polyarylene ether nitrile and sulfonated carbon nanotubes for fuel cells. Int J Hydrogen Energy 2016;41(9):5113–22.

[180] Feng MN, Pu ZJ, Zheng PL, Jia K, Liu XB. Sulfonated carbon nanotubes synergistically enhanced the proton conductivity of sulfonated polyarylene ether nitriles. RSC Adv 2015;5(43):34372–6.

[181] Moreno NG, Gervasio D, García AG, Robles JF. Polybenzimidazole-multiwall carbon nanotubes composite membranes for polymer electrolyte membrane fuel cells. J Power Sources 2015;300:229–37.

[182] Kannan R, Kagalwala HN, Chaudhari HD, Kharul UK, Kurungot S, Pillai VK. Improved performance of phosphonated carbon nanotube–polybenzimidazole composite membranes in proton exchange membrane fuel cells. J Mater Chem 2011;21(20):7223–31.

[183] Vinothkannan M, Kim AR, Yoo DJ. Sulfonated graphene oxide/Nafion composite membranes for high temperature and low humidity proton exchange membrane fuel cells. RSC Adv 2018;8(14):7494–508.

[184] Liao X, Huang Y, Zhou Y, Liu H, Cai Y, Lu S, Yao Y. Homogeneously dispersed HPW/graphene for high efficient catalytic oxidative desulfurization prepared by electrochemical deposition. Appl Surf Sci 2019;484:917–24.

[185] Vinothkannan M, Kim AR, Ryu SK, Yoo DJ. Structurally modulated and functionalized carbon nanotubes as potential filler for Nafion matrix toward improved power output and durability in proton exchange membrane fuel cells operating at reduced relative humidity. J Membr Sci 2022;649:120393.

[186] Ali Z, Yaqoob S, Yu J, D'Amore A. Critical review on the characterization, preparation, and enhanced mechanical, thermal, and electrical properties of carbon nanotubes and their hybrid filler polymer composites for various applications. Composites Part C: Open Access 2024;13:100434.

[187] Ozkan S, Valle F, Mazare A, Hwang I, Taccardi N, Zazpe R, Macak JM, Cerri I, Schmuki P. Optimized polymer electrolyte membrane fuel cell electrode using TiO2 nanotube arrays with well-defined spacing. ACS Appl Nano Mater 2020;3(5):4157–70.

[188] Sivasubramanian G, Hariharasubramanian K, Deivanayagam P, Ramaswamy J. High-performance SPEEK/SWCNT/fly ash polymer electrolyte nanocomposite membranes for fuel cell applications. Polym J 2017;49(10):703–9.

[189] Kannan R, Aher PP, Palaniselvam T, Kurungot S, Kharul UK, Pillai VK. Artificially designed membranes using phosphonated multiwall carbon nanotube−polybenzimidazole composites for polymer electrolyte fuel cells. J Phys Chem Lett 2010;1(14):2109–13.

[190] Kakati N, Das G, Yoon YS. Proton-conducting membrane based on epoxy resin-poly (vinyl alcohol)-sulfosuccinic acid blend and its nanocomposite with sulfonated multiwall carbon nanotubes for fuel-cell application. J Kor Phys Soc 2016;68(2):311–6.

[191] Liu H, Gong C, Wang J, Liu X, Liu H, Cheng F, Wang G, Zheng G, Qin C, Wen S. Chitosan/silica coated carbon nanotubes composite proton exchange membranes for fuel cell applications. Carbohydr Polym 2016;136:1379–85.

[192] Lee DC, Yang HN, Park SH, Kim WJ. Nafion/graphene oxide composite membranes for low humidifying polymer electrolyte membrane fuel cell. J Membr Sci 2014;452:20–8.

[193] Yang HN, Lee WH, Choi BS, Kim WJ. Preparation of Nafion/Pt-containing TiO_2/graphene oxide composite membranes for self-humidifying proton exchange membrane fuel cell. J Membr Sci 2016;504:20–8.

[194] Rajput A, Sharma PP, Yadav V, Kulshrestha V. Highly stable graphene oxide composite proton exchange membrane for electro-chemical energy application. Int J Hydrogen Energy 2020;45(34):16976–83.

[195] Ding Y, Zhang J, Chang L, Zhang X, Liu H, Jiang L. Preparation of high-performance ionogels with excellent transparency, good mechanical strength, and high conductivity. Adv. Mater. 2017;29(47):1704253.

[196] Lim DW, Kitagawa H. Proton transport in metal–organic frameworks. Chem. Rev. 2020;120(16):8416–67.

[197] Lim MY, Kim K. Sulfonated poly (arylene ether sulfone) and perfluorosulfonic acid composite membranes containing perfluoropolyether grafted graphene oxide for polymer electrolyte membrane fuel cell applications. Polymers 2018;10(6):569.

[198] Kim K, Bae J, Lim MY, Heo P, Choi SW, Kwon HH, Lee JC. Enhanced physical stability and chemical durability of sulfonated poly (arylene ether sulfone) composite membranes having antioxidant grafted graphene oxide for polymer electrolyte membrane fuel cell applications. J Membr Sci 2017;525:125–34.

[199] Abouzari-Lotf E, Zakeri M, Nasef MM, Miyake M, Mozarmnia P, Bazilah NA, Emelin NF, Ahmad A. Highly durable polybenzimidazole composite membranes with phosphonated graphene oxide for high temperature polymer electrolyte membrane fuel cells. J Power Sources 2019;412:238–45.

[200] Oh K, Son B, Sanetuntikul J, Shanmugam S. Polyoxometalate decorated graphene oxide/sulfonated poly (arylene ether ketone) block copolymer composite membrane for proton exchange membrane fuel cell operating under low relative humidity. J Membr Sci 2017;541:386–92.

[201] Xu C, Liu X, Cheng J, Scott K. A polybenzimidazole/ionic-liquid-graphite-oxide composite membrane for high temperature polymer electrolyte membrane fuel cells. J Power Sources 2015;274:922–7.

[202] Sun X, Zhang T, Liu X, Ren H, Zhang Q, Feng Y, Ding H. Multi-functionalized acid-base double-shell nanotubes are incorporated into the proton exchange membrane to cope with low humidity conditions. Int J Hydrogen Energy 2020;45 (55):30673–88.

[203] Bai Y, Dou Y, Xie LH, Rutledge W, Li JR, Zhou HC. Zr-based metal–organic frameworks: design, synthesis, structure, and applications. Chem Soc Rev 2016; 45(8):2327–67.

[204] Wu HB, Lou XW. Metal-organic frameworks and their derived materials for electrochemical energy storage and conversion: promises and challenges. Sci Adv 2017;3(12):eaap9252.

[205] Luo R, Zhang K, Qin Y, Xie L, Chai X, Zhang L, Du G, Ge S, Rezakazemi M, Aminabhavi TM, Xu K. Amine-functionalized UiO-66 incorporated electrospun cellulose/chitosan porous nanofibrous membranes for removing copper ions. Chem. Eng. J. 2024;480:148077.

[206] Yang F, Huang H, Wang X, Li F, Gong Y, Zhong C, Li JR. Proton conductivities in functionalized UiO-66: tuned properties, thermogravimetry mass, and molecular simulation analyses. Cryst Growth Des 2015;15(12):5827–33.

[207] Luan Y, Zheng N, Qi Y, Yu J, Wang G. Development of a SO3H-functionalized UiO-66 metal–organic framework by postsynthetic modification and studies of its catalytic activities. Eur J Inorg Chem 2014;2014(26):4268–72.

[208] Phang WJ, Jo H, Lee WR, Song JH, Yoo K, Kim B, Hong CS. Superprotonic conductivity of a UiO-66 framework functionalized with sulfonic acid groups by facile postsynthetic oxidation. Angew Chem Int Ed 2015;54(17):5142–6.

[209] Li F, Chen L, Wei Y, Yin Z, Que K. A novel UiO-66-NH2/graphene oxide composite thin membrane for retarding membrane wetting in membrane distillation. J Ind Eng Chem 2023;123:62–71.

[210] Huazhen S, Beibei T, Peiyi W. Rational design of S-UiO-66@ GO hybrid nanosheets for proton exchange membranes with significantly enhanced transport performance. ACS Appl Mater Interfaces 2017;9(31):26077–87.

[211] Cao J, Zhou H, Huang C, Wu Q, Yao W. ZIF-8-derived Zn, N-codoped porous carbon as a high-performance piezocatalyst for organic pollutant degradation and hydrogen production. J Colloid Interface Sci 2023;645:794–805.

[212] Hu Y, Song X, Zheng Q, Wang J, Pei J. Zeolitic imidazolate framework-67 for shape stabilization and enhanced thermal stability of paraffin-based phase change materials. RSC Adv 2019;9(18):9962–7.

[213] Liu Q, Li Z, Wang D, Li Z, Peng X, Liu C, Zheng P. Metal organic frameworks modified proton exchange membranes for fuel cells. Front Chem 2020;8:694.

[214] Zhang Z, Ren J, Xu J, Meng L, Zhao P, Wang Z. Long-term durable solid state electrolyte membranes based on a metal–organic framework with phosphotungstic acid confined in the mesoporous cages. Int J Hydrogen Energy 2020;45(51):27527–38.

[215] Erkartal M, Usta H, Citir M, Sen U. Proton conducting poly (vinyl alcohol)(PVA)/ poly (2-acrylamido-2-methylpropane sulfonic acid)(PAMPS)/zeolitic imidazolate framework (ZIF) ternary composite membrane. J Membr Sci 2016;499:156–63.

[216] Li Z, He G, Zhao Y, Cao Y, Wu H, Li Y, Jiang Z. Enhanced proton conductivity of proton exchange membranes by incorporating sulfonated metal-organic frameworks. J Power Sources 2014;262:372–9.

[217] Devarajan N, Suresh P. MIL-101-SO$_3$H metal–organic framework as a Brønsted acid catalyst in Hantzsch reaction: an efficient and sustainable methodology for one-pot synthesis of 1, 4-dihydropyridine. New J Chem 2019;43(17):6806–14.

[218] Zhang B, Cao Y, Li Z, Wu H, Yin Y, Cao L, He X, Jiang Z. Proton exchange nanohybrid membranes with high phosphotungstic acid loading within metal-organic frameworks for PEMFC applications. Electrochim Acta 2017;240:186–94.

[219] Hu X, Lu Y, Dai F, Liu C, Liu Y. Host–guest synthesis and encapsulation of phosphotungstic acid in MIL-101 via "bottle around ship": an effective catalyst for oxidative desulfurization. Microporous Mesoporous Mater 2013;170:36–44.

[220] Sun H, Tang B, Wu P. Rational design of S-UiO-66@ GO hybrid nanosheets for proton exchange membranes with significantly enhanced transport performance. Acs Appl. Mater. Interfaces 2017;9(31):26077–87.

[221] Yang P, Liu Q, Liu J, Zhang H, Li Z, Li R, Liu L, Wang J. Interfacial growth of a metal–organic framework (UiO-66) on functionalized graphene oxide (GO) as a suitable seawater adsorbent for extraction of uranium (VI). J. Mater. Chem. A. 2017;5(34):17933–42.

[222] da Trindade LG, Borba KM, Zanchet L, Lima DW, Trench AB, Rey F, Diaz U, Longo E, Bernardo-Gusmão K, Martini EM. SPEEK-based proton exchange membranes modified with MOF-encapsulated ionic liquid. Mater Chem Phys 2019;236:121792.

[223] Askari S, Jafarzadeh M, Christensen DB, Kegnæs S. A synergic activity of urea/ butyl imidazolium ionic liquid supported on UiO-66-NH 2 metal–organic framework for synthesis of oximes. Catal Lett 2020;150:3159–73.

[224] Sun H, Tang B, Wu P. Two-dimensional zeolitic imidazolate framework/carbon nanotube hybrid networks modified proton exchange membranes for improving transport properties. ACS Appl Mater Interfaces 2017;9(40):35075–85.

[225] Ge L, Lin R, Zhu Z, Wang H. A nitrogen-doped electrocatalyst from metal–organic framework-carbon nanotube composite. J Mater Res 2018;33(5):538–45.

[226] Barjola A, Escorihuela J, Andrio A, Giménez E, Compañ V. Enhanced conductivity of composite membranes based on sulfonated poly (ether ether ketone)(SPEEK) with zeolitic imidazolate frameworks (ZIFs). Nanomaterials 2018;8(12):1042.

[227] Pan Y, Sun K, Liu S, Cao X, Wu K, Cheong WC, Chen Z, Wang Y, Li Y, Liu Y, Wang D. Core–shell ZIF-8@ ZIF-67-derived CoP nanoparticle-embedded N-doped carbon nanotube hollow polyhedron for efficient overall water splitting. J Am Chem Soc 2018;140(7):2610–8.

[228] Barjola A, Reyes-Rodríguez JL, Solorza-Feria O, Gimenez E, Compan V. Novel SPEEK-ZIF-67 proton exchange nanocomposite membrane for PEMFC application at intermediate temperatures. Ind Eng Chem Res 2021;60(25):9107–18.

[229] Lee JG, Yoon S, Yang E, Lee JH, Song K, Moon HR, An K. Structural evolution of ZIF-67-derived catalysts for furfural hydrogenation. J Catal 2020;392:302–12.

[230] Anahidzade N, Abdolmaleki A, Dinari M, Tadavani KF, Zhiani M. Metal-organic framework anchored sulfonated poly (ether sulfone) as a high temperature proton exchange membrane for fuel cells. J Membr Sci 2018;565:281–92.

[231] Zheng P, Liu Q, Wang D, Li Z, Meng Y, Zheng Y. Preparation of covalent-ionically cross-linked UiO-66-NH2/sulfonated aromatic composite proton exchange membranes with excellent performance. Front Chem 2020;8:56.

[232] Rao Z, Tang B, Wu P. Proton conductivity of proton exchange membrane synergistically promoted by different functionalized metal–organic frameworks. ACS Appl Mater Interfaces 2017;9(27):22597–603.

[233] Vermoortele F, Ameloot R, Vimont A, Serre C, De Vos D. An amino-modified Zr-terephthalate metal–organic framework as an acid–base catalyst for cross-aldol condensation. Chem. Commun. 2011;47(5):1521–3.

[234] Serra-Crespo P, Van Der Veen MA, Gobechiya E, Houthoofd K, Filinchuk Y, Kirschhock CE, Martens JA, Sels BF, De Vos DE, Kapteijn F, Gascon J. NH2-MIL-53 (Al): a high-contrast reversible solid-state nonlinear optical switch. J Am Chem Soc 2012;134(20):8314–7.

[235] Zhang K, Chen Y, Nalaparaju A, Jiang J. Functionalized metal–organic framework MIL-101 for CO 2 capture: multi-scale modeling from ab initio calculation and molecular simulation to breakthrough prediction. CrystEngComm (Camb) 2013; 15(47):10358–66.

[236] Férey G, Mellot-Draznieks C, Serre C, Millange F, Dutour J, Surblé S, Margiolaki I. A chromium terephthalate-based solid with unusually large pore volumes and surface area. Science. 2005;309(5743):2040–2.

[237] Umeyama D, Horike S, Inukai M, Hijikata Y, Kitagawa S. Confinement of mobile histamine in coordination nanochannels for fast proton transfer. Angew Chem 2011;123(49):11910–3.

[238] Chen Z, Fang P, Zou X, Shi Z, Zhang J, Sun Z, Guo S, Yan F. Interlayer polymerization to construct a fully conjugated covalent organic framework as a metal-free oxygen reduction reaction catalyst for anion exchange membrane fuel cells. Small 2024;20(35):2401880.

[239] James JB, Wang J, Meng L, Lin YS. ZIF-8 membrane ethylene/ethane transport characteristics in single and binary gas mixtures. Ind Eng Chem Res 2017;56(26): 7567–75.

[240] Zhang H, Wu W, Li Y, Liu Y, Wang J, Zhang B, Liu J. Polyelectrolyte microcapsules as ionic liquid reservoirs within ionomer membrane to confer high anhydrous proton conductivity. J Power Sources 2015;279:667–77.

[241] Hou H, Sun G, He R, Wu Z, Sun B. Alkali doped polybenzimidazole membrane for high performance alkaline direct ethanol fuel cell. J Power Sources 2008;182(1): 95–9.

[242] He G, Li Z, Li Y, Li Z, Wu H, Yang X, Jiang Z. Zwitterionic microcapsules as water reservoirs and proton carriers within a Nafion membrane to confer high proton conductivity under low humidity. ACS Appl Mater Interfaces 2014;6(8):5362–6.

[243] Suzuki K, Iizuka Y, Tanaka M, Kawakami H. Phosphoric acid-doped sulfonated polyimide and polybenzimidazole blend membranes: high proton transport at wide temperatures under low humidity conditions due to new proton transport pathways. J Mater Chem 2012;22(45):23767–72.

[244] Fedorova IV, Krestyaninov MA, Kiselev MG, Safonova LP. Solvent effect on proton transfer in the complexes of N, N-dimethylformamide with sulfuric and phosphoric acid: a DFT investigation. J Mol Struct 2016;1106:424–9.

[245] Park CH, Lee SY, Hwang DS, Shin DW, Cho DH, Lee KH, Kim TW, Kim TW, Lee M, Kim DS, Doherty CM. Nanocrack-regulated self-humidifying membranes. Nature 2016;532(7600):480–3.

[246] Haile SM, Pintauro PN. Proton transport for fuel cells. J Mater Chem 2010;20(30): 6211–3.

[247] Che Q, Zhou L, Wang J. Fabrication and characterization of phosphoric acid doped imidazolium ionic liquid polymer composite membranes. J Mol Liq 2015; 206:10–8.

[248] Dang J, Zhao L, Zhang J, Liu J, Wang J. Imidazole microcapsules toward enhanced phosphoric acid loading of polymer electrolyte membrane for anhydrous proton conduction. J Membr Sci 2018;545:88–98.

[249] Mecerreyes D, Grande H, Miguel O, Ochoteco E, Marcilla R, Cantero I. Porous polybenzimidazole membranes doped with phosphoric acid: highly proton-conducting solid electrolytes. Chem Mater 2004;16(4):604–7.

[250] Ou T, Chen H, Hu B, Zheng H, Li W, Wang Y. A facile method of asymmetric ether-containing polybenzimidazole membrane for high temperature proton exchange membrane fuel cell. Int J Hydrogen Energy 2018;43(27):12337–45.

[251] Maity S, Singha S, Jana T. Low acid leaching PEM for fuel cell based on polybenzimidazole nanocomposites with protic ionic liquid modified silica. Polymer 2015;66:76–85.

[252] Li J, Wang S, Liu F, Tian X, Wang X, Chen H, Mao T, Wang Z. HT-PEMs based on nitrogen-heterocycle decorated poly (arylene ether ketone) with enhanced proton conductivity and excellent stability. Int J Hydrogen Energy 2018;43(33): 16248–57.

[253] Tian X, Wang S, Li J, Liu F, Wang X, Chen H, Wang D, Ni H, Wang Z. Benzimidazole grafted polybenzimidazole cross-linked membranes with excellent PA stability for high-temperature proton exchange membrane applications. Appl Surf Sci 2019;465:332–9.

[254] Liu F, Wang S, Li J, Tian X, Wang X, Chen H, Wang Z. Polybenzimidazole/ionic-liquid-functional silica composite membranes with improved proton conductivity for high temperature proton exchange membrane fuel cells. J Membr Sci 2017; 541:492–9.

[255] Mustarelli P, Quartarone E, Grandi S, Carollo A, Magistris A. Polybenzimidazole-based membranes as a real alternative to nafion for fuel cells operating at low temperature. Adv. Mater. 2008;20(7):1339–43.

[256] Lee KS, Spendelow JS, Choe YK, Fujimoto C, Kim YS. An operationally flexible fuel cell based on quaternary ammonium-biphosphate ion pairs. Nat Energy 2016; 1(9):16120.

[257] Chen H, Wang S, Liu F, Wang D, Li J, Mao T, Liu G, Wang X, Xu J, Wang Z. Base-acid doped polybenzimidazole with high phosphoric acid retention for HT-PEMFC applications. J Membr Sci 2020;596:117722.

[258] Hong L, Wang B, Zhao C. Phosphoric acid doped high temperature proton exchange membranes based on comb-shaped polymers with quaternized graft architectures. Appl Surf Sci 2019;483:785–92.

[259] Tian D, Gu T, Yellamilli SN, Bae C. Phosphoric acid-doped ion-pair coordinated PEMs with broad relative humidity tolerance. Energies 2020;13(8):1924.

[260] Wang D, Wang S, Tian X, Li J, Liu F, Wang X, Chen H, Mao T, Liu G. Ethyl phosphoric acid grafted amino-modified polybenzimidazole with improved long-term stability for high-temperature proton exchange membrane applications. Int J Hydrogen Energy 2020;45(4):3176–85.

[261] Singh B, Duong NM, Henkensmeier D, Jang JH, Kim HJ, Han J, Nam SW. Influence of different side-groups and cross-links on phosphoric acid doped radel-based polysulfone membranes for high temperature polymer electrolyte fuel cells. Electrochim Acta 2017;224:306–13.

[262] Bai H, Peng H, Xiang Y, Zhang J, Wang H, Lu S, Zhuang L. Poly (arylene piperidine) s with phosphoric acid doping as high temperature polymer electrolyte membrane for durable, high-performance fuel cells. J Power Sources 2019;443:227219.

[263] Berber MR, Nakashima N. Bipyridine-based polybenzimidazole membranes with outstanding hydrogen fuel cell performance at high temperature and non-humidifying conditions. J Membr Sci 2019;591:117354.

[264] Farrokhi M, Abdollahi M. Enhancing medium/high temperature proton conductivity of poly (benzimidazole)-based proton exchange membrane via blending with poly (vinyl imidazole-co-vinyl phosphonic acid) copolymer: proton conductivity-copolymer microstructure relationship. Eur Polym J 2020;131: 109691.

[265] Erdemi H, Bozkurt A. Synthesis and characterization of poly (vinylpyrrolidone-co-vinylphosphonic acid) copolymers. Eur Polym J 2004;40(8):1925–9.

[266] Teixeira FC, de Sá AI, Teixeira AP, Ortiz-Martínez VM, Ortiz A, Ortiz I, Rangel CM. New modified Nafion-bisphosphonic acid composite membranes for enhanced proton conductivity and PEMFC performance. Int J Hydrogen Energy 2021;46(33):17562–71.

[267] Tanaka M, Takeda Y, Wakiya T, Wakamoto Y, Harigaya K, Ito T, Tarao T, Kawakami H. Acid-doped polymer nanofiber framework: three-dimensional proton conductive network for high-performance fuel cells. J Power Sources 2017;342:125–34.

[268] Taherkhani Z, Abdollahi M, Sharif A. Proton conducting porous membranes based on poly (benzimidazole) and poly (acrylic acid) blends for high temperature proton exchange membranes. Solid State Ionics 2019;337:122–31.

[269] Quartarone E, Angioni S, Mustarelli P. Polymer and composite membranes for proton-conducting, high-temperature fuel cells: a critical review. Materials 2017; 10(7):687.

[270] Chia MY, San Thiam H, Leong LK, Koo CH. Effect of filler content on transport properties of sulfonated polyether ether ketone (SPEEK) composite proton exchange membranes. InIOP Conference Series: Mater. Sci. Eng. 2018;409(1): 012003.

[271] Xu C, Wu X, Wang X, Mamlouk M, Scott K. Composite membranes of polybenzimidazole and caesium-salts-of-heteropolyacids for intermediate temperature fuel cells. J Mater Chem 2011;21(16):6014–9.

[272] Ooi YX, Ya KZ, Maegawa K, Tan WK, Kawamura G, Muto H, Matsuda A. CHS-WSiA doped hexafluoropropylidene-containing polybenzimidazole composite membranes for medium temperature dry fuel cells. Int J Hydrogen Energy 2019; 44(60):32201–9.

[273] Ya KZ, Nbelayim P, Kikuchi T, Maegawa K, Kawamura G, Muto H, Matsuda A. Effect of mixed alkali metal ions in highly proton conductive K/Cs-hydrogen sulfate-phosphotungstic acid composites prepared by mechanical milling. Solid State Ionics 2019;340:115022.

[274] Wang S, Sun P, Hao X, Li Z, Liu G, Jin L, Yin X. Ferric sulfophenyl phosphate bonded with phosphotungstic acid as a novel intercalated high-temperature inorganic-organic proton conductor. Mater Chem Phys 2018;213:35–43.

[275] Lu JL, Fang QH, Li SL, Jiang SP. A novel phosphotungstic acid impregnated meso-Nafion multilayer membrane for proton exchange membrane fuel cells. J Membr Sci 2013;427:101–7.

[276] Xie Q, Li Y, Chen X, Hu J, Li L, Li H. Composite proton exchange membranes based on phosphosilicate sol and sulfonated poly (ether ether ketone) for fuel cell applications. J Power Sources 2015;282:489–97.

[277] Xie Q, Li Y, Hu J, Chen X, Li H. A CsH2PO4-based composite electrolyte membrane for intermediate temperature fuel cells. J Membr Sci 2015;489: 98–105.

[278] Wu H, Shen X, Cao Y, Li Z, Jiang Z. Composite proton conductive membranes composed of sulfonated poly (ether ether ketone) and phosphotungstic acid-loaded imidazole microcapsules as acid reservoirs. J Membr Sci 2014;451:74–84.

[279] Li J, Wang S, Xu J, Xu L, Liu F, Tian X, Wang Z. Organic-inorganic composite membrane based on sulfonated poly (arylene ether ketone sulfone) with excellent long-term stability for proton exchange membrane fuel cells. J Membr Sci 2017; 529:243–51.

[280] Furtado Filho AA, Gomes AS. Sulfonated bisphenol-A-polysulfone based composite PEMs containing tungstophosphoric acid and modified by electron beam irradiation. Int J Hydrogen Energy 2012;37(7):6228–35.

[281] Li W, Zhang F, Yi S, Huang C, Zhang H, Pan M. Effects of casting solvent on microstructrue and ionic conductivity of anhydrous sulfonated poly (ether ether ketone)-inoic liquid composite membranes. Int J Hydrogen Energy 2012;37(1): 748–54.

[282] Hooshyari K, Javanbakht M, Adibi M. Novel composite membranes based on dicationic ionic liquid and polybenzimidazole mixtures as strategy for enhancing thermal and electrochemical properties of proton exchange membrane fuel cells applications at high temperature. Int J Hydrogen Energy 2016;41(25):10870–83.

[283] Tian X, Wang S, Li J, Liu F, Wang X, Chen H, Ni H, Wang Z. Composite membranes based on polybenzimidazole and ionic liquid functional Si–O–Si network for HT-PEMFC applications. Int J Hydrogen Energy 2017;42(34): 21913–21.

[284] Thanganathan U, Nogami M. Investigations on effects of the incorporation of various ionic liquids on PVA based hybrid membranes for proton exchange membrane fuel cells. Int J Hydrogen Energy 2015;40(4):1935–44.

[285] Altaf F, Batool R, Gill R, Rehman ZU, Majeed H, Ahmad A, Shafiq M, Dastan D, Abbas G, Jacob K. Synthesis and electrochemical investigations of ABPBI grafted montmorillonite based polymer electrolyte membranes for PEMFC applications. Renew Energy 2021;164:709–28.

[286] Wang L, Liu Z, Liu Y, Wang L. Crosslinked polybenzimidazole containing branching structure with no sacrifice of effective NH sites: towards high-performance high-temperature proton exchange membranes for fuel cells. J Membr Sci 2019;583:110–7.

[287] Kumari M, Sodaye HS, Bindal RC. Cross-linked sulfonated poly (ether ether ketone)-poly ethylene glycol/silica organic–inorganic nanocomposite membrane for fuel cell application. J Power Sources 2018;398:137–48.

[288] Hasegawa S, Hiroki A, Ohta Y, Iimura N, Fukaya A, Maekawa Y. Thermally stable graft-type polymer electrolyte membranes consisting based on poly (ether ether ketone) and crosslinked graft-polymers for fuel cell applications. Radiat Phys Chem 2020;171:108647.

[289] Kim K, Heo P, Ko T, Kim KH, Kim SK, Pak C, Lee JC. Poly (arlyene ether sulfone) based semi-interpenetrating polymer network membranes containing cross-linked poly (vinyl phosphonic acid) chains for fuel cell applications at high temperature and low humidity conditions. J Power Sources 2015;293:539–47.

[290] Sithambaranathan P, Nasef MM, Ahmad A, Ripin A. Crosslinked composite membrane by radiation grafting of 4-vinylpyridine/triallyl-cyanurate mixtures onto poly (ethylene-co-tetrafluoroethylene) and phosphoric acid doping. Int J Hydrogen Energy 2017;42(14):9333–41.

[291] Wang Y, Chen P, Weng Q, Chen X, An Z. Quinoxaline-based semi-interpenetrating polymer network of sulfonated poly (arylene ether) s and sulfonated polyimides as proton exchange membranes. Polym Bull 2021;78(8):4333–54.

[292] Tutgun MS, Sinirlioglu D, Celik SU, Bozkurt A. Investigation of nanocomposite membranes based on crosslinked poly (vinyl alcohol)–sulfosuccinic acid ester and hexagonal boron nitride. J Polym Res 2015;22:1. 1.

[293] Zhou T, Li Y, Wang W, He L, Cai L, Zeng C. Application of a novel PVA-based proton exchange membrane modified by reactive black KN-B for low-temperature fuel cells. Int J Electrochem Sci 2019;14(9):8514–31.

[294] Ramly NN, Aini NA, Sahli N, Aminuddin SF, Yahya MZ, Ali AM. Dielectric behaviour of UV-crosslinked sulfonated poly (ether ether ketone) with methyl cellulose (SPEEK-MC) as proton exchange membrane. Int J Hydrogen Energy 2017;42(14):9284–92.

[295] Mahimai BM, Sivasubramanian G, Sekar K, Kannaiyan D, Deivanayagam P. Sulfonated poly (ether ether ketone): efficient ion-exchange polymer electrolytes for fuel cell applications–a versatile review. Mater Adv 2022;3(15):6085–95.

[296] Segale M, Seadira T, Sigwadi R, Mokrani T, Summers G. A new frontier towards development of efficient SPEEK polymer membranes for PEM fuel cells applications: a review. Mater Adv 2024.

[297] Nabilla Ramly N. Physical properties analysis of UV-crosslinked sulfonated poly ether ether ketone and methyl cellulose. J Mech Eng 2016;13(2):97–110.

[298] Lv S, Li X, Lu M, Lu T, Lv W, Liu W, Dong X, Liu Z, Yang B. Recent advances in non-perfluorinated sulfonic acid proton exchange membranes in the energy field. J. Mater. Chem. A. 2024.

[299] Bahar T. Development of reasonably stable chitosan based proton exchange membranes for a glucose oxidase based enzymatic biofuel cell. Electroanalysis 2020;32(3):536–45.

[300] Kamjornsupamitr T, Sangthumchai T, Saejueng P, Sumranjit J, Hunt AJ, Budsombat S. Composite proton conducting membranes from chitosan, poly (vinyl alcohol) and sulfonic acid-functionalized silica nanoparticles. Int J Hydrogen Energy 2021;46(2):2479–90.

[301] Zhao G, Chen Y, Li XF, Zhang S, Situ Y. Fabrication of highly proton-conductive chitosan whole-bio-membrane materials functionalized with adenine and adenosine monophosphate. Green Chem 2020;22(8):2426–33.

[302] Munavalli BB, Kariduraganavar MY. Enhancement of fuel cell performance of sulfonated poly (arylene ether ketone) membrane using different crosslinkers. J Membr Sci 2018;566:383–95.

[303] Chen H, Wang S, Li J, Liu F, Tian X, Wang X, Mao T, Xu J, Wang Z. Novel cross-linked membranes based on polybenzimidazole and polymeric ionic liquid with improved proton conductivity for HT-PEMFC applications. J Taiwan Inst ChemEng 2019;95:185–94.

[304] Wang C, Li Z, Sun P, Pei H, Yin X. Preparation and properties of covalently crosslinked polybenzimidazole high temperature proton exchange membranes doped with high sulfonated polyphosphazene. J Electrochem Soc 2020;167(10):104517.

[305] Li X, Ma H, Wang P, Liu Z, Peng J, Hu W, Jiang Z, Liu B. Construction of high-performance, high-temperature proton exchange membranes through incorporating SiO2 nanoparticles into novel cross-linked polybenzimidazole networks. ACS Appl Mater Interfaces 2019;11(34):30735–46.

[306] Karas F, Hnát J, Paidar M, Schauer J, Bouzek K. Determination of the ion-exchange capacity of anion-selective membranes. Int J Hydrogen Energy 2014;39(10):5054–62.

[307] Ying YP, Kamarudin SK, Masdar MS. Silica-related membranes in fuel cell applications: an overview. Int J Hydrogen Energy 2018;43(33):16068–84.

[308] Geng H, Wu H, Li J, He X, Shi B, Fan C, Qiu M, Mao X, Jiang Z. Preparing proton exchange membranes via incorporating silica-based nanoscale ionic materials for the enhanced proton conductivity. Solid State Ionics 2020;349:115294.

[309] Zeng J, Zhou Y, Li L, Jiang SP. Phosphotungstic acid functionalized silica nanocomposites with tunable bicontinuous mesoporous structure and superior proton conductivity and stability for fuel cells. Phys Chem Chem Phys 2011;13(21):10249–57.

[310] Unnikrishnan L, Mohanty S, Nayak SK, Jayan NP. Sulfonated polysulfone/TiO 2 nanocomposite membranes for fuel cell application. Int. J. Plast. Technol. 2011;15:1–20.

[311] Elakkiya S, Arthanareeswaran G, Ismail AF, Das DB, Suganya R. Polyaniline coated sulfonated TiO2 nanoparticles for effective application in proton conductive polymer membrane fuel cell. Eur Polym J 2019;112:696–703.

[312] Devrim Y, Durmuş GN. Composite membrane by incorporating sulfonated graphene oxide in polybenzimidazole for high temperature proton exchange membrane fuel cells. Int J Hydrogen Energy 2022;47(14):9004–17.

[313] Kim AR, Gabunada JC, Yoo DJ. Amelioration in physicochemical properties and single cell performance of sulfonated poly (ether ether ketone) block copolymer composite membrane using sulfonated carbon nanotubes for intermediate humidity fuel cells. Int J Energy Res 2019;43(7):2974–89.

[314] Hernández-Fernández P, Montiel M, Ocón P, de La Fuente JG, García-Rodríguez S, Rojas S, Fierro JL. Functionalization of multi-walled carbon nanotubes and application as supports for electrocatalysts in proton-exchange membrane fuel cell. Appl Catal, B 2010;99(1–2):343–52.

[315] Ahmed S, Ali M, Cai Y, Lu Y, Ahmad Z, Khannal S, Xu S. Novel sulfonated multi-walled carbon nanotubes filled chitosan composite membrane for fuel-cell applications. J Appl Polym Sci 2019;136(22):47603.

[316] Wang S, Lin Y, Yang J, Shi L, Yang G, Zhuang X, Li Z. UiO-66-NH2 functionalized cellulose nanofibers embedded in sulfonated polysulfone as proton exchange membrane. Int J Hydrogen Energy 2021;46(36):19106–15.

[317] Donnadio A, Narducci R, Casciola M, Marmottini F, D'Amato R, Jazestani M, Chiniforoshan H, Costantino F. Mixed membrane matrices based on nafion/UiO-66/SO3H-UiO-66 nano-MOFs: revealing the effect of crystal size, sulfonation, and filler loading on the mechanical and conductivity properties. ACS Appl Mater Interfaces 2017;9(48):42239–46.

[318] Li J, Gong JL, Zeng GM, Zhang P, Song B, Cao WC, Fang SY, Huan SY, Ye J. The performance of UiO-66-NH2/graphene oxide (GO) composite membrane for removal of differently charged mixed dyes. Chemosphere 2019;237:124517.

[319] Feng L, Hou HB, Zhou H. UiO-66 derivatives and their composite membranes for effective proton conduction. Dalton Trans 2020;49(47):17130–9.

[320] Kahraman H, Akın Y. Recent studies on proton exchange membrane fuel cell components, review of the literature. Energy Convers. Manage. 2024;304:118244.

[321] Dong F, Xu S, Wu X, Jin D, Wang P, Wu D, Leng Q. Cross-linked poly (vinyl alcohol)/sulfosuccinic acid (PVA/SSA) as cation exchange membranes for reverse electrodialysis. Sep Purif Technol 2021;267:118629.

[322] Inoue T, Uma T, Nogami M. Performance of H2/O2 fuel cell using membrane electrolyte of phosphotungstic acid-modified 3-glycidoxypropyl-trimethoxysilanes. J Membr Sci 2008;323(1):148–52.

[323] Ho WF, Lim KM, Yang KL. In situ formation of leak-free polyethylene glycol (PEG) membranes in microfluidic fuel cells. Lab Chip 2016;16(24):4725–31.

[324] Chalykh AE, Khasbiullin RR, Aliev AD, Matveev VV, Gerasimov VK, Slesarenko NA, Avilova IA, Volkov VI, Tverskoy VA. The effect of Divinylbenzene on the structure and properties of polyethylene films with related radiation chemical grafted polystyrene and Sulfocationite membranes. Membranes 2023;13(6):587.

[325] Zhou W, Xiao J, Chen Y, Zeng R, Xiao S, Nie H, Li F, Song C. Sulfonated carbon nanotubes/sulfonated poly (ether sulfone ether ketone ketone) composites for polymer electrolyte membranes. Polym Adv Technol 2011;22(12):1747–52.

[326] Wang YM, Zhang X, Yang D, Wu L, Zhang J, Lei T, Yang R. Highly stable metal-organic framework UiO-66-NH2 for high-performance triboelectric nanogenerators. Nanotechnology 2021;33(6):065402.

[327] Shi S, Weber AZ, Kusoglu A. Structure/property relationship of Nafion XL composite membranes. J Membr Sci 2016;516:123–34.

[328] Liu J, Suraweera N, Keffer DJ, Cui S, Paddison SJ. On the relationship between polymer electrolyte structure and hydrated morphology of perfluorosulfonic acid membranes. J Phys Chem C 2010;114(25):11279–92.

[329] Kang DW, Kang M, Hong CS. Post-synthetic modification of porous materials: superprotonic conductivities and membrane applications in fuel cells. J Mater Chem 2020;8(16):7474–94.

[330] Yin C, Chen D, Hu M, Jing H, Qian L, He C. Composite proton exchange membrane featuring a three-layer structure: enhanced thermal stability, proton conductivity, and fuel cell performance. J Membr Sci 2024;707:122997.

[331] Lin Q, Sun X, Chen X, Shi S. Effect of pretreatment on microstructure and mechanical properties of Nafion™ XL composite membrane. Fuel Cells 2019;19(5):530–8.

[332] Patil Y, Kulkarni S, Mauritz KA. In situ grown titania composition for optimal performance and durability of Nafion® fuel cell membranes. J Appl Polym Sci 2011;121(4):2344–53.

[333] Xiaomin GA, Yonghua LI, Jinlong LI. Review on modification of sulfonated poly(-ether-ether-ketone) membranes used as proton exchange membranes. Mater Sci 2015;21(4):574–82.

[334] Li Y, Nguyen QT, Schaetzel P, Lixon-Buquet C, Colasse L, Ratieuville V, Marais S. Proton exchange membranes from sulfonated polyetheretherketone and sulfonated polyethersulfone-cardo blends: conductivity, water sorption and permeation properties. Electrochim Acta 2013;111:419–33.

[335] Qu E, Hao X, Xiao M, Han D, Huang S, Huang Z, Wang S, Meng Y. Proton exchange membranes for high temperature proton exchange membrane fuel cells: challenges and perspectives. J Power Sources 2022;533:231386.

[336] Li Q, He R, Jensen JO, Bjerrum NJ. PBI-based polymer membranes for high temperature fuel cells–preparation, characterization and fuel cell demonstration. Fuel cells 2004;4(3):147–59.